Applied Physics Department

Energy efficiency improvement of hybrid ground coupled HVAC systems from thermal energy generation and storage management

PhD-Thesis

Author: Nicolás Pardo García
Supervisors: Álvaro E. Montero Reguera, Javier F. Urchueguía Schölzel and Pedro Fernández de Córdoba Castellá

A mis mujeres...
y a mis hombres.

Buenos dias D. Canuto...
(N. García)

Resumen

El incremento del consumo energético de los últimos tiempos esta produciendo serios cambios en la naturaleza tales como el calentamiento global. Alrededor del 40 % de los gases de efecto invernadero en los países desarrollados proceden de los equipos en las edificaciones donde aproximadamente el 60% son producidos en los sistemas de climatización. En este contexto, las bombas de calor acopladas al terreno son una solución atractiva como sistema de climatización en los edificios comerciales debido a su alta eficiencia comparada con los sistemas convencionales basados en bombas de calor aire-agua. De hecho, la Agencia de Protección Medioambiental Americana reconoce que este tipo sistemas son los más eficientes y confortables. Sin embargo, la eficiencia de las bombas de calor acopladas al terreno podría mejorarse aún más mediante la adecuada gestión de los distintos equipos que las configuran.

El objetivo de la investigación de la tesis doctoral será el desarrollo de estrategias de gestión energética a través de simulaciones en los sistemas de climatización basados en bombas de calor acoplados al terreno para mejorar la eficiencia energética de los mismos y a la vez mantener las condiciones de confort térmico dentro del área climatizada. Las estrategias de gestión energética estarán orientadas en tres aspectos: combinación de varios sistemas de generación (bomba de calor acoplada al terreno y bomba de calor aire-agua), desacoplo de la generación energética de la distribución energética (mediante un deposito de almacenamiento térmico) y estrategias basadas en la gestión equipos de la instalación (mediante su regulación continua).

De los resultados de la investigación se pueden obtener dos conclusiones fundamentales. La primera de ellas es que una adecuada gestión de un sistema compuesto por un depósito de almacenamiento, una bomba de calor aire-agua y una bomba de calor acoplada al terreno produce una mejora en la eficiencia energética de entorno al 40% respecto al sistema convencional y de entorno al 18% respecto al sistema geotérmico. La segunda conclusión

de la tesis es que una adecuada estrategia de regulación en continuo sobre los elementos que configuran un sistema de bomba de calor acoplada al terreno produce un ahorro de alrededor del 24% respecto a los sistemas convencionales de gestión.

Resum

L'incrementa del consum energètic dels últims temps està produint seriosos canvis en la natura tals com l'escalfament global. Al voltant del 40% dels gasos d'efecte hivernacle als països desenvolupats procedeixen dels equipaments en les edificacions on aproximadament el 60% són produïts als sistemes de climatització. En aquest context, les bombes de calor acoplades al terreny són una solució atractiva com a sistema de climatització als edificis comercials a causa de la seua alta eficiència comparada amb els sistemes convencionals basats en bombes de calor aire-aigua. De fet, l'Agència de Protecció Mediambiental Americana reconeix que aquests tipus de sistemes són els més eficients i confortables. Tanmateix, l'eficiència de les bombes de calor acoblades al terreny podria millorar-se encara més mitjançant l'adequada gestió dels diferents equips que les configuren.

L'objectiu de la investigació de la tesi doctoral serà el desenvolupament d'estratègies de gestió energètica a través de simulacions en els sistemes de climatització basats en bombes de calor acoplades al terreny per millorar l'eficiència energètica dels mateixos i alhora mantenir les condicions de confort tèrmic dins de l'àrea climatitzada. Les estratègies de gestió energètica estaran orientades en tres aspectes: combinació de diversos sistemes de generació (bomba de calor acoplada al terreny i bomba de calor aire-aigua), desacoplament de la generació energètica de la distribució energètica (mitjançant un depòsit d'emmagatzenament tèrmic) i estratègies basades en la gestió dels equipaments de la instal·lació (mitjançant la seua regulació contínua).

Dels resultats de la investigació es poden obtenir dues conclusions fonamentals. La primera d'elles és que una adequada gestió d'un sistema compost per un depòsit d'emmagatzenament, una bomba de calor aire-aigua i una bomba de calor acoplada al terreny produeix una millora de la eficiència energètica d'entorn del 40% respecte al sistema convencional i d'entorn del 18% respecte al sistema geotèrmic. La segona conclusió de la tesi és que una

adequada estratègia de regulació en continu sobre els elements que configuren un sistema de bomba de calor acoplada al terreny produeix un estalvi del voltant del 24% respecte als sistemes convencionals de gestió.

Abstract

Nowadays, the increasing of the energy consumption is producing serious changes in the natural environment as the global warming. Around the 40% of all greenhouse gas emissions in developed countries come from the building equipments, where approximately 60% are produced by the air conditioning systems. In this context, ground coupled heat pumps are an attractive solution as air conditioning systems in commercial buildings due to their higher efficiency compared with the conventional air to water heat pump. In fact, the American Environmental Protection Agency recognizes ground coupled heat pump systems among the most efficient and comfortable systems available today. Nevertheless, the energy efficiency of the ground coupled heat pumps could be improve by means a properly management of the different equipments which form them.

The objective of the research of this PhD thesis will be the development of management strategies in the air conditioning system based on the ground coupled heat pumps to improve its energy efficiency at the same time that we keep the thermal comfort in the conditioned areas. The energy management strategies will be oriented in the three ways: combining of several generation systems (ground coupled heat pump and air to water heat pump), decoupling thermal generation from thermal distribution (by means a thermal storage device) and strategies based on the management of the devices of the system (by means of continuous regulation of them).

From the results of this research we can obtain two main conclusions. The first one is that a properly management of a system composed by a thermal storage, an air to water heat pump and a ground coupled heat pump produce an improvement of the energy efficiency around a 40% respect to a conventional system and around a 18% respect to a geothermal system. The second main conclusion of this thesis is that a properly management strategy in continuous regulation of the devices which are part of a ground coupled heat pump system produce a energy savings around of the 24% respect to

the conventional management systems.

Acknowledgments

La realización de este trabajo de investigación no podría haberse llevado a cabo sin la ayuda y la colaboración de todo un grupo humano que me ha acompañado desde el inicio de esta tarea. A todos ellos he de agradecer sus aportaciones tanto científicas como personales.

Quisiera agradecer en primer lugar a mis directores de trabajo J.F. Urchueguía, Á. Montero y P. Fernández de Córdoba por toda su dedicación y la confianza depositada en mi persona. También he de agradecer al resto de mis compañeros que me han ayudado en todos y cada uno de los problemas que han ido surgiendo en el desarrollo de presente trabajo. Quisiera hacer una mención especial a J. Martos por toda la ayuda que me ha prestado y que han sido una guía en los momentos más problemáticos de este trabajo pero sobre todo por su amistad y su gran apoyo.

Finalmente a mi familia y mis amigos por todo el apoyo personal que me han ofrecido. Ellos han llenado los huecos en los momentos difíciles y en especial a V. Rajdlova que me apoya y me quiere como nadie podría hacer nunca.

Contents

Chapter 1
General introduction

In this chapter we would like to set up the reasons which have motivated the development of this thesis, the current context of the geothermal systems, the objectives of our research and the structure of this work. The contents are as follows: in the first section the motivation or this dissertation is presented. The second section introduces the state of the art of the different aspects which are implicated in the geothermal systems to contextualize this work. Afterwards, we define the main objectives which have been achieved in this research. Finally, the last section presents the final structure of this thesis.

1.1 Motivation

The energy sector is one of the most important in modern economic systems. The recent fluctuation of the oil prices has produced measures to solve this problem and particularly in the oil importing countries. These measures are oriented to solve growing uncertainties about the quantities and prices related with the oil imports. Nevertheless, we have to bear in mind other considerations to plan the future strategies with respect to the production and consumption of the energy. One of the most important is the threat of global climate change. This phenomenon is caused by the greenhouse gasses emissions to the atmosphere by human actions during the recent decades.

Greenhouse gas emissions caused by human activity are generally considered the most important single source of potential future warming. The International Energy Agency (IEA) recognizes that the equipments from the service sector (buildings used for commercial or public purposes) and from the residential sector (buildings used by single family dwellings and apartments) produce around 40% of the total amount of the greenhouse gas emissions in developed countries, where approximately 60% are produced in cooling and heating systems, [1]. In this context, the development of new management

strategies for the Heating, Ventilation and Air Conditioning (HVAC) systems which employ technologies based on renewable energies could be a good way to improve its energy efficiency and to reduce the environmental impact.

A Ground Coupled Heat Pump (GCHP) unit is an assembly of an electrically driven compressor, two heat exchangers, an expansion valve and a ground heat exchanger. Its primary aim is the utilization of the renewable energy from the ground. In the winter season, the ground is used as heat source, absorbing heat contained in it, whereas in the summer season, it is used as heat sink, rejecting heat in it. This process is done by means of a fluid (water or water with antifreeze) flowing inside the ground heat exchanger, which is usually formed by a series of plastic pipes installed below the ground surface or submerged in a water reservoir (lake, river, sea, ocean...).

These units represent a technically viable technology for heating, cooling and domestic hot water systems in buildings. They offer several interesting characteristics for the potential user, such as a lower electrical demand and maintenance requirements than conventional systems. Furthermore, the Environmental Protection Agency (EPA) recognizes the GCHP systems as the most efficient and comfortable heating and cooling systems available today, [2].

Several experimental studies have proved higher energy efficiency of geothermal systems versus conventional air conditioning systems. An energy efficiency comparison was done between a conventional heating system and a GCHP system by Healy et al. in cold climate conditions. This study showed that the conventional one had a lower coefficient of performance than the GCHP system in the particular conditions of this study, [3]. The research made by Petit et al. concluded the best energy efficiency and viability of the system based on the GCHP system versus the air heat pump system in the South Africa climatic conditions, [4]. Hwang et al. designed and constructed a GCHP system for a university building in South Korea. The results of the experiment showed that the energy efficiency of the installation driven by the GCHP was 74% higher than when the installation was driven by a conventional air to water heat pump system, [5]. Finally, Urchueguía et al. did a comparison between the energy performance of a ground coupled water to water heat pump system and an air to water heat pump system for heating and cooling in Mediterranean coast climate conditions. In this study, the geothermal system saved, in terms of primary energy consumption, around 43% in the heating season and 37% in the cooling season of the energy consumed by the conventional one, [6].

From a non-economical point of view, GCHP systems offer competitive levels of comfort compared with standard technologies, reduced noise levels and visual contamination, savings of greenhouse gas emissions and reasonable environmental safety. Proof of the goodness of this technology is the estimation around 1.1 million of installed units in 2005 in all the world, [7].

1.2 State of the art

The environment in which we live often requires artificial modification to provide healthy, safe, and livable conditions. From the origin of the times, the human beings have developed different systems to achieve this objective. For example, the Romans circulate aqueduct water through the walls of houses to cool them. Medieval Persian used cisterns to collect rain water and wind towers placed over them blow the generated cool air into the buildings. And in Egypt was invented and used widely the fan during the Middle Age, [8] and [9].

In the 1700s, the studies of the American scientist Benjamin Thompson and the British chemist Sir Humphry Davy triggered research resulting in the understanding that heat is a form of energy. This fact was finally proven by James Joule, a British physicist, and J.R. von Mayer and Hermann von Helmoholz, both German physicist in the mid-1800s.

In 1748, Dr. William Cullen at the University of Glasgow was the first to demonstrate artificial refrigeration by evaporating ether in a partial vacuum. His work led to further research into the chemical and mechanical systems that allow to obtain low temperatures. Early in the 1800s, close-cycle compression refrigeration was proposed. In 1820, British scientist and inventor Michael Faraday discovered that compressing and liquefying ammonia could chill air when the liquefied ammonia was allowed to evaporate. In 1842, Floridan physician John Garrie used compressor technology to create ice. He even envisioned centralized air conditioning that could cool entire cities. Nevertheless, the first commercial applications of air conditioning were manufactured to cool air for industrial processing rather than personal comfort. In 1902 the first modern air conditioning device was invented by Willis Carrier to improve manufacturing process control in a printing plant. And afterwards, in the 1950s was when has its expansion in the residential market.

In 1912 the Swiss patent issued to Heinrich Zoelly is the first known refe-

rence to ground source heat pump systems, [10]. Before World War II, some ground source heat pump systems were installed, [11]. At the same time, several projects involving researches in laboratory and in actual monitoring installation were undertaken. From the theoretical point of view, Ingersoll et al. proposed the line source model, [12], and Carslaw et al. proposed the cylindrical source model, [13], which provided some of the basis for later design programs. During the years after Word War II, the interest in further researches waned due to problems with drying around horizontal ground loop heat exchangers, [14], leakages, [15], and undersizing, [16]. This situation produced that gradually this kind of installation began to decrease.

Research began again in the late 1970s, after the oil crisis, and initially followed much of the same paths as the 1940s research, with an emphasis on experimental testing. This research did lead to solutions for several of the problems associated with the 1940s installations: drying around horizontal ground loop heat exchangers was resolved with better backfilling techniques, leakage problems were substantially resolved with the use of heat fusion and high-density polyethylene pipe, and undersizing problems were alleviated to some degree with new sizing algorithms, [17].

At the same time, the number of installation in residential buildings became to increase. In reference [18] numerous case studies of GCHP systems applied to commercial buildings may be found. This increased focus on commercial systems drove research in several areas:

Computer simulation: Computer simulation of ground coupled heat pump systems is one of the most important research topics. This is involved in the high initial cost due to drill of deep boreholes. To reduce cost, precise system design becomes very important. Various design tools have been developed. The line source model and the cylindrical source model assume infinite length for borehole. Hart and Couvillion proposed an equation for the ground temperature around a line source in terms of a power series of the ratio of radial distance and far field distance, [19]. The definition of far field distance depends on the radius of the borehole. The International Ground Source Heat Pump Association (IGSHPA) adopted the line source model but developed formulae to approximate the exponential integral appearing in the line source solution, [20]. Hellström applied a numerical inversion technique to solve the inverse Laplace transform of the governing differential equation for one-dimensional transient heat conduction equation in polar coordinates and developed an alternative form for the cylindrical source solution, [21]. Hikari et al. derived simplified forms for the cylindrical source solution at

borehole surface depending on the Fourier number, [22]. Eskilson calculated the ground temperature around single borehole using finite-difference method, assuming no temperature change on the ground surface (by superimposing an identical mirror borehole above the ground surface with negative strength). He proposed a g-function to describe the performance of borehole, and developed g-function curves based on selected borefield configurations, [23]. The finite line source model quoted by Zeng et al. adopted similar methodology, but used an analytical expression developed from point source solution for calculating the ground temperature change instead of using the finite-difference method, [24]. Lamarche and Beauchamp developed alternative forms for the finite line source solution with shorter computation time, [25]. Finally, Bandos et al. proposed new approximation expressions for the mean dimensionless ground temperature around a deep borehole for the intermediate and long time intervals for the external heat conduction problem, [26].

All the above models calculate the performance of a single borehole based on constant loading along the borehole in the time domain. To deal with load varying with time, the method of load aggregation was employed. The load profile was divided into various constant load steps starting at particular time instants. The overall performance is the summation of effects from each load step. To reduce computing time, Yavuzturk postulated that load occurring after certain time could be lumped together into larger blocks, [27]. Bernier et al. suggested a multiple load aggregation algorithm to calculate the performance of a single borehole at variable load based on the cylindrical source model. For cases involving more than one borehole, the method of superposition was applied, [28].

Nowadays, researchers continue improving the models adding new effects of the ground and employing better techniques to solve these systems. Lee et al. developed a three dimensional finite difference method using rectangular coordinate system to discretize the borefield where the borehole was represented by a square column, [29]. Li et al. proposed to use the Delaunay triangulation method to mesh the borefield, in this way, the original geometric structure in the borehole remained intact, [30]. Esena et al. with the employment of new computer technics based on neuro-fuzzy inference system allowed predicting the daily performance of a GCHP system, [31]. Yang et al. proposed a two-region analytical solution model, which divided the heat transfer region of vertical U-tube GHE into two parts at the boundary of borehole wall, [32]. In the area of geothermal piles several models and experiments have been done. Gao et al. developed and validated several

numerical models for different types of pile-foundation heat exchangers to determine the most efficient of them to be used in a district heating and cooling system, [33]. Katsura et al. developed an algorithm which allowed modeling several configurations in serial or parallel circuits for multiple ground heat exchangers which was proven in a residential GCHP system with geothermal piles, [34]. Finally, researches have been also interested in another configurations of ground heat exchangers. As an example, Demir et al. modeled and performed the experimental verification for the heat transfer in a horizontal parallel pipe ground heat exchanger, [35].

Geothermal hybrid systems: In most areas, rejected heat to the ground and extracted heat from the ground by a GCHP are not equal. In the heating dominated areas occurs that the heating period is longer. Therefore, the heating load is higher than the load in the cooling period. In cooling dominated area takes place the opposite phenomenon. This inconsistency between heat extracted and heat rejected produces, respectively, the gradually decreasing or increasing of the temperature on the surroundings of the heat exchanger. Therefore, this situation produce with the time a deterioration of the soil properties due to long-term operation of the system.

In this context, this situation may be mitigated by increasing the size of the ground loop heat exchanger. Alternatively, the GCHP system can be integrated with another generation system balancing the amount of heat extracted and rejected load into the ground. Theses kinds of systems are called 'Hybrid Ground Coupled Heat Pump System (HGHP)'. For example, in heating dominated areas the solar energy is one of the most suitable options for this kind of integrated systems. Several studies have probed that combination of thermal solar panels and a ground coupled heat pump allows to diminish the extracted load from the ground during the cooling season, balancing the thermal load rejected and absorbed in the ground. Ozgener et al. did an experimental evaluation of a vertical solar assisted ground coupled heat pump system where a solar collector was directly installed into the ground coupled loop, [36]. Hepbasli studied the exergetic aspects of a ground solar heat pump system where a solar domestic hot water tank was integrated, [37]. This combination of GCHP system, solar panels and hot water tanks was studied in actual conditions. Trillat et al. designed and built a family house in region of Savoie, France, to evaluate these kind of systems, [38], and a similar study was done by Han et al. in another family house in the countryside of Tianjin, China, [39]. In addition, Wang et al. presented a new management strategy to improve the efficiency of these systems while the energy balance in the ground was kept at the same time, [40].

Finally, the integration of solar panels with a ground coupled heat pump with another types of ground heat exchangers are studied. In this context a model and a experiment of a solar assisted ground coupled heat pump system with a vertical double-spiral ground heat exchanger was done by Bi et al., [41].

In cooling dominated areas the employment of a cooling tower or an air to water heat pump in combination with a GCHP allows to balance the load in the soil where the ground heat exchanger is placed. The ASHRAE manual discusses the advantages of these systems in reducing the initial costs and ground area requirement compared with conventional GCHP systems. The manual proposes a design procedure for cooling towers with GCHP system for cooling dominated buildings and it offers a series of general guidelines to integrate supplemental heat rejecters, [42]. Gilbreath conducted a more detailed study based on this kind of systems and presented some design suggestions from a installation in an office building, [43]. Kavanaugh investigate the impact of the supplemental heat rejected and suggested that this one should be sized according to the peak loads and its nominal capacity should be calculated according to the difference between cooling and heating loads, [44]. Phetteplace et al. described the operating performance of this kind of system with, 70 vertical closed-loop boreholes and a 275 KW of thermal capacity, using the measured data over a 22 month period, [45]. Spitler et al. presented a system simulation approach to compare the advantages and disadvantages of several control strategies for the operation of the GCHP supported with a cooling tower system, [46]. Finally, Yi et al. developed a hourly model by modeling the heat transfer process of the main components. He also investigated several design methods and control strategies, [47].

In this sense, it should be mention that the employment of a thermal storage device in an air conditioning system allows decoupling energy generation from energy distribution. This possibility gives us two important advantages. First, the thermal energy demanded can be generated by means of a generation device with a lower thermal capacity than in the systems where the thermal load is only satisfied directly by the generator system. And second, it is possible to minimize the effects of the thermal load peaks generating the thermal energy when the environmental conditions are more favourable. Therefore, the incorporation of a thermal storage device could produce high energy savings in an air conditioning system, in particular, for the systems driven for a heat pump in a cooling dominated area. For example, Hasnain et al. studied the employment of a thermal storage coupled with a conventional air conditioning system in Saudi Arabia conditions. The study anticipated that the employment of this equipment could reduce the

peak cooling-load demand and the peak electrical demand around 30-40% and 10-20% respectively, [48]. And Nagota et al. studied the energy-saving effects of the electric driven heat pump for a district heating and cooling system where heat pumps could be operated at full load by utilizing the thermal storage capability. The results showed that the thermal storage contributed significantly to save electrical energy in cooling mode, [49].

Geothermal response tests: These geothermal tests are oriented to determine the effective thermal conductance of the ground where is going to be placed a ground heat exchanger. The thermal conductance is one of the most essential parameters when measuring geothermal probes, energy piles and components with ground contact. In general, in a response tests, a constant amount of heat is applied to the subsoil and the temperature response is measured. The conventional evaluation of the response test is mostly done according to the line source theory which allows calculating the effective conductivity of the ground with the measure data.

The idea of measuring the thermal response of the ground in situ was first presented by Mogensen, who suggested a system with a chilled heat carrier fluid, [50]. The first mobile test for thermal response tests were developed independently at Luleå Technical University in Sweden, [51] and [52], and at Oklahoma State University in USA, [53] and [54]. They were both based on Mogensen's concept but used heated instead of chilled carrier fluid.

Similar test equipments have later been developed in several countries with small variations from the initials. The Ecole Polytechnique Fédérale de Lausanne (EPFL) in Switzerland presented its own version in 2002, [55]. Afterwards, a compact version was developed from these equipments, [56]. The first thermal response test in Germany was performed in Langen in 1999 with the equipment of UBeG GbR and used as a basis for sizing a large borehole heat exchanger field, [57]. In Netherlands a test unit has been developed with a reversible heat pump instead of electrical resistance to control the fluid temperature. And therefore, it is possible to choose between heat extraction and heat injection, [58].

Grouts: The reduction of the length of the borehole for the ground heat exchanger can be achieved increasing the thermal conductivity of grout used to seal the space between the borehole and the heat exchanger loop. The grout provides a heat transfer medium between the U-loop and the surrounding formation, controls groundwater movement and prevents contaminations of underground aquifers. Kavanaugh et al. and Philippacopoulos

et al. studied the thermal properties of sand, cement and bentonite grouts which nowadays are accepted as standard fill materials for the geothermal boreholes, [59] and [60]. Philippacopoulos et al. also tested the permeability and infiltration of the cement grouts, [61]. Nevertheless recently, Allan has studied and assessed a new superplasticized cement-sand grouts and he proved that this new kind of grouts have performance advantages over cement grout as higher thermal conductivity, better physical and mechanical bonding characteristics, [62].

1.3 Objectives

After presenting the motivation of the employment of the GCHP as air conditioning system and the state of the art of this technology, we want to present the actual situation of the employment in this system in Europe. Figure 1.1 shows that in spite of the North of Europe (heating dominated areas) is an old and strong technology, in the South of Europe and particularly in the countries of the Mediterranean area (cooling dominated areas) is an emerging technology, [63]. Due to this situation the research in the improvement of the energy efficiency of the air conditioning system driven by a ground coupled heat pump has been focused for the conditions in the heating dominated areas leaving, until nowadays, the necessary researches for conditions in the cooling dominated areas.

The objective of this research is to improve the energy efficiency of HVAC systems driven by a GCHP at the same time that we keep the thermal comfort in a cooling dominated building in the Mediterranean area. To do it, we have developed several management strategies for this air conditioning systems to improve the thermal energy generation and the thermal energy distribution throughout the following ideas:

Combining several generation systems. We can develop management strategies to improve the efficiency of the GCHP systems by combining it with another generation systems. The energy efficiency of an air to water heat pump depends on environmental conditions and, therefore, there are specific situations in which its efficiency can be comparable with the efficiency of the ground source systems. Then, a suitable management of a HVAC system combining both generation procedures could produce a performance better than each one working independently.

Decoupling thermal generation from thermal distribution. A

Figure 1.1: GCHP deployment in Europe.

management strategy which employs a thermal storage device could improve the efficiency of the HVAC system. As we said previously, this device allows minimizing the effects of the thermal load peaks and decreasing the thermal capacity of the GCHP system.

Managing properly the different devices of the GCHP system. The capacity of an air conditioning system is determined by the thermal demand of the coldest or warmest day along the year. Therefore, most of the time, the system is working under its designed capacity. In this context, the development of management strategies for the operation of the air conditioning system and, particularly, for the system based on the ground coupled heat

pumps, allowing to optimize the procedure to generate the thermal energy is a good way to improve the energy efficiency. From this idea, a continuous regulation of the different devices of the HVAC system can allow designing a more efficient way to generate the demanded thermal energy.

The experimental evaluation of the different management strategies developed in this thesis supposes high costs and long duration. Therefore, numerical simulations are a good alternative to test them. For this reason this thesis has been developed with TRNSYS which is a specific package software which allows us to evaluate the different aspects of the air conditioning systems driven by a GCHP, [64]. Finally, we want to mention that we have also included in this thesis, when we have been considered necessary, other aspects related with the GCHP installation as the cost assessment and the control technology to manage correctly the different devices of these air conditioning systems.

1.4 Contents of the thesis

In chapter 2, *'Ground coupled heat pump background'*, we describe the behaviour of the main elements which configure a ground coupled heat pump system: the ground where is linked to the heat exchanger, the heat pump device which cools or heats the desired area and the ground heat exchanger of which we present a classification of its different possible types. Finally, we include several actual examples of GCHP systems.

In chapter 3, *'Efficiency improvement of ground coupled heat pumps when combined with air source heat pump and thermal storage'*, we study the effects in the energy efficiency of an air conditioning system when the following ideas are applied: the combination of several generation systems (a ground coupled heat pump and an air to water heat pump) and the employment of a thermal storage to decouple thermal energy generation with the thermal energy distribution. To do it, we develop several air conditioning configurations to evaluate these two ideas, in first place separately and, afterwards, jointly.

In chapter 4, *'Efficiency improvement of ground coupled heat pumps from energy generation and distribution management'*, we study the power consumption behaviour of an air conditioning system driven only by a ground coupled heat pump. From this study we develop a new management strategy which manages the different devices to reduce the electrical energy consump-

tion while the desired thermal comfort is kept. Finally, we compare the total power consumption of the HVAC system when it is managed by the new strategy and by a conventional one.

In chapter 5, *'Conclusions'*, we summarize the main results obtained in the development of this thesis and we also propose several future research works.

We have also included four appendixes which contain some aspects which can help to clarify details of the present thesis:

In appendix A, *'Thermal energy model of the heat pump and the ground heat exchanger'*, is explained with more detail the thermal model of the water to water heat pumps and the air to water heat pump as well as the 'Duct Ground Heat Storage Model' which is employed to model the ground heat exchanger in the presented thesis.

In appendix B, *'Control devices'*, is explained how works the On-Off controller and the PID controller used to implement the management strategies presented in chapter four.

In appendix C, *'Fanger's PMV Model'*, is explained the 'Predicted Mean Vote' which is the parameter chosen to evaluate the thermal comfort state in our simulations.

In appendix D, *'Climatic Areas'*, is presented the subdivision into climatic areas of the South of Europe in order to identify the different Mediterranean climatic areas.

In appendix E, *'TRNSYS software package'*, we introduce the software package employed to model and to evaluate the different air conditioning layouts and the energy management strategies studied in this thesis.

In appendix F, *'Accuracy of the simulations results for the air conditioning layout configurations presented in Chapter 3'*, we present a study of the accuracy of the simulation results for the different air conditioning layouts presented in Chapter 3.

Finally, we include the employed nomenclature, the list of the tables and the figures, the contributions obtained from this research and the bibliography.

Chapter 2
Ground coupled heat pump background

2.1 Introduction

Ground coupled heat pump systems are a highly efficient renewable energy technology for space heating and cooling. This technology is based on the fact that ground temperature is fairly constant a few meters of surface soil. The ground is warmer in the middle of winter and cooler in the middle of summer than the outside air. Therefore, a GCHP system simply, during the winter season, removes heat from the earth and transfers it to the indoor air. And during summer season, this system extracts heat from indoor air and transferred to the earth.

In this chapter, we want to show a more practical point of view of the GCHP systems. To do it, the main elements employed in them (ground, heat pump and ground heat exchanger) are described with detail. We also present several actual examples of offices or public buildings located in the Mediterranean area (cooling dominated area) which employ air conditioning system driven by GCHPs.

This chapter is structured as follows. First, we explain the thermal behaviour of the ground and the reasons which make suitable to be used as heat source or heat sink. Next, it is described the operation circle in a heat pump and how it can move heat from the ground to the indoor air or vice versa. Afterwards, we present a classification of the different types of ground heat exchangers that can be used in a geothermal system. Finally, we describe several actual examples of office and public buildings located in the Mediterranean area (cooling dominated areas) which employ air conditioning systems driven by ground coupled heat pumps.

2.2 Ground thermal behaviour

The ground transports heat slowly and has a high heat storage capacity, its temperature changes slowly on the order of months or even years, depending on the depth of the measurement. As a consequence of this low thermal conductivity, the soil can transfer some heat from the cooling season to the heating season as we see in Figure 2.1, [65]. Heat absorbed by the earth during the summer effectively can be used in the winter. This yearly, continuous cycle between the air and the soil temperature gives a thermal energy potential that can be used to heat or to cool a building.

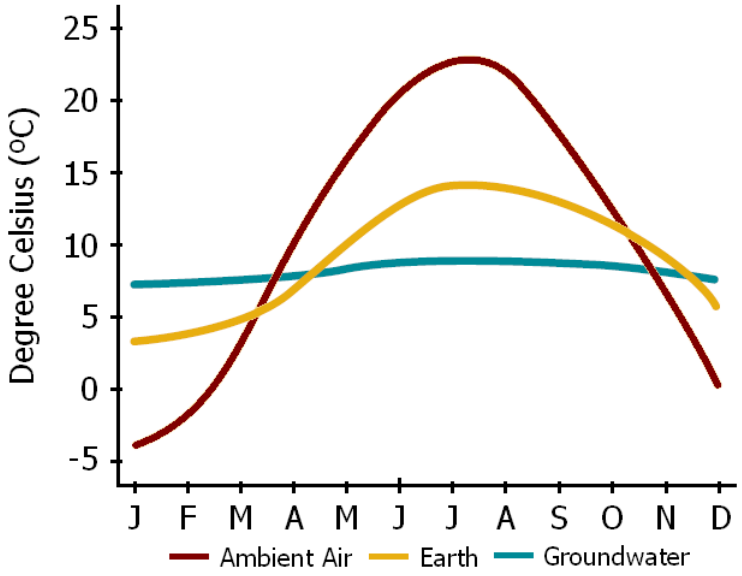

Figure 2.1: Average Monthly Temperature.

Another thermal characteristic of the ground is that a few meters from the surface soil the variation of the earth temperature and the groundwater temperature are lower in comparison with the air temperature above the soil as we see in Figure 2.2, [65]. This thermal fluctuations further helps to move the heating or cooling load to the season where it is needed. The earth is warmer than the ambient air in the winter and cooler than the ambient air in the summer.

This ground below the surface provides a free renewable source of energy that can easily provide enough energy along the year to heat and cool, for example, an average suburban residential home. A ground coupled heat pump

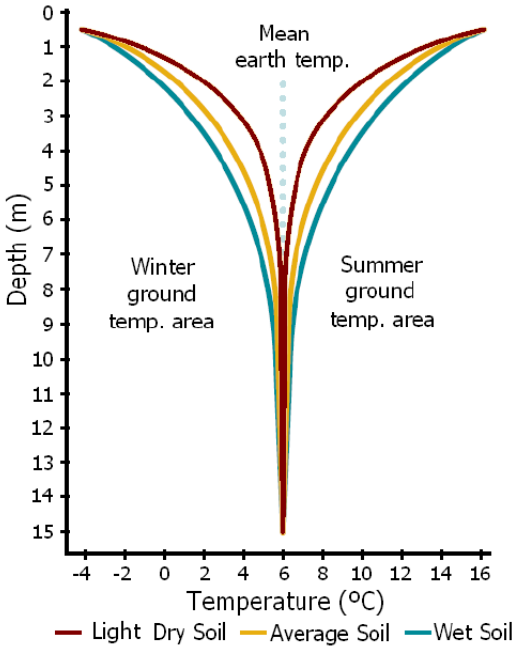

Figure 2.2: Soil Temperature Variation.

transforms this earth energy into useful energy to heat and cool buildings. It provides low temperature heat by extracting it from the ground or a body of water and provides cooling by reversing this process. Its principal application is space heating and cooling, though many also supply hot water, such as for domestic use.

2.3 Heat pump

A heat pump is a device that cool a fluid stream on the evaporator side while rejecting heat to a fluid on the condenser side. Then, this device can be employed to cool or heat an area of a building depending on if in the building is located the evaporator or the condenser. Normally the pump works by exploiting the physical properties of an evaporating and condensing fluid known as refrigerant.

The operation circle in the heat pump is as follows. The refrigerant, in its gaseous state, is pressurized and circulated through the system by a compressor. On the discharge side of the compressor, the now hot and highly pressurized gas is cooled in a heat exchanger, called a condenser, until it condenses into a high pressure, moderate temperature liquid. The condensed

refrigerant then passes through a pressure-lowering device like an expansion valve. This device then passes the low pressure, liquid refrigerant to another heat exchanger, the evaporator where the refrigerant evaporates into a gas via heat absorption. The refrigerant then returns to the compressor and the cycle is repeated.The four components in the vapor compression circle are shown in Figure 2.3

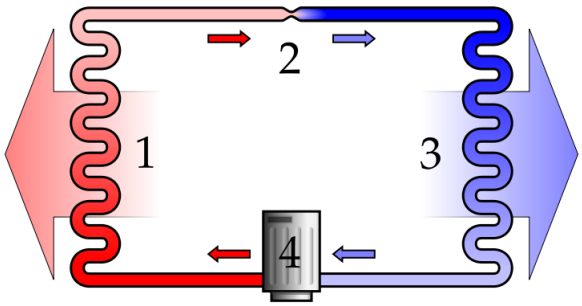

Figure 2.3: Diagram of a heat pump's vapor-compression circle: 1) Condenser, 2) Expansion valve, 3) Evaporator, 4) Compressor.

The efficiency of a heat pump is estimated with the Coefficient of Performance index (COP) which is the ratio between useful energy generated by the heat pump and the work of the compressor. Therefore, the COP for the heat pump in a heating or cooling application is:

$$COP_{heating} = \frac{Q_{heat}}{W_{compressor}} \tag{2.1}$$

$$COP_{cooling} = \frac{Q_{cool}}{W_{compressor}} \tag{2.2}$$

In our particular work two kinds of heat pumps are employed to cool or heat the areas of a building: air to water heat pumps and water to water hear pumps. The air to water heat pump extracts or rejects heat to the outdoor air to heat or cool the water which is pumped to the internal hydraulic circuit of the building. And the water to water heat pump has connected to its external hydraulic circuit a ground heat exchanger which allows extracting or rejecting heat to the ground to heat or cool the water which is pumped to the internal hydraulic circuit of the building.

2.4 Ground heat exchangers

The ground system links the heat pump to the underground and allows extracting of heat from the ground or injecting of heat into the ground. These systems can be classified generally as open or closed systems, with a third category for those not truly belonging to one or the other:

- **Open systems:** Groundwater is used as a heat carrier, and is brought directly to the heat pump. Between rock/soil, ground water, and the heat pump evaporator there is no barrier, hence this type is called 'open'.
- **Closed systems:** Heat exchangers are located in the underground (either in a horizontal, vertical or oblique fashion), and a heat transfer fluid is circulated within the heat exchangers, transporting heat from the ground to the heat pump (or vice versa). The heat carrier is separated from the rock/soil and groundwater by the wall of the heat exchanger, making it a 'closed' system.
- **Other systems:** Not always the system can be attributed exactly to one of the above categories, e.g., if there is a certain distinction between groundwater and the heat carrier fluid, but no true barrier. Standing column wells, mine water or tunnel water are examples for this category.

To choose the right system for a specific installation, several factors have to be considered: geology and hydrogeology of the underground (sufficient permeability is a must for open systems), area and utilization on the surface (horizontal closed systems require a minimum area), existence of potential heat sources like mines, and the heating and cooling characteristics of the buildings. In the design phase, accurate data are necessary to size the ground system in such a way that optimum performance is achieved with minimum cost.

2.4.1 Open-loop systems

Open-loop systems consist primarily of extraction wells, extraction and reinjection wells, or surface water systems (see figure 2.4). This system reinjects the majority of the return water back into the source well, minimising the need for a reinjection well and the amount of surface discharge water. There are several special factors to consider in open-loop systems. First, it is water quality. In open-loop systems, the primary heat exchanger between the refrigerant and the groundwater is subject to fouling, corrosion, and blockage.

Second, it is the adequacy of available water because the necessary amount of water is high and can be affected by local water resource regulations. And third, it is what to do with the discharge stream. The groundwater must either be reinjected into the ground by separate wells or discharged to a surface system such as a river or lake. Local codes and regulations may affect the feasibility of open-loop systems.

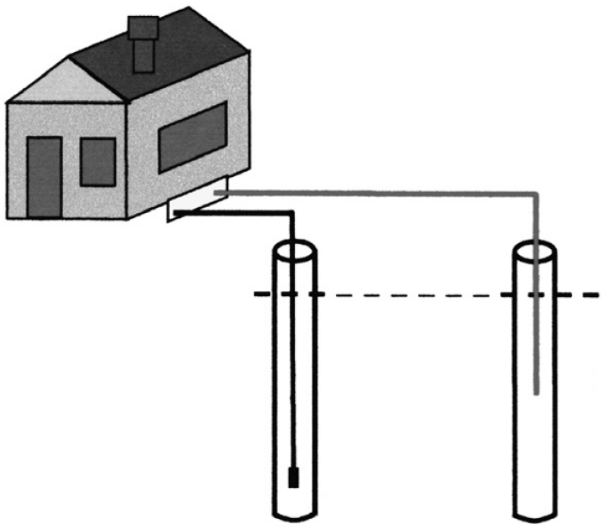

Figure 2.4: Open-loop ground heat exchanger.

Depending on the well configuration, open-loop systems can have the highest pumping load requirements of any of the ground-coupled configurations. In ideal conditions, however, an open-loop application can be the most economical type of ground-coupling system.

2.4.2 Closed-loop systems

In this case heat exchangers are located underground, either in horizontal, vertical or oblique position, and a heat transfer fluid is circulated within the heat exchanger, transferring the heat from the ground to a heat pump or vice versa.

Horizontal-loop systems

This configuration is usually the most cost-effective when adequate yard space is available and trenches are easy to dig. The trenchers have a depth

of 1-2 m in the ground and usually a series of parallel plastic pipes is used (see figures 2.5 and 2.6). Fluid runs through the pipes in a closed system. Horizontal ground loops are the easiest to install while a building is under construction. However, new types of digging equipment allow horizontal boring and thus it is possible to retrofit such systems into existing houses with minimal disturbance of the topsoil and even allow loops to be installed under existing buildings or driveways.

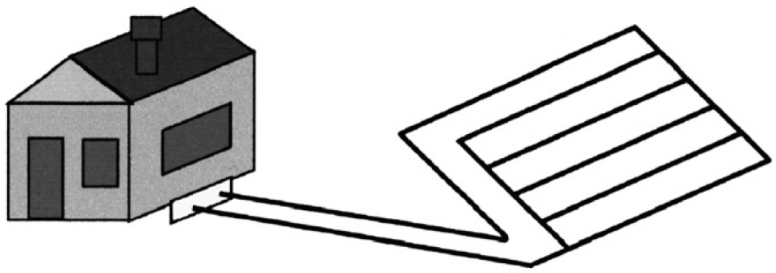

Figure 2.5: Horizontal-type ground heat exchangers connection in parallel.

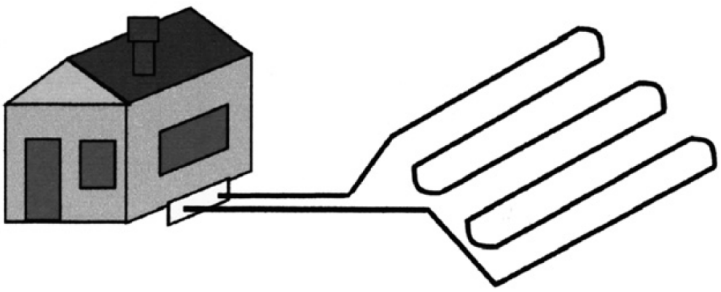

Figure 2.6: Horizontal-type ground heat exchangers connection in series.

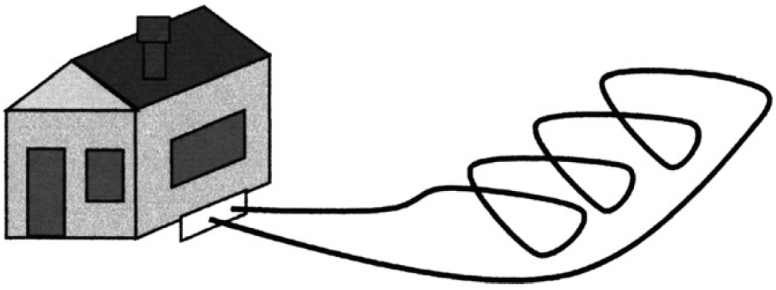

Figure 2.7: Slinky-type ground heat exchanger..

Some special ground heat exchangers have been developed for heat pump systems, in which the pipe is curled into a slinky shape (see figure 2.7). In this way, it is possible to place more pipes into shorter trenches in order to reduce the amount of land space needed. These collectors are best suited for heating and cooling in places where natural temperature recharge of the ground is not vital.

Vertical-loop systems

Vertical ground heat exchangers or borehole heat exchangers are widely used when there is a need to install sufficient heat exchange capacity under a confined surface area such as when the earth is rocky close to the surface, or where minimum disruption of the landscape is desired (see figure 2.8). This is possible because the temperature below a certain depth remains constant over the year. In a standard borehole, which in typical applications is 50-150 meters deep, plastic pipes are installed, and the space between the pipe and the hole is filled with an appropriate material to ensure good contact between the pipe and the undisturbed ground and reduce the thermal resistance.

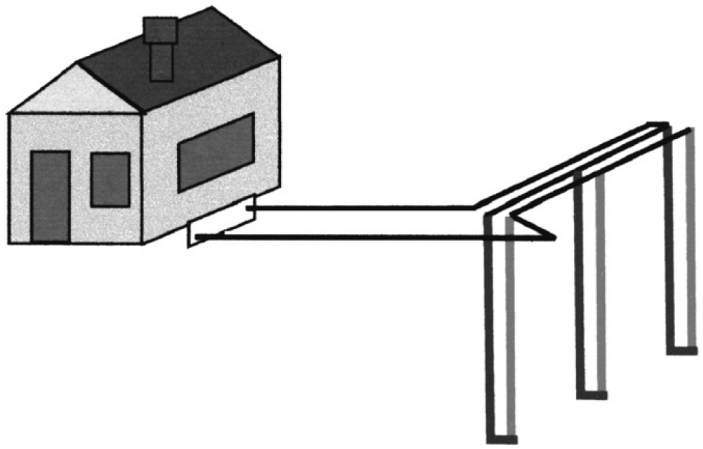

Figure 2.8: Vertical ground heat exchangers.

Vertical loops are generally more expensive to install, but require less piping than horizontal loops because the earth deeper down is cooler in summer and warmer in winter, compared to the ambient air temperature.

2.5 Examples of the GCHP systems

In this section we present several actual examples of office or public buildings located in the Mediterranean area (cooling dominated areas) which employ air conditioning systems driven by ground coupled heat pumps, [66]. We consider these examples represent well the kind of situations where the different energy management strategies developed in this thesis could be applied. Finally, for each installation a brief description of them and several comments about their energy efficiency are included.

Office building of Universidad Politécnica de Valencia

The building is located in Valencia city in Spain (see figure 2.9). The total area comprises 250 m^2 which includes a corridor, nine offices, a computer room, and a chamber with photocopiers and a coffee dispenser. The ground heat exchanger of this installation is composed by six U-tube vertical boreholes of fifty meters depth placed in parallel and the water to water heat pump has the particularity that employs propane as refrigerant with nominal capacities of 19.3 KW and 15.9 KW in heating and cooling mode respectively.

Figure 2.9: Office building of Universidad Politécnica Valencia.

In this installation was also included a conventional air to water heat pump system in order to compare the electrical energy consumption of both systems. The obtained results showed that geothermal system saved in terms of primary energy around 41% during the heating season and a 38% during the cooling season with respect to the conventional system. Finally, the

seasonal performance factor for the geothermal system was 3.46 and 4.36 in heating mode and cooling mode respectively.

Office building of 'Caisse Allocations Familiales' of Lyon city

The building is located in the centre of Lyon city which is located in the south part of France where the climatology is relatively warm. This building was built in 1997 and it has an area of 16.633 m^2 and six floors (see figure 2.10). The GCHP system is composed by two water to water heat pumps with a total thermal capacity of 600 KW. The ground heat exchanger is an open-loop system which uses two water pumps of 100 $m^3/hour$ in order to extract water from an aquifer.

Figure 2.10: Office building of CAF de Lyon.

An energy efficiency study was done in this installation. To do it, measures of the thermal energy generated and the electrical consumption were done from 1998 to 2006. The results show that the electrical energy consumption of the air conditioning system was around 67.6 KWh/m^2 per year where the 53.9% was from the heat pumps, the 27.8% was from the water pumps and 18.3% was from the ventilation system. And the annual performance factor of the GCHP system obtained during this period was 3.83.

Town hall of Pylaia

The Town hall of Pylaia is located in Thessaloniki city in Greece with a total area of 2500 m^2 (see figure 2.11). This building was built in 2001 and the GCHP system was installed in 2002. The system employs eleven geothermal heat pumps in order to cover totally the thermal demands. And the ground heat exchanger is composed by 21 boreholes of 80 meters depth.

During 2003 several measures where done in this GCHP system which showed that the seasonal performance factors of the heat pump where 4 and 3.5 in heating and cooling mode respectively.

Figure 2.11: Town hall of Pylaia.

Office building of National Technical University of Athens

The office building of total area 6.000 m^2 is situated in Zografou, Athens. The office building was built in two phases: the first wing during the years 1986-1990 and the second wing during the years 1995-1999. The geothermal

Figure 2.12: Office building of National Technical University of Athens (CRES).

system was installed in the second wing during 1999-2000 in order to cover

totally its load in heating mode or cooling mode.

In this project two ground source heat pump were installed. The first heat pump (328 kW_{th} - 291 kW_c) uses ground water from a well and the second one (198 kW_{th} - 170 kW_c) uses ground water from a well as well as a borehole heat exchanger.

Chapter 3

Efficiency improvement of ground coupled heat pumps when combined with air source heat pump and thermal storage

3.1 Introduction

Ground coupled heat pumps are an attractive solution for cooling and heating commercial buildings due to their higher efficiency compared with the conventional air to water heat pump. Nevertheless, we can develop management strategies to improve the efficiency of these systems by combining it with other generation systems. For example, the energy efficiency of an air to water heat pump depends on the environmental conditions and, therefore, there are specific situations in which its efficiency is comparable with the efficiency of the ground source system. Hence, a suitable combination of both generation systems could produce a new one with a performance better than each one working independently.

Another way to improve the energy efficiency of the system could be decoupling energy generation from energy distribution through of a thermal storage device. This possibility gives us two important advantages. First, the thermal energy demanded can be generated with a generation device with a lower thermal capacity than in the systems where the thermal load is only satisfied directly by the generator system. And second, it is possible to minimize the effects of the thermal load peaks generating the thermal energy when the environmental conditions are more favorable.

In this chapter, we evaluate the improvement in the energy efficiency

when these two ideas are applied in an air conditioning system in a cooling dominated building in the Mediterranean area. To do it, several air conditioning layouts which combine a ground coupled heat pump, an air to water heat pump and a thermal storage device are developed and linked to a cooling dominated building. Because in this conditions the energy demand in the cooling mode is much higher than in the heating mode, this air conditioning layouts are designed to improve the energy efficiency during this period.

Our study is focused in the Mediterranean area, for this reason a subdivision of the South of Europe into climatic areas has been done in order to identify the different Mediterranean climatic areas, [67]. Following this subdivision we have chosen the weather of the cities of Athens (climatic area type 3C), Rome (climatic area type 4C) and Valencia (climatic area type 5C) as representatives. Finally, the thermal comfort criteria employed to obtain the thermal load in the modeled office building is the Predicted Mean Vote index (PMV). This comfort index predicts the mean value of votes of a large group of people in the Thermal Sensation Scale and it is defined by the ISO7730-1994 standard, [68].

The procedure to evaluate the energy efficiency when implementing these ideas is as follows. First, we evaluate the electrical energy consumptions of the air conditioning system when is driven only by an air to water heat pump or a ground coupled heat pump. These values are used as a reference for comparison with the consumptions of the implemented layouts. Second, we present an air conditioning configuration composed by a ground coupled heat pump which is supported by an air to water heat pump to study the behaviour of the combination of both systems. Third, we combine a thermal storage device with a ground coupled heat pump or with an air to water heat pump to study the behaviour when is decoupled energy generation from energy distribution. Finally, we present three hybrid configurations (HA, HB and HC) which combine the three elements in different layouts. In HA configuration, we use the air to water heat pump during the night to cool the thermal storage device. During the day, the thermal storage device and the ground coupled heat pump are the elements which cool the thermal load. In HB configuration, during the night the air to water heat pump cools the thermal storage as in HA configuration. During the day, the thermal storage device and the ground coupled heat pump cool the thermal load and the air to water heat pump supports them when is needed. Finally, HC configuration works as HB configuration but the ground coupled heat pump is the element which cools the thermal storage device during the night. Therefore, the air to water heat pump only supports the thermal storage device and the

ground coupled heat pump in the peaks of the thermal load.

For the three climatic areas, the electrical energy consumptions for each device are calculated in the different configurations and an evaluation of the energy efficiency is presented. We analyze the advantages and disadvantages of each configuration to define the factors which allow deciding which one is the most appropriate. We also include the cost assessment for the air conditioning configurations. Finally, the model and the evaluation of this study has been done with TRNSYS which is a specific package software for this kind of systems, [64].

This chapter is structured as follows. First two sections describe the PMV index and the simulated office building to define the thermal load which has to be satisfied by the different air conditioning configurations in the three climatic areas. Afterwards, we present the air conditioning system configurations and the energy model of the air conditioning devices.

Finally, we present and discuss the results obtained in our simulations from the energy efficiency point of view and also from the economic cost point of view.

3.2 Comfort criteria

We choose the Predicted Mean Vote (PMV) index to evaluate the comfort in our simulation. This index is the criteria to estimate the comfort state proposed by the ISO7730-1994 standard and predicts the mean value of the votes of a large group of persons on the seven point Thermal Sensation Scale (see appendix C).

The PMV index for the air conditioning system is calculated in the simulation at each time step. To do it, three parameters, activity, thermal resistance of clothing and mean air velocity have to be estimated. We follow ISO7730-1994 recommendations for this purpose. The value for the activity parameter is 1.2 met for moderated office activity. The thermal resistance of clothing is 1.0 clo, when the considered working clothes are shirts, trousers, jackets, and shoes. Finally, the value for the mean air velocity is estimated in 0.1 m/s. The other three parameters, air temperature, mean radiant temperature and partial water vapour pressure are computed at each time step.

3.3 Simulated office area

The model of the office building adopted for this study features three floors with a length of 30 m, a width of 20 m and a height of 3 m with eight thermal zones per floor (see figure 3.1). Thus, each floor has an area of 600 m^2 and the entire building 1800 m^2 with a total of 32 thermal zones.

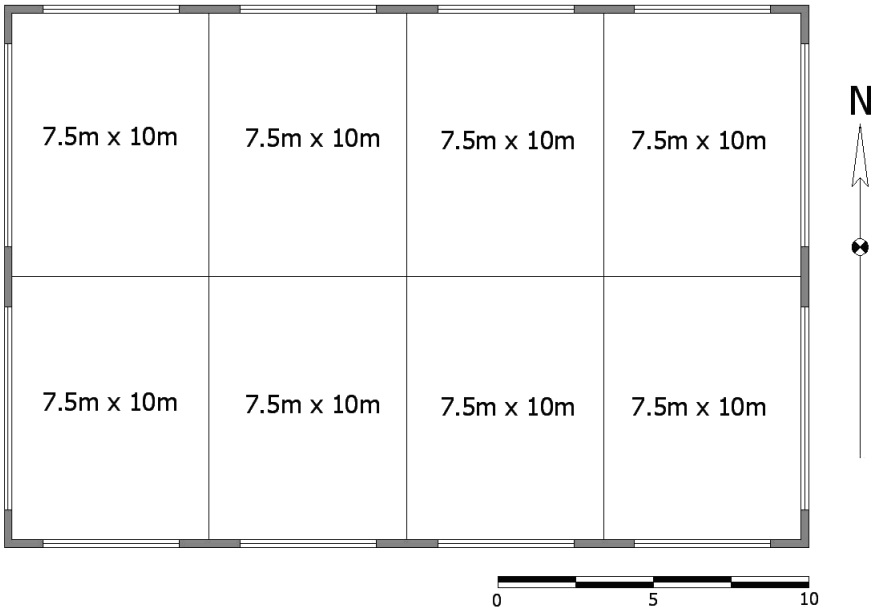

Figure 3.1: Layout of the windows and thermal zones in a floor of the office building.

External walls are defined as ventilated façades composed by four elements: perforated brick, 5 cm of insulation, air chamber and a Naturex plate cover; its global heat transfer coefficient is 0.51 W/m^2K. The window fraction is approximately 22% in each façade; the windows are composed by a glass, with solar radiation transmissivity equal to 0.837 and conductivity equal to 5.74 W/m^2K, dedicating a 15% of this area to the frame surface with a heat transfer coefficient equal to 0.588 W/m^2K. The internal and external shadow factor for these windows is estimated in 0.7.

The peak building occupancy is 11 $m^2/person$. Each office worker contributes 132 W of internal gain, where 54% are assumed to be sensible and 46% latent and the peak lighting density is 20 W/m^2. The occupancy and

the lighting schedules for a day are shown in figure 3.2.

We want to mention that the design of the office building satisfies the standard for the thermal conditions in buildings which is reflected in the NBE-CT-79 for the climatic area of the Spanish coast, [69]. For this reason, we have considered that this office building can be used as standard in the Mediterranean area.

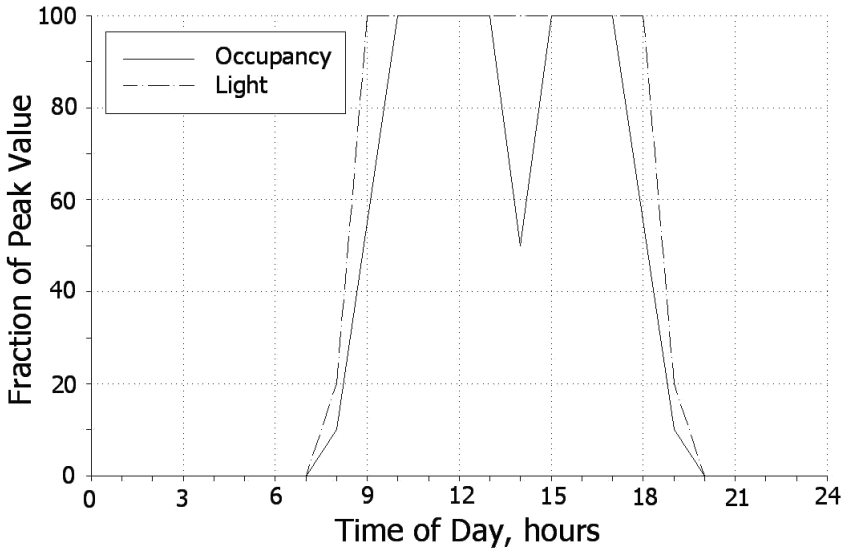

Figure 3.2: Occupancy and lighting schedule.

All these parameters are included throughout the TRNBuild tool specifically designed to simulate the thermal behaviour in a multi-zone building area. A subdivision of the South of Europe into climatic areas has been done in order to identify the different Mediterranean climatic areas, [67]. Following this subdivision we have chosen the weather of the cities of Athens (climatic area type 3C), Rome (climatic area type 4C) and Valencia (climatic area type 5C) as representatives to cover all the Mediterranean climatic areas. Finally, we consider that the heating season is from January to March and from November to December, and the cooling season is from April to October.

Figure 3.3 shows the daily heating load provided to the thermal load in the heating season and the daily heating load extracted to the thermal load in the cooling season which satisfies the neutral thermal comfort conditions, PMV equal to zero, in the office building for the three climatic areas. In the simulation conditions, the weather database employed models the Mediterranean

weather, which is characterized to have hot summers and warm winters and the occupancy period coincides when the external ambient temperature and the solar radiation are the highest during the day. The combination of these two factors with the internal thermal loads due to the occupancy and the lighting density produce that the thermal energy demand in cooling mode is much higher than in heating mode. These obtained thermal loads for the three climatic areas are consistent with the thermal studies for several standard buildings in the Mediterranean area presented in the reports of the European Project Geocool, [67]. Finally, the oscillations of the daily thermal load are due to the variation of the daily external ambient temperature of the weather database. Notice the decreasing trend of the daily heating load when we approach to the cooling season.

3.4 Air conditioning configurations

In this subsection, we present the different air conditioning configurations linked to the office building and the energy models of the employed devices. As we mention previously, we evaluate the electrical energy consumption and the energy efficiency of several air conditioning layouts in a cooling dominated building. The different air conditioning configurations combine properly the following elements: a ground coupled heat pump, an air to water heat pump and a thermal storage device.

The developed air conditioning configurations are oriented to improve the energy efficiency during the cooling season because in our particular cooling dominated building the thermal load is much higher during this period than during the heating season. These configurations are designed to evaluate the improving of the thermal efficiency during the cooling season following two ideas: first one, decoupling energy generation from energy distribution using a thermal storage device and second one, combining properly the ground coupled heat pump and the air to water heat pump. During the heating season the thermal load can be satisfied directly by the principal generator device of the air conditioning configurations. This is because this element is designed for cooling season and, in our particular case, it has enough thermal capacity to satisfy the low thermal load in the heating season.

The studied air conditioning system layouts are the following ones. First, we study the air conditioning system when is only composed by an air to water heat pump or a ground coupled heat pump. These systems are used as reference to evaluate the efficiency improvement achieved by the other air

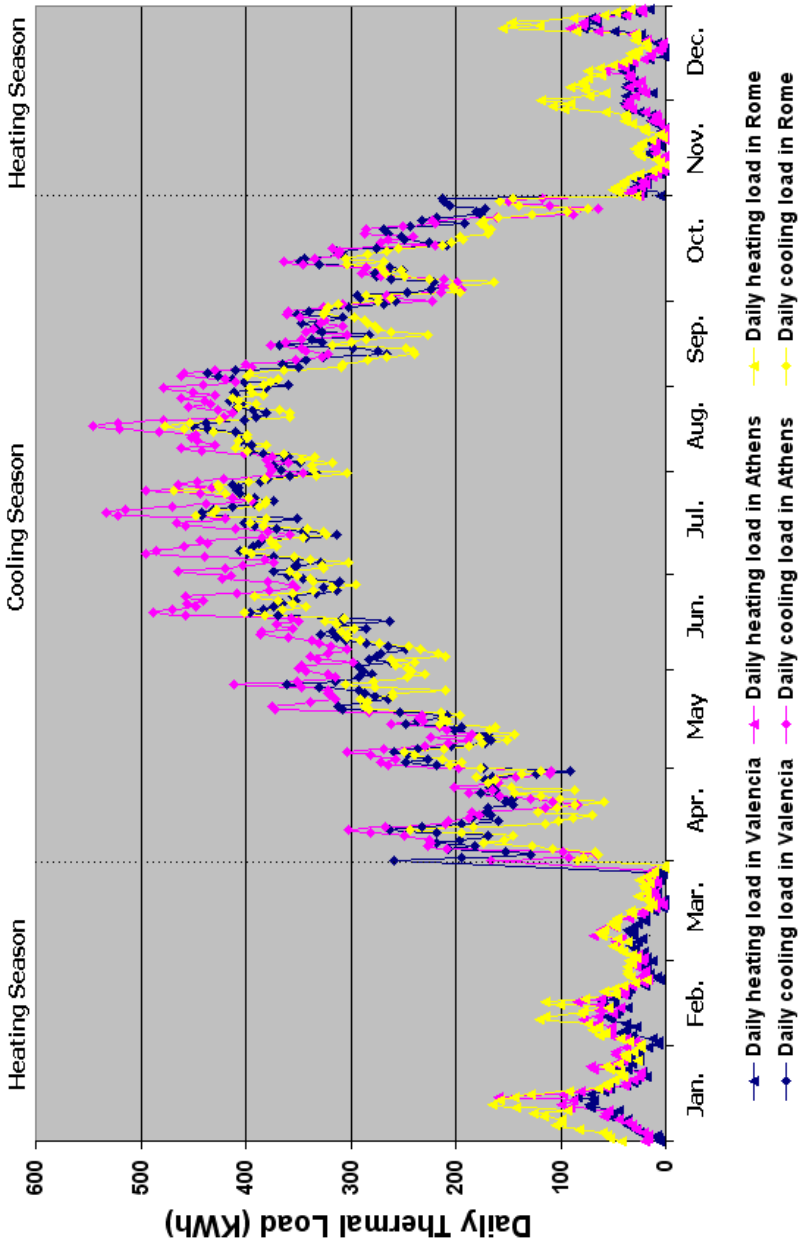

Figure 3.3: Daily heating load provided to the thermal load in the heating season and daily cooling load extracted to the thermal load in the cooling season for the three climatic areas: Athens, Rome and Valencia.

conditioning configurations. Second, we study the air conditioning system composed by a ground coupled heat pump supported by an air to water heat pump in the peaks of the thermal load. This configuration is analysed to evaluate the effect produced by the combination of both generation systems. Third, we study the combination of a thermal storage device with a ground coupled heat pump or with an air to water heat pump. This case is thought to analyse the effect of decoupling energy generation from energy distribution. And finally, we present three hybrid configurations which combine properly the three elements: ground coupled heat pump, air to water heat pump and the thermal storage device.

3.4.1 Air conditioning strategies in the cooling season

Air to water heat pump configuration ('Air')

The air conditioning system is composed by an air to water heat pump (AWHP), an internal water pump (IWP) and air fan (AF) (see figure 3.4). The internal water pump transports the generated cooled water in the evaporator of the air to water heat pump to the thermal load and the air fan is used to dispel the rejected heat in the condenser to the air outside the office building. In this configuration the cooled water only is generated and supplied by the air to water heat pump in the instant when is demanded by the building.

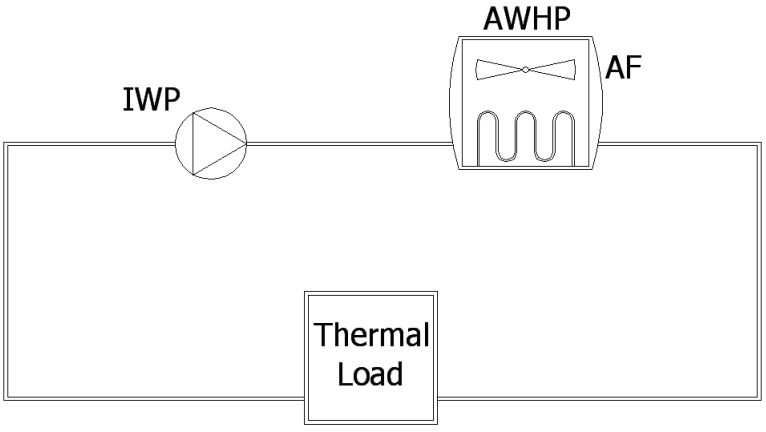

Figure 3.4: Air to water heat pump configuration, 'Air'.

Ground coupled heat pump configuration ('GCHP')

The air conditioning system is composed by a water to water heat pump (WWHP), a ground heat exchanger (GHE) and an internal and an external water pump (IWP, EWP). This configuration is shown in figure 3.5. The external water pump is used to pump water through the ground heat exchange to dispel the rejected heat in the condenser of the water to water heat pump. The internal water pump transports the generated cooled water in the evaporator of the water to water heat pump to the thermal load. In this configuration the cooled water only is generated and supplied by the ground coupled heat pump in the instant when is demanded by the building.

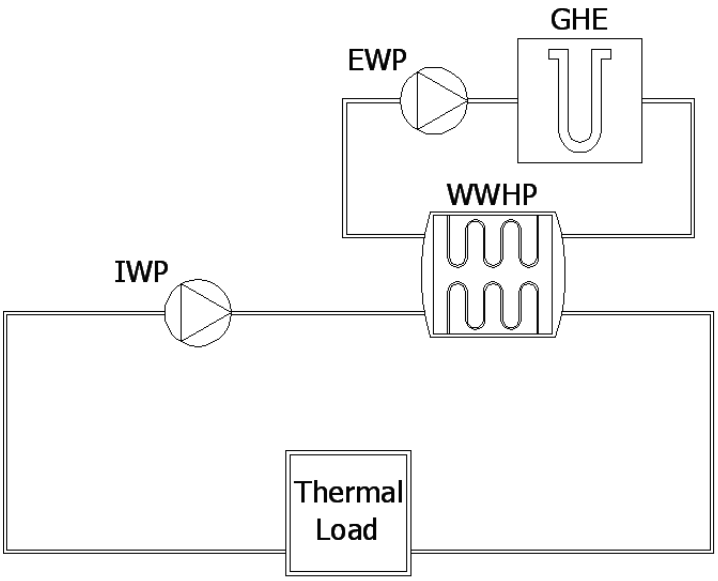

Figure 3.5: Ground coupled heat pump configuration, 'GCHP'.

Ground coupled heat pump and air to water heat pump configuration ('GCHP + Air': GAI, GAII, GAIII and GAIV)

This configuration combines the two generation systems: a ground coupled heat pump and an air to water heat pump (see figure 3.6). The cooled water is supplied directly to the thermal load and the ground coupled heat pump is the principal generator system because its coefficient of performance is the highest of both. Therefore, in the first instant the ground coupled heat pump tries to satisfy directly the thermal load. If this element has not enough capacity, the air to water heat pump is switched on and supports to the ground coupled heat pump increasing the cooling capacity of the air conditioning configuration.

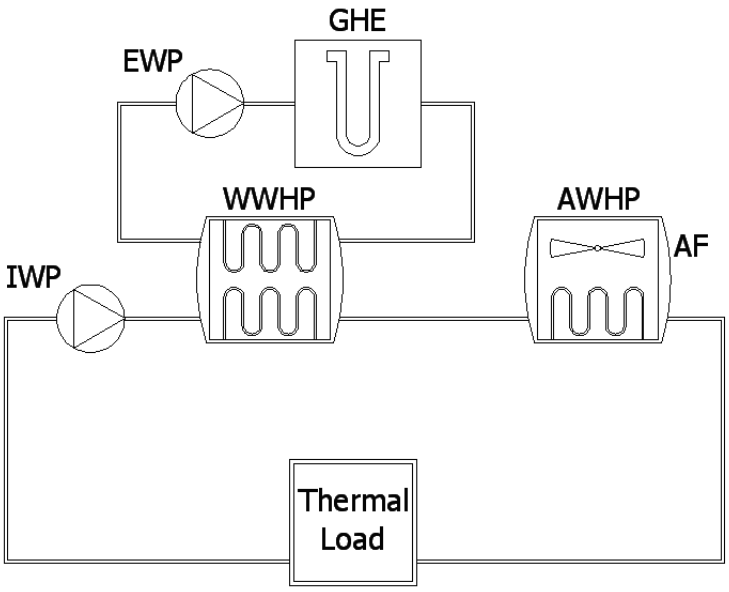

Figure 3.6: Ground coupled heat pump with air to water heat pump configuration, 'GCHP + Air': GAI, GAII, GAIII and GAIV.

Air to water heat pump with thermal storage device configuration ('Air + S')

This air conditioning system is similar to the 'Air' configuration but it is incorporated a thermal storage device (TSD). This configuration is shown in figure 3.7. A period during the night, the air to water heat pump, the internal water pump and the air fan are switched on to cool the thermal storage device. The difference of the temperature between the evaporator and the condenser is less during the night. As a consequence, the air to water heat pump electrical energy consumption needed to produce a given quantity of cooled water is lower during the night.

In first instance, the thermal load in the office building is satisfied by the cool water previously stored during the night. If the thermal storage device has not enough capacity, this element is supported by the air to water heat pump until completing the thermal load. Finally, the thermal storage device is by-passed when the water outlet temperature of this device is higher than its water inlet temperature and, from this instant, only the air to water heat pump satisfies the thermal load. Notice that the internal water pump is the element which pumps the water through the hydraulic circuit and the air fan

is only connected when the air to water heat pump is switched on.

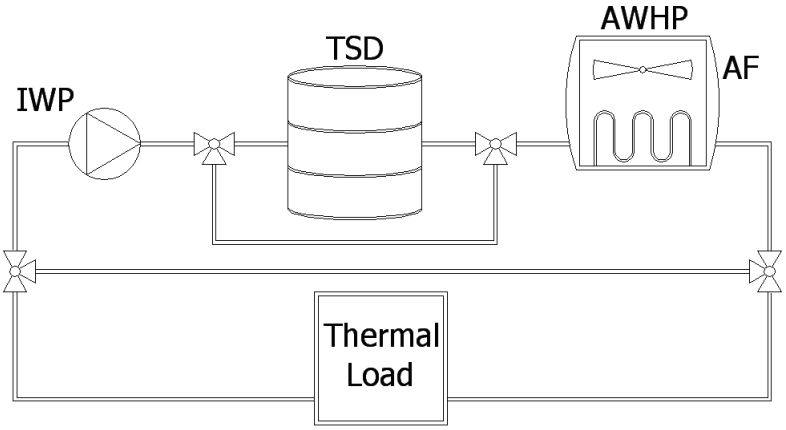

Figure 3.7: Air to water heat pump with thermal storage device configuration, 'Air + S'.

Ground coupled heat pump with thermal storage device configuration ('GCHP + S')

This air conditioning system is similar to the 'Air + S' configuration but the air to water heat pump is replaced by a water to water heat pump with a ground heat exchanger (see figure 3.8).

During a period in the night the water to water heat pump and the internal and external water pumps are switched on to cool the thermal storage device. Afterwards, during the occupancy of the office building, the thermal load is satisfied by the thermal storage device and therefore the internal water pump is switched on. When this element has not enough capacity, the water to water heat pump and external water pump are switched on to support the thermal storage device. In the moment when the water outlet temperature of the thermal storage device is higher than its water inlet temperature, this element is by-passed and only the ground coupled heat pump can cool the thermal load. Notice that the external water pump is only switched on when the water to water heat pump is connected.

Hybrid configuration type A ('HA': HAI, HAII, HAIII and HAIV)

In this air conditioning configuration the three elements are combined: the ground coupled heat pump, the air to water heat pump and the thermal

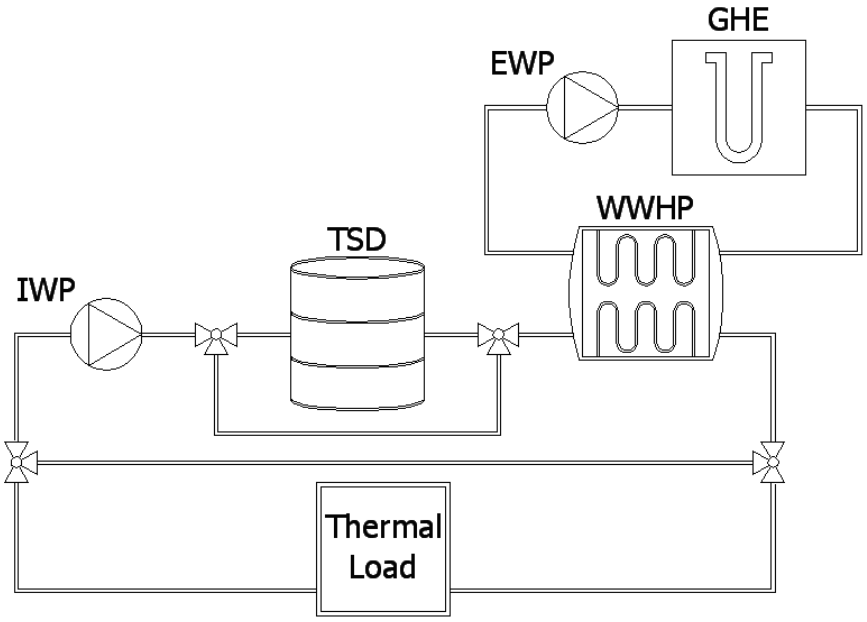

Figure 3.8: Ground coupled heat pump with thermal storage device configuration, 'GCHP + S'.

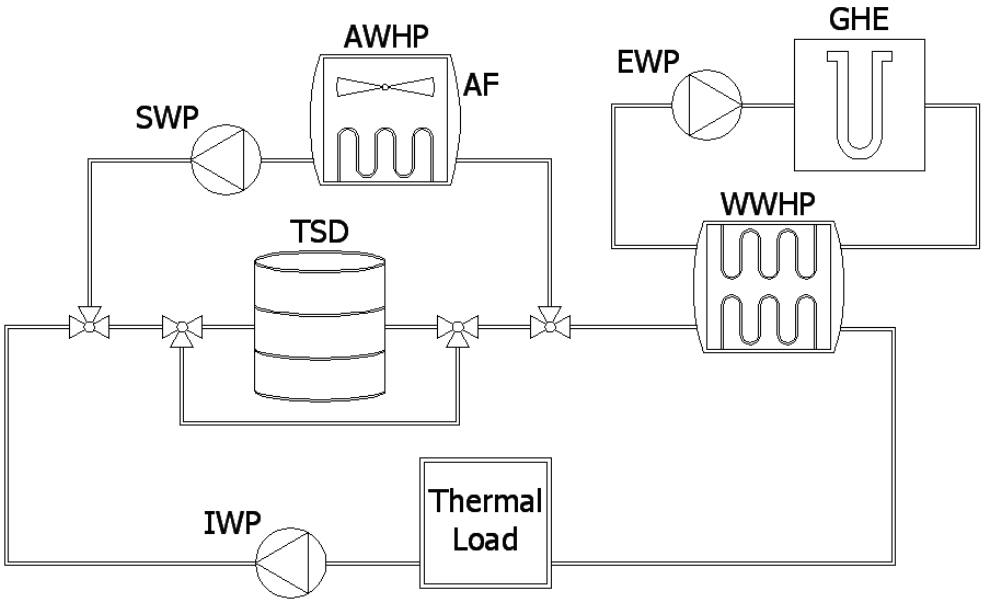

Figure 3.9: Hybrid configuration type A, 'HA': HAI, HAII, HAIII and HAIV.

storage device (see figure 3.9). The idea behind this configuration is based on the fact that the environmental air temperature is lower than the ground temperature during the night, so in this period the air is a better sink than the ground.

The strategy implemented in this air conditioning configuration is as follows. The air to water heat pump, the air fan and the storage water pump (SWP) are switched on to cool the thermal storage device during a period in the night. During the day these elements are switched off and the water to water heat pump, the internal and external water pumps and the thermal storage device work following the same procedure presented in 'GCHP + S'.

Hybrid configuration type B ('HB': HBI, HBII and HBIII)

This configuration is similar to the previous one, but the air to water heat pump is also used to satisfy directly the thermal load (see figure 3.10). The air to water heat pump has to support to the other two equipments when the peaks of the thermal load are exceptionally high. As a consequence, we can reduce the thermal capacity of the water to water heat pump which is installed.

In this strategy, the air to water heat pump is used to cool the thermal storage device during a period in the night. During the day this element tries to satisfy the thermal load. If the thermal storage device has not enough capacity, the water to water heat pump and the external water pump are switched on to support it. If these two elements are still not enough, the air to water heat pump and the air fan are switched on, and both generation systems with the thermal storage device cool the thermal load. Finally, the thermal storage device is by-passed when its water outlet temperature is higher than its water inlet temperature and, from this instant, only the ground coupled heat pump and the air to water heat pump can satisfy the thermal load.

Hybrid configuration type C ('HC': HCI, HCII and HCIII)

This configuration is similar to the hybrid configuration type B but the ground coupled heat pump cools the thermal storage device during a period in the night (see figure 3.11). Therefore, the air to water heat pump and the air fan only are switched on when the peaks of the thermal load are

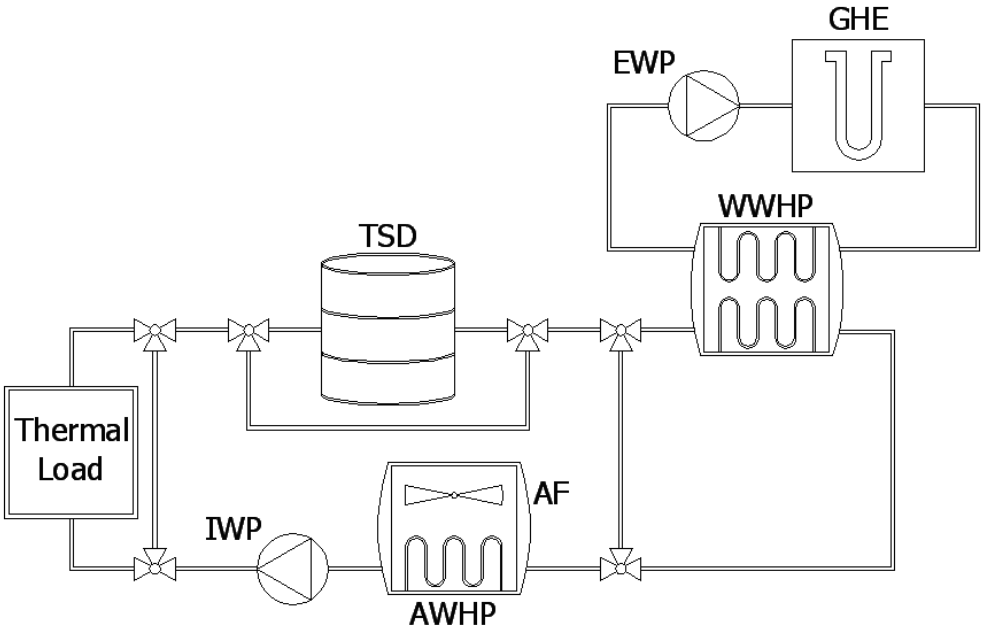

Figure 3.10: Hybrid configuration type B, 'HB': HBI, HBII and HBIII.

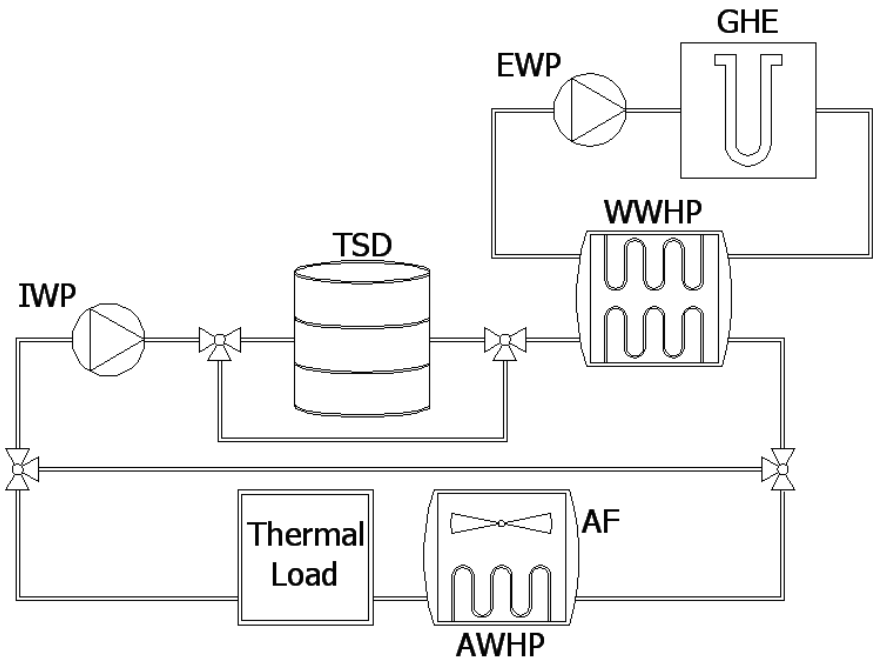

Figure 3.11: Hybrid configuration type C, 'HC': HCI, HCII and HCIII.

exceptionally high.

3.4.2 Air conditioning configuration designs

The choice of the parameters for each air conditioning configuration has been done considering the following features of the heat pump in cooling mode, [70]:

- The nominal COP for the water to water heat pump is 4.5
- The nominal COP for the air to water heat pump is 2.5
- The cooling water inlet temperature to the thermal load has to be 7°C.
- The thermal storage device supplies the 40% of the thermal energy.

Table 3.1, table 3.2 and table 3.3 show the values of these parameters for the climatic areas of Athens, Rome and Valencia respectively. For each configuration it is include the nominal cooling capacity of the water to water heat pump (P_{WWHP}), the nominal cooling capacity of the air to water heat pump (P_{AWHP}), the air fan power consumption (P_{AF}), the air volume flow ($\dot{m}_{AF}$), the external water pump power consumption (P_{EWP}), the water mass flow in the external circuit ($\dot{m}_{EWP}$), the internal water pump power consumption (P_{IWP}), the water mass flow in the internal circuit ($\dot{m}_{IWP}$), the storage water pump power consumption (P_{SWP}), the water mass flow in the storage circuit ($\dot{m}_{EWP}$), the number of boreholes ($N.B.$), the size of the thermal storage device (TSD) and the period in which the thermal storage device is storing thermal energy (t_{stor}).

3.5 Energy model of the air conditioning devices

The following paragraphs detail the model describing the behaviour of the components employed in the simulations. We also derive the way to compute the electrical power consumption of each one for given conditions.

Ground Heat Exchanger (GHE). The objective of the ground heat exchanger is to interchange heat with the ground. A heat carrier fluid is circulated through the ground heat exchanger and either rejects heat to, or absorbs heat from the ground depending on the temperatures of the heat carrier fluid and the ground. In typical U-tube ground heat exchanger applications, a vertical borehole is drilled into the ground. A U-tube heat

	P_{WWHP} (KW)	P_{AWHP} (KW)	P_{AF} (KW)	$\dot{m}_{AF}$ (m^3/h)	P_{EWP} (KW)	$\dot{m}_{EWP}$ (Kg/h)	P_{IWP} (KW)	$\dot{m}_{IWP}$ (Kg/h)	P_{SWP} (KW)	$\dot{m}_{SWP}$ (Kg/h)	$N.B.$	TSD (m^3)	t_{stor}
Air-A	——	52.0	5.0	21000	——	——	1.91	10500	——	——	——	——	——
GCHP-A	52.0	——	——-	——	0.92	10500	1.91	10500	——	——	15	——	——
GAI-A	47.0	5.0	0.25	2100	0.87	9500	1.77	9500	——	——	15	——	——
GAII-A	42.0	10.0	0.75	4100	0.83	8500	1.63	8500	——	——	14	——	——
GAIII-A	37.0	15.0	1.25	6000	0.78	7500	1.5	7500	——	——	14	——	——
GAIV-A	32.0	20.0	1.75	8000	0.74	6500	1.35	6500	——	——	12	——	——
Air+S-A	——	37.0	3.47	14800	——	——	1.50	7500	——	——	——	55	1h-6h
GCHP+S-A	37.0	——	——	——	0.78	7500	1.50	7500	——	——	10	55	1h-6h
HAI-A	37.0	37.0	3.47	14800	0.78	7500	1.50	7500	0.78	7500	9	55	1h-6h
HAII-A	37.0	32.0	2.97	12800	0.78	7500	1.50	7500	0.74	6500	9	55	0h-6h
HAIII-A	37.0	27.0	2.46	10800	0.78	7500	1.50	7500	0.70	5500	9	55	23h-6h
HAIV-A	37.0	22.0	1.96	8800	0.78	7500	1.50	7500	0.66	4500	9	55	22h-6h
HBI-A	32.0	32.0	2.97	12800	0.74	6500	1.35	6500	——	——	9	40	0h-6h
HBII-A	27.0	27.0	2.46	10800	0.70	5500	1.21	5500	——	——	9	32	23h-6h
HBIII-A	22.0	22.0	1.96	8800	0.66	4500	1.07	4500	——	——	8	26	22h-6h
HCI-A	32.0	6.0	0.35	2600	0.74	6500	1.35	6500	——	——	10	40	0h-6h
HCII-A	27.0	11.0	0.85	4500	0.70	5500	1.21	5500	——	——	9	32	23h-6h
HCIII-A	22.0	16.0	1.35	6500	0.66	4500	1.07	4500	——	——	8	26	22h-6h

Table 3.1: Parameters of the different devices for the air conditioning configurations in Athens

	P_{WWHP} (KW)	P_{AWHP} (KW)	P_{AF} (KW)	$\dot{m}_{AF}$ (m^3/h)	P_{EWP} (KW)	$\dot{m}_{EWP}$ (Kg/h)	P_{IWP} (KW)	$\dot{m}_{IWP}$ (Kg/h)	P_{SWP} (KW)	$\dot{m}_{SWP}$ (Kg/h)	$N.B.$	TSD (m^3)	t_{stor}
Air-R	——	45.0	4.30	18000	——	——	1.70	9000	——	——	——	——	——
GCHP-R	45.0	——	——	——	0.85	9000	1.70	9000	——	——	13	——	——
GAI-R	39.7	6.0	0.35	2600	0.805	8000	1.56	8000	——	——	13	——	——
GAII-R	35.0	10.0	0.74	4100	0.76	7000	1.42	7000	——	——	12	——	——
GAIII-R	29.6	15.5	1.30	6200	0.715	6000	1.28	6000	——	——	12	——	——
GAIV-R	24.6	20.5	1.80	8300	0.67	5000	1.14	5000	——	——	10	——	——
Air+S-R	——	35.0	3.27	14000	——	——	1.42	7000	——	——	——	45	1h-6h
GCHP+S-R	35.0	——	——	——	0.76	7000	1.42	7000	——	——	9	45	1h-6h
HAI-R	35.0	35.0	3.27	14000	0.76	7000	1.42	7000	0.76	7000	8	45	1h-6h
HAII-R	35.0	29.6	2.72	11800	0.76	7000	1.42	7000	0.715	6000	8	45	0h-6h
HAIII-R	35.0	24.5	2.21	10000	0.76	7000	1.42	7000	0.67	5000	8	45	23h-6h
HAIV-R	35.0	19.4	1.70	7800	0.76	7000	1.42	7000	0.63	4000	8	45	22h-6h
HBI-R	29.6	29.6	2.72	11800	0.715	6000	1.28	6000	——	——	8	35	0h-6h
HBII-R	24.6	24.6	2.21	10000	0.67	5000	1.14	5000	——	——	8	28	23h-6h
HBIII-R	19.4	19.4	1.70	7800	0.63	4000	1.00	4000	——	——	7	22	22h-6h
HCI-R	29.6	6.0	0.35	2600	0.715	6000	1.28	6000	——	——	9	35	0h-6h
HCII-R	24.6	9.0	0.65	3700	0.67	5000	1.14	5000	——	——	8	28	23h-6h
HCIII-R	19.4	14.3	1.18	5800	0.63	4000	1.00	4000	——	——	7	22	22h-6h

Table 3.2: Parameters of the different devices for the air conditioning configurations in Rome

	P_{WWHP} (KW)	P_{AWHP} (KW)	P_{AF} (KW)	$\dot{m}_{AF}$ (m^3/h)	P_{EWP} (KW)	$\dot{m}_{EWP}$ (Kg/h)	P_{IWP} (KW)	$\dot{m}_{IWP}$ (Kg/h)	P_{SWP} (KW)	$\dot{m}_{SWP}$ (Kg/h)	$N.B.$	TSD (m^3)	t_{stor}
Air-V	——	45.0	4.30	18000	——	——	1.70	9000	——	——	——	——	——
GCHP-V	45.0	——	——	——	0.85	9000	1.70	9000	——	——	13	——	——
GAI-V	39.7	6.0	0.35	2600	0.805	8000	1.56	8000	——	——	13	——	——
GAII-V	35.0	10.0	0.74	4100	0.76	7000	1.42	7000	——	——	12	——	——
GAIII-V	29.6	15.5	1.30	6200	0.715	6000	1.28	6000	——	——	12	——	——
GAIV-V	24.6	20.5	1.80	8300	0.67	5000	1.14	5000	——	——	10	——	——
Air+S-V	——	35.0	3.27	14000	——	——	1.42	7000	——	——	——	40	1h-6h
GCHP+S-V	35.0	——	——	——	0.76	7000	1.42	7000	——	——	8	40	1h-6h
HAI-V	35.0	35.0	3.27	14000	0.76	7000	1.42	7000	0.76	7000	8	40	1h-6h
HAII-V	35.0	29.6	2.72	11800	0.76	7000	1.42	7000	0.715	6000	8	40	0h-6h
HAIII-V	35.0	24.5	2.21	10000	0.76	7000	1.42	7000	0.67	5000	8	40	23h-6h
HAIV-V	35.0	19.4	1.70	7800	0.76	7000	1.42	7000	0.63	4000	8	40	22h-6h
HBI-V	29.6	29.6	2.72	11800	0.715	6000	1.28	6000	——	——	8	32	0h-6h
HBII-V	24.6	24.6	2.21	10000	0.67	5000	1.14	5000	——	——	7	27	23h-6h
HBIII-V	19.4	19.4	1.70	7800	0.63	4000	1.00	4000	——	——	7	21	22h-6h
HCI-V	29.6	6.0	0.35	2600	0.715	6000	1.28	6000	——	——	8	32	0h-6h
HCII-V	24.6	9.0	0.65	3700	0.67	5000	1.14	5000	——	——	7	27	23h-6h
HCIII-V	19.4	14.3	1.18	5800	0.63	4000	1.00	4000	——	——	7	21	22h-6h

Table 3.3: Parameters of the different devices for the air conditioning configurations in Valencia

exchanger is then pushed into the borehole. The top of the ground heat exchanger is typically several centimetres below the surface of the ground. Finally, the borehole is filled with a fill material. We use 'Duct Ground Heat Storage Model' to simulate our GHE, [21].

We employ the method proposed in [65] to estimate the size of the ground heat exchanger and its length is normalized to boreholes of one hundred meters depth which are linked in parallel. Finally, table 3.4 includes the properties of the soil where the ground heat exchanger is placed and the description parameters for the boreholes, [70].

Parameter	Value
Borehole depth	100 m
Borehole radius	0.1016 m
Ground Heat Capacity	2016 $kJ/m^3/K$
Ground thermal conductivity	2 W/mK
Pipe thermal conductivity	0.42 W/mK
Outer radius of U-tube pipe	0.01664 m
Inner radius of U-tube pipe	0.01372 m
Centre to centre half distance	0.0254 m

Table 3.4: Properties of the soil where is placed the ground heat exchanger and the description parameters for the boreholes.

Water to Water Heat Pump (WWHP). The water to water heat pump is a component which supplies thermal energy to the office area. In cooling mode this device extracts heat from the office building which is dispelled to the ground.

The electrical energy consumption for the heat pump is defined as the following expression:

$$P_{HP_{ww}} = \frac{G_{ww}}{COP_{ww}} f_{flp,ww}(PLR_{ww}) \tag{3.1}$$

and the G_{ww}, COP_{ww} and $f_{flp,ww}$ quantities needed to calculate $P_{HP,ww}$ are related on different ways with the operational variables (see appendix A.2).

Air to Water Heat Pump (AWHP). The air to water heat pump is a component which supplies thermal energy to the office area. In cooling

mode this device extracts heat from the office building which is dispelled to the external ambient.

The electrical energy consumption for the heat pump is defined as the following expression:

$$P_{HP_{aw}} = \frac{G_{aw}}{COP_{aw}} f_{flp,aw}(PLR_{aw}) \tag{3.2}$$

and the G_{aw}, COP_{aw} and $f_{flp,aw}$ quantities needed to calculate $P_{HP,aw}$ are related on different ways with the operational variables (see appendix A.2).

Thermal Storage Device (TSD). A thermal storage device in an air conditioning system allows decoupling thermal energy generation from thermal energy distribution. As a consequence, we can generate and store this energy whenever the conditions are more favourable. And therefore, an increasing of the number of running hours with a reduction of the installed thermal capacity of the air conditioning system is produced.

We employ a stratified water tank as thermal storage device. The model assumes that the stratification could be modelled considering that the tank is composed by ten fully mixed equal volume segments, with an energy balance equation for each one. The expression which allows calculating the variation of the temperature in each segment is as follows:

$$m_i Cp_{water} \frac{dT_i}{dt} = \dot{Q}_i^{dp} + \dot{Q}_i^{cond} + \dot{Q}_i^{loss} \tag{3.3}$$

where m_i is the mass of node i, Cp_{water} is the specific heat of water, dT_i/dt is the variation of the temperature in node i, $\dot{Q}_i^{dp}$ is the energy change of the node i due to charging or discharging via direct inlet or outlet flow including flow upward or downward in the tank, $\dot{Q}_i^{cond}$ represents the thermal conduction to neighboring nodes of the node i, $\dot{Q}_i^{loss}$ are the losses to the ambient of the node i. Notice that we obtain a set of ten differential equations which can be solved as a function of time.

Water Pump (EWP, IWP, SWP). We use single speed water pumps for the hydraulic circuits. In the model, the water pumps supply the water mass flows and consume electricity only in the instants when its control signals indicate that the pumps are in operation. The electrical power consumption of these devices is computed as:

$$P_{pump} = \gamma_{pump} \cdot P_{rated,pump} \tag{3.4}$$

where $P_{rated,pump}$ is the rated pump power consumption and γ_{pump} is the control signal of the water pump which has a value of zero or one depending on if it is switched off or switched on.

Air Fan (AF). A single speed air fan is used to dispel the rejected heat on the condenser side of the air to water heat pump. This device only supplies the air mass flow and consumes electricity in the instants when its control signal indicates that is switched on. Its electrical power consumption is modelled with the following equation:

$$P_{fan} = \gamma_{fan} \cdot P_{rated,fan} \tag{3.5}$$

where $P_{rated,fan}$ is the rated fan power consumption and γ_{fan} is the control signal for the air fan which has a value of zero or one depending on if it is switched off or switched on.

3.6 Behaviour of the air conditioning layouts

The purpose of this section is to show the behaviour of the different air conditioning layouts. To do it, we present the evolution of the water temperature in the hydraulic circuit and the thermal load for each configuration from the 19th of August at 12:00 (hour 5532 of the year) to the 22th of August at 18:00 (hour 5610 of the year) in the climatic area of Valencia.

Behaviour of the 'Air' configuration

Figure 3.12 shows the evolution of the water temperature in the hydraulic circuit for the 'Air' configuration. In the figure is presented the outlet water temperature of the thermal load and the outlet water temperature of the AWHP.

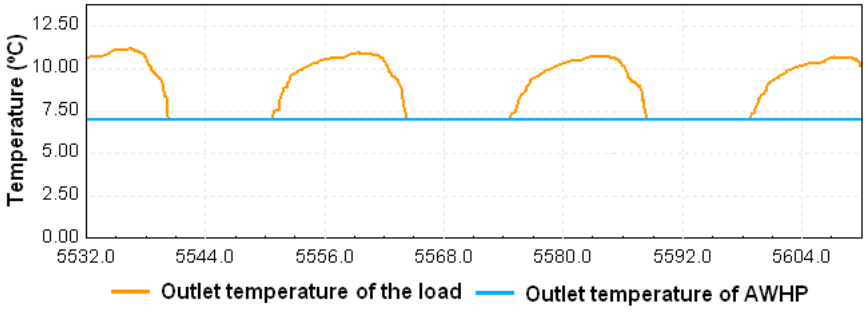

Figure 3.12: Behaviour of the 'Air' configuration

The periods when is produced a variation between the inlet and outlet water temperature of the thermal load indicate that the air conditioning system is switched on and the air conditioning system is cooling the thermal load.

The simulation shows that the inlet water temperature of the thermal load is always 7ºC. This is because when the air conditioning system is switched on the AWHP has enough thermal capacity to cool the water to this temperature. And afterwards, the system keeps this temperature because it was the last one before to switch off the air conditioning system.

Behaviour of the 'GCHP' configuration

Figure 3.13 shows the evolution of the water temperature in the hydraulic circuit for the 'GCHP' configuration. In the figure is presented the outlet water temperature of the thermal load and the outlet water temperature of the WWHP.

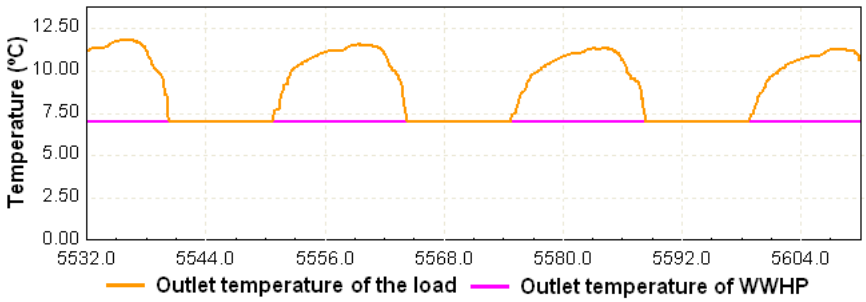

Figure 3.13: Behaviour of the 'GCHP' configuration

The behaviour in this air conditioning configuration is similar to the 'Air' configuration because for both layouts the thermal load, the water mass flow of the internal water pump and the thermal capacity of the heat pump are the same.

Behaviour of the 'GCHP + Air' configuration

Figure 3.14 shows the evolution of the water temperature in the hydraulic circuit for the 'GCHP + Air' configuration. In the figure is presented the outlet water temperature of the thermal load, the outlet water temperature of the WWHP and the outlet water temperature of the AWHP.

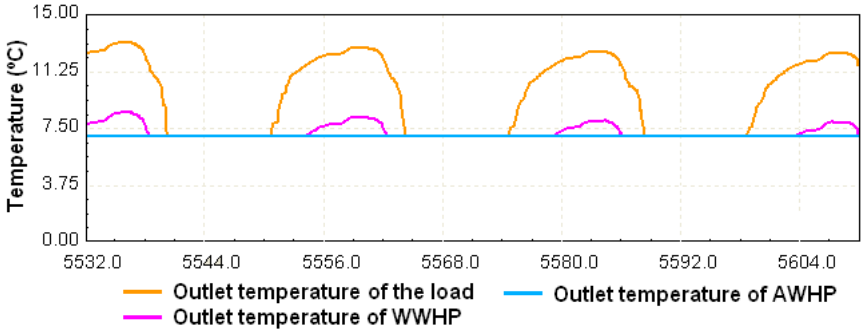

Figure 3.14: Behaviour of the 'GCHP + Air' configuration.

In this configuration the lower thermal capacity of the WWHP produces that the outlet water temperature of its evaporator can not arrive to the 7ºC in some periods. In this conditions, the AWHP is is switched on cooling this warm water to this temperature.

Behaviour of the 'Air + S' configuration

Figure 3.15 shows the evolution of the water temperature in the hydraulic circuit for the 'Air + S' configuration. In the figure is presented the outlet water temperature of the thermal load, the water temperature on the top and on the bottom of the tank, the average temperature of the tank and the outlet water temperature of the AWHP.

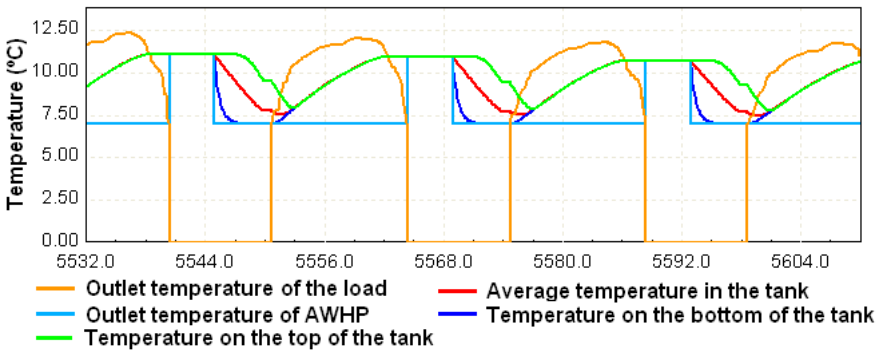

Figure 3.15: Behaviour of the 'Air + S' configuration

In this simulation, the periods when the outlet water temperature in the

thermal load is bigger than zero indicates that the air conditioning system is cooling the thermal load. The other periods are zero because the software package assigns this value after to do the necessary changes in the position of the valves of the hydraulic circuit to cool the thermal storage during the night. This assigned value do not affect to the results of the simulation because in the moment when the air conditioning system has to cool the thermal load the correct value of the outlet water temperature which correspond to thermal load is assigned in the simulation. This happens in all the configuration which incorporate a thermal storage device.

The figure shows clearly how the water temperature in the thermal storage decrease when is cooled by the AWHP during the night and how this temperature increase when thermal load rejects heat in it. In the instant when its inlet water temperature, which is the water from the thermal load, is lower than its outlet water temperature, this device is by-passed and it maintains the temperature until the AWHP starts to cool it again.

Finally when the outlet water temperature of thermal storage is warmer than 7ºC, the AWHP supports it cooling the inlet water to the thermal load until this temperature. Notice that the outlet water temperature of the AWHP is equal to the water temperature of thermal storage device after finishing the thermal demand of the thermal load. This is because in this moment the air conditioning is switched off an the changes in the position of the valves of the hydraulic circuit to cool the thermal storage is produced.

Behaviour of the 'GCHP + S' configuration

Figure 3.16 shows the evolution of the water temperature in the hydraulic

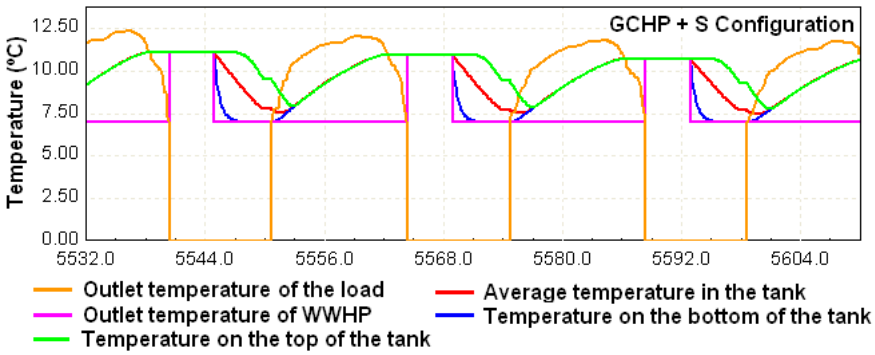

Figure 3.16: Behaviour of the 'GCHP + S' configuration

circuit for the 'GCHP + S' configuration. In the figure is presented the outlet water temperature of the thermal load, the water temperature on the top and on the bottom of the tank, the average temperature of the tank and the outlet water temperature of the WWHP.

The behaviour in this air conditioning configuration is similar to the 'Air + S' configuration because for both layouts the thermal load, the parameter of the devices and the thermal capacity of the heat pumps are the same.

Behaviour of the 'HA' configuration

Figure 3.17 shows the evolution of the water temperature in the hydraulic circuit for the 'HA' configuration. In the figure is presented the outlet water temperature of the thermal load, the water temperature on the top and on the bottom of the tank, the average temperature of the tank the outlet water temperature of the AWHP and the outlet water temperature of the WWHP. In this particular case, the water temperature on the top of the tank is not reflected in the figure because its representation in under the other ones.

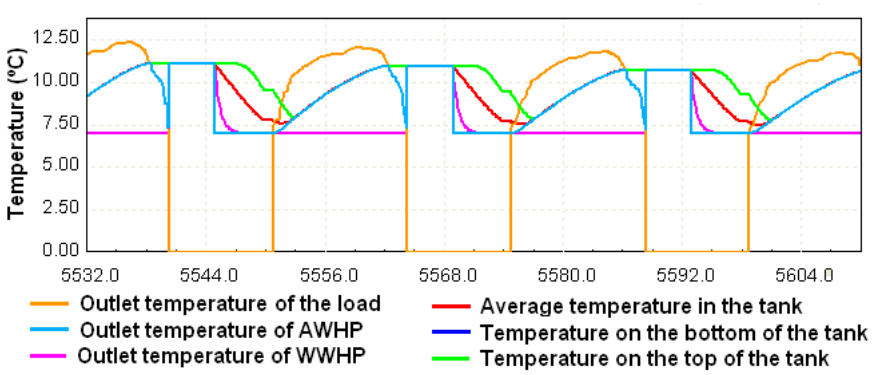

Figure 3.17: Behaviour of the 'HA' configuration

In this configuration the behaviour of the thermal storage device is similar to the 'Air + S' and 'GCHP + S' configurations. During the periods when it is cooled the thermal load and the outlet water temperature of thermal storage is warmer than 7ºC, the WWHP is switched on cooling the inlet water to the thermal load until this temperature.

Behaviour of the 'HB' configuration: HBI, HBII and HBIII

Figure 3.18 shows the evolution of the water temperature in the hydraulic

circuit for the 'HB' configuration. In the figure is presented the outlet water temperature of the thermal load, the water temperature on the top and on the bottom of the tank, the average temperature of the tank the outlet water temperature of the WWHP and the outlet water temperature of the AWHP. In this particular case, the water temperature on the top of the tank is not reflected in the figure because its representation in under the other ones.

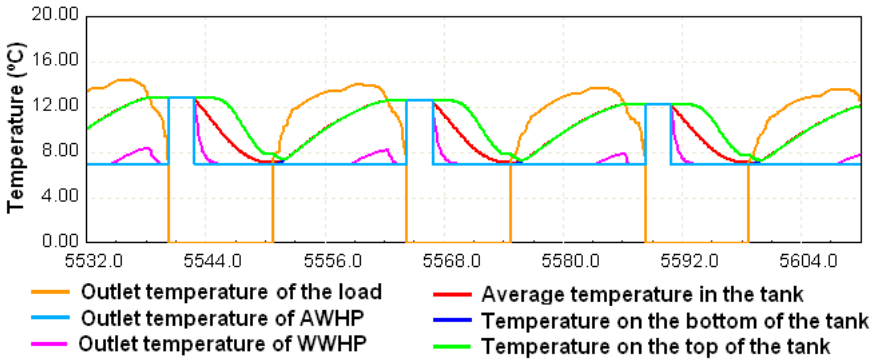

Figure 3.18: Behaviour of the 'HB' configuration

This configuration has a similar behaviour to the 'HA' configuration one but the AWHP has to support the WWHP when the thermal capacity of this device is not enough to cool the inlet water of the thermal load. This effect is shown in the figure when the outlet temperature of the WWHP can not arrive to the 7ºC. In this conditions, this warm water arrives to the AWHP and this device is switched on cooling the water to this temperature.

Behaviour of the 'HC' configuration: HCI, HCII and HCIII

Figure 3.19 shows the evolution of the water temperature in the hydraulic circuit for the 'HC' configuration. In the figure is presented the outlet water temperature of the thermal load, the water temperature on the top and on the bottom of the tank, the average temperature of the tank, the outlet water temperature of the WWHP and the outlet water temperature of the AWHP.

This configuration has a similar behaviour as the 'HB' configuration but the WWHP is the device which cools the thermal storage device during the night. The AWHP only has to support the other devices cooling the inlet water to the thermal load when is necessary.

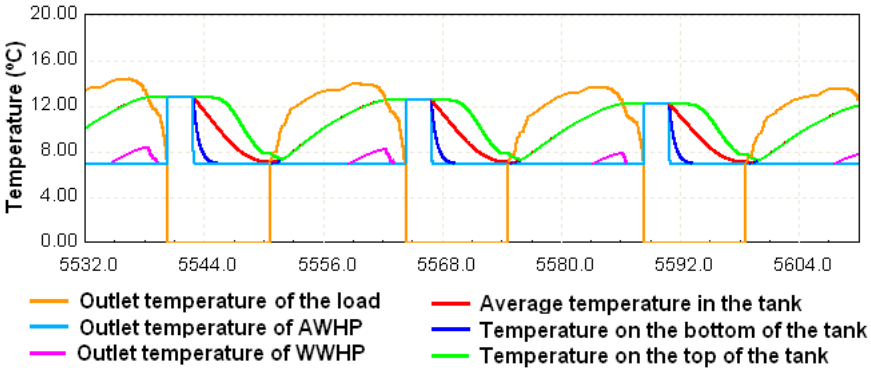

Figure 3.19: Behaviour of the 'HC' configuration

3.7 Simulation results and discussion

In this section, we present and discuss the results of our simulations. For the three climatic areas the total electrical energy consumption of each device employed for the different air conditioning configurations is calculated during cooling season (see table 3.5, table 3.6 and table 3.7). An analysis of the electrical energy consumption is included comparing the consumption of the heat pumps, the water pumps and the air fan. We also study the energy efficiency for each case through the Cooling Mode Performance Factor, CMPF. We define this parameter as the ratio between the total cooling thermal load and the total electrical energy consumption in cooling mode:

$$CMPF = \frac{Q_{load,cool}}{W_{elec,cool}} \tag{3.6}$$

We think that this parameter is a good choice to describe the energy efficiency of the air conditioning layouts because of the following. We pointed out that during heating season the thermal load can be directly satisfied by the main generator device of the air conditioning configuration. This is because this element is designed for a cooling dominated building and the main generation device has enough thermal capacity to satisfy the low thermal load in the heating season. For this reason, the study of the improving of the energy efficiency through decoupling energy generation from energy distribution and combining several generation systems is only applicable during cooling season. Therefore, a proper choice to evaluate the efficiency of each system is the ratio between the total cooling thermal load and the total electrical energy consumption in cooling mode.

	WWHP (KWh)	*AWHP (KWh)*	*AF (KWh)*	*IWP (KWh)*	*EWP (KWh)*	*SWP (KWh)*
Air-A	——	16729	14005	5355	——	——
GCHP-A	14766	——	——	5355	2577	——
GAI-A	14716	0.85	1.54	4958	2437	——
GAII-A	14747	36.06	64.5	4565	2325	——
GAIII-A	14615	208	429.3	4201	2185	——
GAIV-A	141608	817	1347	3781	2073	——
Air+S-A	——	9515	13502	5837	——	——
GCHP+S-A	9217	——	——	2837	3035	——
HAI-A	8461	624.1	3782	4129	2147	850.2
HAII-A	8361	625	3885	4129	2147	967.9
HAIII-A	8414	630.6	3751	4129	2147	1067
HAIV-A	8535	641.1	3414	4129	2147	1150
HBI-A	8541	622.6	4100	5482	2037	——
HBII-A	8425	768.4	4401	5176	1927	——
HBIII-A	7988	1253	4608	4809	1817	——
HCI-A	9207	22.54	16.99	5547	3041	——
HCII-A	9096	201.7	221.5	5236	3029	——
HCIII-A	8651	668.4	820.4	4863	3000	——

Table 3.5: Total electrical energy consumption of the WWHP, AWHP, AF, IWP, EWP and SWP for the different air conditioning configurations in Athens

	WWHP (KWh)	*AWHP (KWh)*	*AF (KWh)*	*IWP (KWh)*	*EWP (KWh)*	*SWP (KWh)*
Air-R	——	13691	11728	4636	——	——
GCHP-R	12392	——	——	4636	2318	——
GAI-R	12370	13	10.05	4255	2196	——
GAII-R	12341	120.2	176.4	3873	2073	——
GAIII-R	11980	500.1	747.3	3491	1950	——
GAIV-R	11168	1413	1863	3109	1827	——
Air+S-R	——	7446	12483	5421	——	——
GCHP+S-R	7754	——	——	5421	2901	——
HAI-R	7063	477.4	3564	3782	2024	828.4
HAII-R	7134	479.7	3558	3782	2024	935.2
HAIII-R	7169	483.90	3372	3782	2024	1022
HAIV-R	7286	490.7	2961	3782	2024	1097
HBI-R	7024	487.6	3604	5083	1904	——
HBII-R	7040	611.5	3861	4774	1784	——
HBIII-R	6665	1063	3935	4407	1678	——
HCI-R	7696	10.77	10.36	5165	2885	——
HCII-R	7621	190.5	163.6	4848	2849	——
HCIII-R	7220	586.5	669.9	4471	2817	——

Table 3.6: Total electrical energy consumption of the WWHP, AWHP, AF, IWP, EWP and SWP for the different air conditioning configurations in Rome

	WWHP (KWh)	*AWHP (KWh)*	*AF (KWh)*	*IWP (KWh)*	*EWP (KWh)*	*SWP (KWh)*
Air-V	——	15230	11961	4729	——	——
GCHP-V	13436	——	——	4729	2364	——
GAI-V	13429	8.39	12.97	4339	2239	——
GAII-V	13387	141.6	209.1	3950	2114	——
GAIII-V	12953	600.7	909.5	3560	1989	——
GAIV-V	11997	1683	2188	3171	1864	——
Air+S-V	——	8669	12661	5498	——	——
GCHP+S-V	8620	——	——	5498	2943	——
HAI-V	7997	497.0	3564	3869	2071	828.4
HAII-V	7966	500.2	3558	3869	2071	935.2
HAIII-V	7997	504.3	3372	3869	2071	1022
HAIV-V	8100	512.0	2965	3869	2071	1099
HBI-V	7992	535.1	3795	5162	1948	——
HBII-V	7726	716.8	4101	4846	1825	——
HBIII-V	7270	1265	4158	4467	1716	——
HCI-V	8578	26.89	28.58	5235	2924	——
HCII-V	8328	244.3	211.9	4910	2886	——
HCIII-V	7856	765.4	826.6	4526	2851	——

Table 3.7: Total electrical energy consumption of the WWHP, AWHP, AF, IWP, EWP and SWP for the different air conditioning configurations in Valencia

In figure 3.20 we present the total electrical energy consumption of each air conditioning layout during cooling season and its corresponding CMPF for the three climatic areas. The total electrical energy consumption is composed by three parts: the electrical energy consumption of the heat pumps (AWHP and WWHP), the electrical energy consumption of the water pumps(IWP, EWP and SWP) and the electrical energy consumption of the air fan (AF). For our particular office building, the total cooling thermal load is 70015 KWh for Athens, 57811 KWh for Rome and 63789 KWh for Valencia.

These results are calculated from simulations with time step equal to three minutes. We want to point out that we have performed a convergence study of the results for different time steps and obtained that the numerical error is lower than 1‰ for the presented results. Furthermore, there is a clear tendency towards a value independent of the time step employed (see appendix F).

In the following paragraphs we discuss the obtained values for each air conditioning layout.

We see in figure 3.20 that the behaviour in the electrical energy consumption and the CMPF of the different air conditioning configuration are similar for the three climatic areas.

The 'Air' configuration is the system which consumes more electrical energy. The electrical consumption of the 'GCHP' configuration is significantly lower than the 'Air' one because the outdoor air temperature during the day is higher than the ground temperature and, therefore, the ground is a much better heat sink than the air. In addition, the COP of the air to water heat pump is lower than the one for the water to water heat pump.

The 'GCHP + Air' configuration combines the two thermal generation systems. The air to water heat pump is employed as auxiliary generation system, allowing reducing the thermal capacity of the ground coupled heat pump and the water mass flow capacity of the internal and external water pumps. For the three climatic areas we study different cases which correspond to the combination of different sizes of both generation systems (see table 3.1, table 3.2 and table 3.3 for details). In this configuration, the electrical energy consumptions of the water to water heat pump and the water pumps decrease and appear the electrical consumptions of the auxiliary system (see table 3.5, table 3.6 and table 3.7). In figure 3.20, we can see for the three climatic areas that this configuration has an improvement of the CMPF with respect to the 'GCHP' configuration because the electrical energy savings achieved by reducing the sizes of the water to water heat pump and water pumps are higher than the electrical energy consumption of the auxiliary system (air to water heat pump and air fan). Nevertheless, in the cases GAIV-R and GAIV-V the weights of the electrical energy consumption of the auxiliary systems (specially their air fans) are higher than the electrical energy savings achieved by the size reduction of the water to water heat pumps and the water pumps and, therefore, their CMPF is lower than 'GCHP-R' and 'GCHP-V' respectively. This gives us a range of sizes in which combining both systems is better than using any of them separately for each climatic area.

The employment of a stratified water tank as a thermal storage device allows reducing the thermal capacity of the heat pumps, the water pump capacity of the water pumps and the air blown capacity of the air fan because they have more time to generate the thermal energy consumed by the thermal load. In the three climatic areas, an improvement of the CMPF is produced in all air conditioning configurations which store cooled water during the night as can be seen in figure 3.20. In these configurations it is reduced the

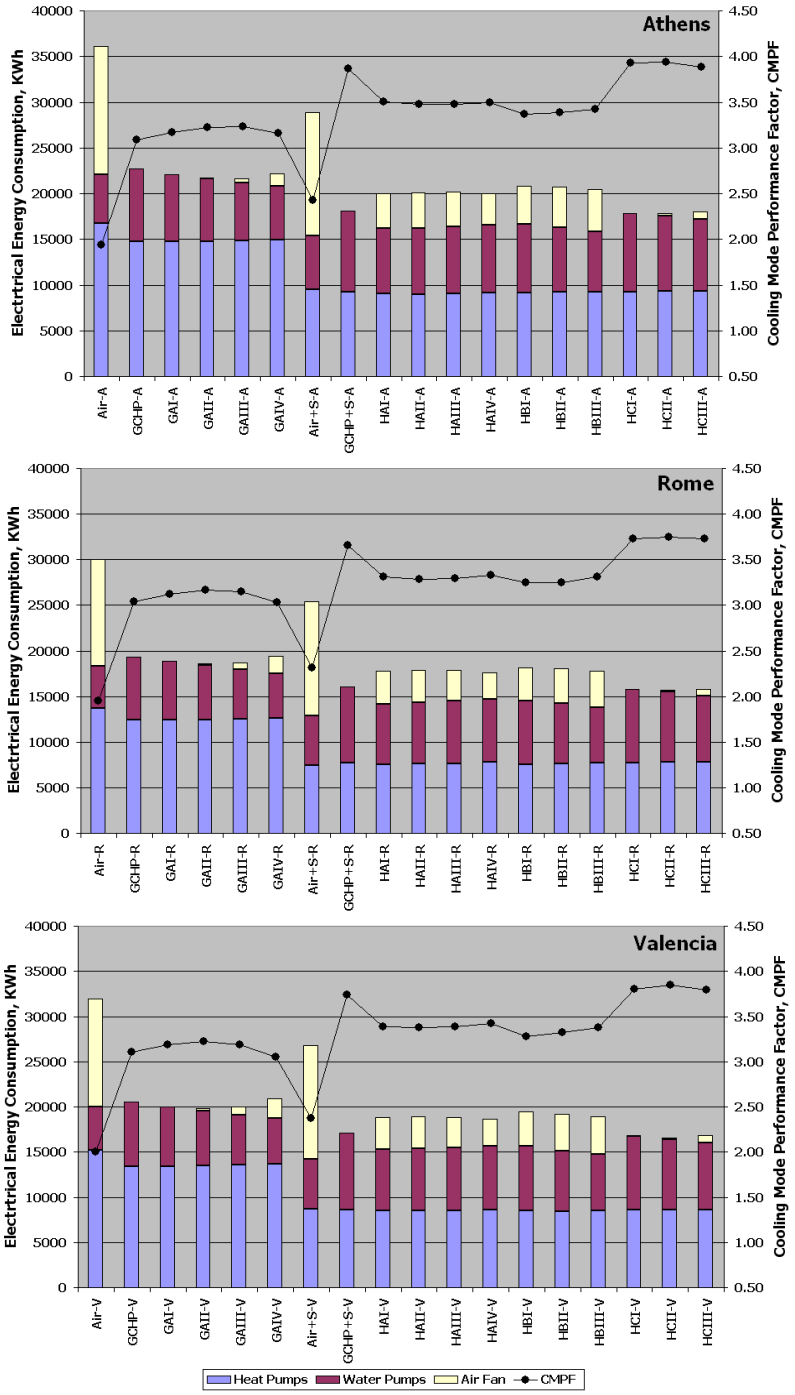

Figure 3.20: Total electrical energy consumption in cooling mode and the Cooling Mode Performance Factor (CMPF) for the air conditioning configurations in Athens, Rome and Valencia.

electrical energy consumption of the heat pumps in spite of the increasing of the electrical energy consumption of the air fan and the water pumps. This is clearly seen when is compared the electrical energy consumptions of the devices of the 'Air' and 'GCHP' configurations respectively with the 'Air + S' and 'GCHP + S' configurations (see electrical consumption results presented in table 3.7, table 3.5 and table 3.6).

As we said in previous sections, the hybrid configurations combine the three elements: the ground coupled heat pump, the air to water heat pump and the thermal storage device. In 'HA' and 'HB' configurations the air to water heat pump is used to cool the thermal storage device. In principle, this should be more efficient than using the ground coupled heat pump because during the night the outdoor air temperature is lower than the ground temperature and, then, in this period the air is a better heat sink than the ground. The results show that these two configurations have better CMPF than the 'Air', 'GCHP', 'GCHP + Air' and 'Air + S' configurations for the three climatic areas. Nevertheless, the better coefficient of performance of the water to water heat pump and the high electrical consumption of the air fan to dispel the rejected heat in the condenser of the air to water heat pump produce that the 'GCHP + S' configuration consumes less electrical energy than these two configurations as can be seen in figure 3.20. So, although the air is a better heat sink during the night it is better to cool the water storage device with the ground coupled heat pump. Notice that the 'HB' configuration has a higher electrical consumption than the 'HA' configuration. This is because in the 'HB' configuration the air to water heat pump and the air fan are switched on during more time because these elements have to support to the ground coupled heat pump when the thermal load is high.

Finally, the highest CMPF is obtained by the 'HC' configuration for the three climatic areas. This layout is the one that takes better profit of the combination of both generation systems and decoupling energy generation from energy distribution. From figure 3.20 we see that this configuration is an improvement of the 'GCHP + S' configuration following the idea of 'GCHP + Air' one, i.e., supporting it by a small auxiliary system based on an air to water heat pump.

3.8 Cost assessment

The installation of any air conditioning system involves considerable initial capital cost and, therefore, an assessment of the cost effectiveness is essential.

In this section we present the capital investment and the final economic cost of the thermal energy for the different configurations in the three climatic areas. We also analyze the different aspect which involves the economic behaviour of the studied configurations.

In table 3.8, table 3.9 and table 3.10 we present the capital investment for the equipments employed for each air conditioning configuration in the climatic areas of Athens, Rome and Valencia respectively. The prices employed for the different devices are based on from several catalogues, [70], [71] and [72]. And in these tables, we have included the price of the air fan in the price of the AWHP because usually both devices are in the same equipment.

In figure 3.21 we present the final economy cost of the thermal energy in cooling mode at the end of the useful life of the air conditioning system versus the annual increase of the price of the electricity for the three different areas. We define this final economic cost as the ratio between the total cooling thermal energy generated during the useful life of the air conditioning system and its total economy cost, which includes the initial investment of the installation as well as the economy cost from the electrical energy consumption along the time in cooling mode.

	WWHP €	*AWHP* €	*IWP* €	*EWP* €	*SWP* €	*GHE* €	*TSD* €
Air-A	——	13479	——	910	——	——	——
GCHP-A	8528	——	759	910	——	46500	0
GAI-A	7961	3449	697	837	——	46500	——
GAII-A	7393	4516	636	763	——	43400	——
GAIII-A	6826	5583	574	689	——	43400	——
GAIV-A	6258	6650	513	616	——	37200	——
Air+S-A	——	10278	——	689	——	——	44000
GCHP+S-A	6826	——	574	689	——	31000	44000
HAI-A	6826	10278	574	689	574	27900	44000
HAII-A	6826	9211	574	689	513	27900	44000
HAIII-A	6826	8144	574	689	452	27900	44000
HAIV-A	6826	7077	574	689	390	27900	44000
HBI-A	6258	9211	513	616	——	27900	32000
HBII-A	5691	8144	452	542	——	27900	25600
HBIII-A	5123	7077	390	468	——	24800	20800
HCI-A	6258	3662	513	616	——	31000	32000
HCII-A	5691	4729	452	542	——	27900	25600
HCIII-A	5123	5796	390	468	——	24800	20800

Table 3.8: Capital investment for the equipment employed for air conditioning configurations in the climatic area of Athens

	WWHP €	*AWHP* €	*IWP* €	*EWP* €	*SWP* €	*GHE* €	*TSD* €
Air-R	——	11985	——	800	——	——	——
GCHP-R	7734	——	667	800	——	40300	——
GAI-R	7132	3662	605	726	——	40300	——
GAII-R	6599	4516	544	653	——	37200	——
GAIII-R	5986	5690	482	579	——	37200	——
GAIV-R	5418	6757	421	505	——	31000	——
Air+S-R	——	9851	——	653	——	——	36000
GCHP+S-R	6599	——	544	653	——	27900	36000
HAI-R	6599	9851	544	653	544	24800	36000
HAII-R	6599	8699	544	653	482	24800	36000
HAIII-R	6599	7610	544	653	421	24800	36000
HAIV-R	6599	6522	544	653	360	24800	36000
HBI-R	5986	8699	482	579	——	24800	28000
HBII-R	5418	7632	421	505	——	24800	22400
HBIII-R	4828	6522	360	432	——	21700	17600
HCI-R	5986	3662	482	579	——	27900	28000
HCII-R	5418	4303	421	505	——	24800	22400
HCIII-R	4828	5434	360	432	——	21700	17600

Table 3.9: Capital investment for the equipment employed for air conditioning configurations in the climatic area of Rome

	WWHP €	*AWHP* €	*IWP* €	*EWP* €	*SWP* €	*GHE* €	*TSD* €
Air-V	——	11985	——	800	——	——	——
GCHP-V	7734	——	667	800	——	40300	——
GAI-V	7132	3662	605	726	——	40300	——
GAII-V	6599	4516	544	653	——	37200	——
GAIII-V	5986	5690	482	579	——	37200	——
GAIV-V	5418	6757	421	505	——	31000	——
Air+S-V	——	9851	——	653	——	——	32000
GCHP+S-V	6599	——	544	653	——	24800	32000
HAI-V	6599	9851	544	653	544	24800	32000
HAII-V	6599	8699	544	653	482	24800	32000
HAIII-V	6599	7610	544	653	421	24800	32000
HAIV-V	6599	6522	544	653	360	24800	32000
HBI-V	5986	8699	482	579	——	24800	25600
HBII-V	5418	7632	421	505	——	21700	21600
HBIII-V	4828	6522	360	432	——	21700	16800
HCI-V	5986	3662	482	579	——	24800	25600
HCII-V	5418	4303	421	505	——	21700	21600
HCIII-V	4828	5434	360	432	——	21700	16800

Table 3.10: Capital investment for the equipment employed for air conditioning configurations in the climatic area of Valencia

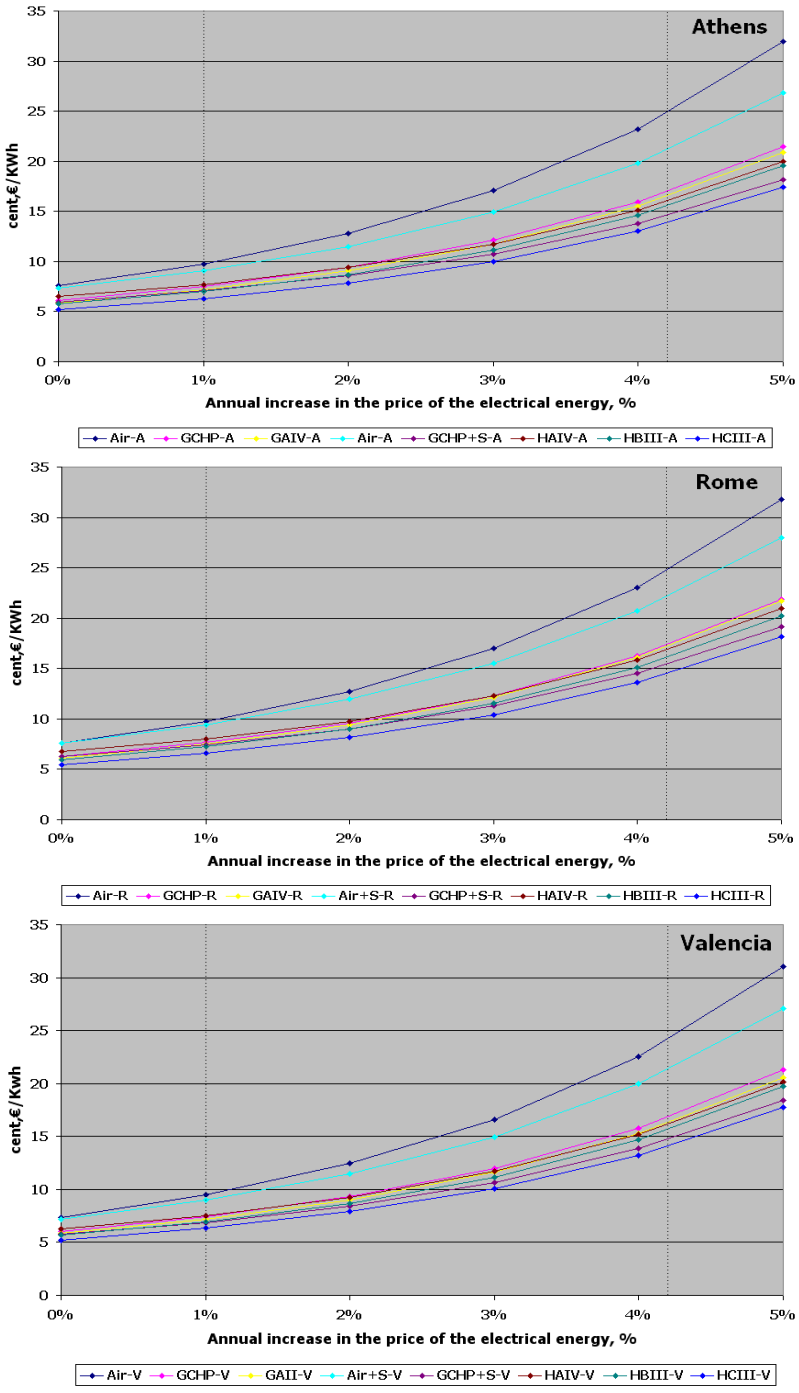

Figure 3.21: Final economy cost of the air conditioning configuration versus to the annual increase of the price of the electrical energy for Athens, Rome and Valencia.

$$FCost_{cool} = \frac{TCost}{Q_{total,cool}} \tag{3.7}$$

In this study the following considerations have been done: First, we consider that the useful life of the air conditioning system is fifty years. Second, the tariff employed in this study is 13.93 cent,euro/KWh which is the mean tariff for the Mediterranean countries, [73]. Third, the forecast of the increasing of the price of the electrical energy for the European Union goes from 1% to 4.2%, [74], and this range is shown in the figure with two vertical dotted lines. Finally, we only include the cases with the best cost effectiveness for the 'GCHP + Air', 'HA', 'HB' and 'HC' configurations for each climatic area.

From this economic study we see that for the three climate areas the initial investment for the 'Air' configuration is the lowest (see table 3.8, table 3.9 and table 3.10 for details). This is because the installation of a stratified water tank (as a thermal storage) and a GCHP (due to the ground heat exchanger) produce a high increase in the initial cost in an air conditioning system. Nevertheless, figure 3.21 shows that this configuration has the highest final economic cost for the thermal energy. Figure 3.21 also shows that a incorporation of a thermal storage device produce an improvement in the cost effectiveness. This is clearly seen when is compared the final economic cost of the 'Air' and 'GCHP' configurations respectively with the 'Air + S' and 'GCHP + S' configuration for the three climatic areas. The 'GCHP + Air' configuration, which combine both generation systems, has around the same thermal energy cost than the 'GCHP' configuration in the three climatic areas. Finally, the hybrid configurations, which combine the three equipments, has the best cost effectiveness in the three climatic areas. This is specially good for the HC configuration which has the best CMPF and the best cost effectiveness.

Notice that the increase in the price of the electricity has lower influence in the most efficient configurations.

Chapter 4

Efficiency improvement of ground coupled heat pumps from energy generation and distribution management

4.1 Introduction

In the standard design of an air conditioning system, the references taken to estimate the heating and cooling capacity of the heat pump to be installed are usually based on the coldest and the warmest day along the year. Therefore, the thermal energy required by the thermal load is under the design point of the air conditioning system during most part of the time. In this context, the development of strategies for the operation of the air conditioning system and, particularly for the system based on GCHPs, allowing to optimize the procedure to generate the required thermal energy is a good way to improve the energy efficiency while satisfying the thermal comfort.

In this chapter we evaluate the energy savings that a new management strategy can produce in an air conditioning system composed by a GCHP and a central fan coil linked to a standard office space. In this new management strategy, the air mass flow in the fan, the water mass flows in the internal and external hydraulic systems and the set point temperature in the heat pump, usually fixed in conventional strategies, have the possibility of a continuous regulation which allows us to design a more efficient way to achieve the desired thermal comfort.

This new management strategy is based on five capacity levels developed from the total electrical power equation of the air conditioning system. In

our particular case, this equation indicates that to achieve energy savings is desirable to work with low water flows. For this reason, the new management strategy tries to achieve a steady state in which the water mass flow is maintained as low as possible, using first all other possibilities to supply energy.

An office space in the Mediterranean coast (cooling dominated area) is modeled to evaluate the energy performance of an air conditioning system driven by a GCHP when it is managed by the new management strategy and by a conventional one. The thermal comfort criterion which has to be satisfied is the Predicted Mean Vote index (PMV). This comfort index predicts the mean value of votes of a large group of people in the Thermal Sensation Scale and it is defined by the ISO7730-1994 standard.

In our simulation, we compare the annual electrical energy consumption for both strategies. We also analyze the factors which allow improving the energy efficiency of the system by means of the new management strategy. Finally, the model and the evaluation of this study has been done with TRNSYS which is a specific package software for this kind of systems, [64].

This chapter is structured as follows. First two sections describe the PMV index and the simulated office building where is linked our air GCHP system. Afterwards, the air conditioning system configuration, the energy model of its devices and the total electrical power equation obtained from the particular consumption of each element. Next, we define the new management strategy and the conventional one. And finally, we present and discuss the results obtained in our simulation.

4.2 Comfort criteria

We choose the Predicted Mean Vote (PMV) index to evaluate the thermal comfort in our simulation. This index is a criteria to estimate the comfort state proposed by the ISO7730-1994 standard and predicts the mean value of the votes of a large group of persons on the seven point Thermal Sensation Scale (see the appendix C).

The PMV index for the air conditioned space is calculated at each simulation step time. To do it, three parameters, activity, thermal resistance of clothing and mean air velocity have to be estimated. We follow ISO7730-1994 recommendations for this purpose. The value for the activity parameter is

1.2 *met* for moderated office activity. The thermal resistance of clothing is 1.0 *clo*, when the considered working clothes are shirts, trousers, jackets, and shoes. Finally, the value for the mean air velocity is estimated in 0.1 m/s. The other three parameters, air temperature, mean radiant temperature and partial water vapour pressure are computed at each time step.

4.3 Simulated office area

The simulated office area comprises 108 m^2 (12 m x 9 m) with two windows in the north and south façades and three in the east and west façades. To perform the simulation the office area is characterized by its building materials, its dimensions, distribution and orientation. There are four different kinds of construction elements: external walls, floor, roof and window glasses. External walls are defined as ventilated façades composed by four elements: perforated brick, 5 *cm* of insulation, air chamber and a Naturex plate cover; its global conductivity is 0.51 W/m^3K. The floor and the roof are built with hollow blocks with 5 cm of insulation; its global conductivity is 0.51 W/m^2K. Finally, the window is composed by a glass, with a solar radiation transmissivity equal to 0.837 and conductivity equal to 5.74 W/m^2K, and a window frame, with conductivity equal to 0.588 W/m^2K. The windows size is 1.5 square meters, dedicating a 15% of this area to the frame surface. The internal and external shadow factor for these windows is estimated in 0.7. The orientation of the office area, the layout of windows and the fan coils is shown in figure 4.1.

All these parameters are included through the TRNBuild tool specifically designed to simulate the thermal behaviour in a multi-zone building area. Finally, the weather data base of the Spanish city of Valencia is used to characterize the Mediterranean coast weather (cooling dominated area).

4.4 Air conditioning system

The air conditioning system linked to the simulated office area is based on a GCHP. This system is composed by two parts: the external circuit composed by the external water pump (EWP) and the geothermal heat exchanger (GHE), and the internal circuit, composed by the internal water pump (IWP) and a central fan coil (FC) linked to the office area. The water to water heat pump (WWHP) is a reversible heat pump and it is the connecting element between both circuits. In figure 4.2 we include a schematic diagram showing

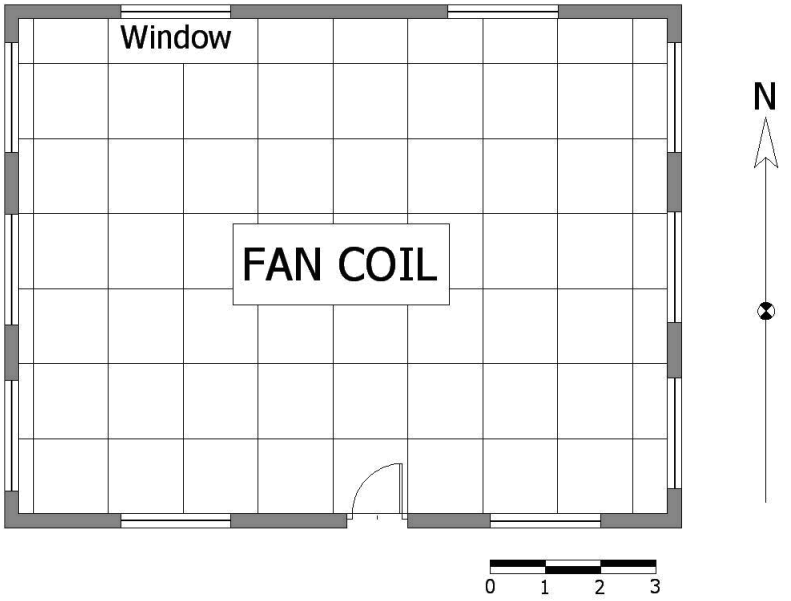

Figure 4.1: Layout of windows and the fan coil in the air conditioned area.

the layout of these devices.

The only difference between the hydraulic circuit for the new management strategy and the conventional management strategy is in the active devices (WWHP, EWP, IWP, EMF) employed. For the new one the active devices have a continuous regulation, whereas for the conventional strategy these devices have only two positions: switched on or switched off.

The following paragraphs detail the model describing the behaviour of each component. We also derive the way to compute the electrical power consumption of each one, for given working conditions. Notice that the purpose of this study is to improve the energy efficiency of the system keeping the comfort requirements. Therefore, the knowledge of this power consumption behaviour allows us to develop a suitable management strategy to achieve this objective.

Ground Heat Exchanger (GHE). The objective of the ground heat exchanger is to interchange heat with the ground. A heat carrier fluid is circulated through the ground heat exchanger and either rejects heat to, or absorbs heat from the ground depending on the temperatures of the heat

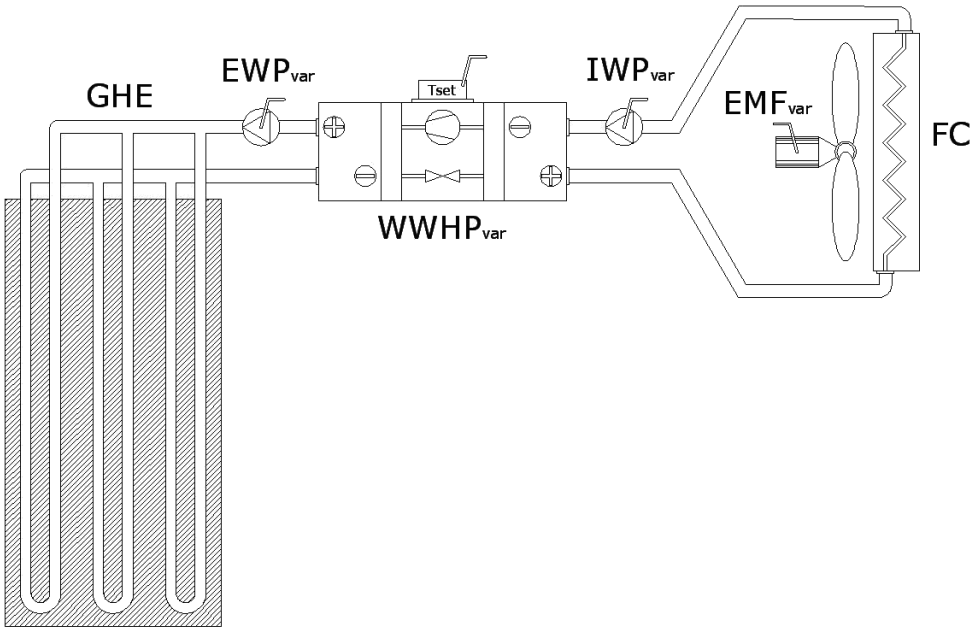

Figure 4.2: Air conditioning system: geothermal heat exchanger (GHE), external water pump (EWP), internal water pump (IWP), water to water heat pump (WWHP), fan coil (FC), electric motor of the fan (EMF).

carrier fluid and the ground. In typical U-tube ground heat exchanger applications, a vertical borehole is drilled into the ground. A U-tube heat exchanger is then pushed into the borehole. The top of the ground heat exchanger is typically several centimeters below the surface of the ground. Finally, the borehole is filled with a fill material. We use 'Duct Ground Heat Storage Model' to simulate our GHE, [21].

Our GHE is composed by three U-tube vertical boreholes of fifty meters depth placed in parallel. The boreholes are filled with bentonite. Finally, description parameters for the GHE used in the simulation are shown in table 4.1, [70].

Water to Water Heat Pump (WWHP). The water to water heat pump is the component that supplies thermal energy to the office area. It is a reversible heat pump; when the system is working in heating mode this device extracts heat from the ground which is used to heat the offices. When the system works in cooling mode makes the opposite action. The model chosen to describe the behaviour of the WWHP allows the possibility of varying

Parameter	Value
Number of boreholes	3
Borehole length	50 m
Borehole radius	0.1016 m
Storage thermal conductivity	2 W/mK
Storage Heat Capacity	2016 $kJ/m^3/K$
Outer radius of U-tube pipe	0.01664 m
Inner radius of U-tube pipe	0.01372 m
Center to center half distance	0.0254 m
Fill thermal conductivity	1.3 W/mK
Pipe thermal conductivity	0.42 W/mK

Table 4.1: Description parameters of the Ground Heat Exchangers.

the set point temperature. This is one of the four variables that we are going to use as manipulated variable.

The electrical energy consumption for the heat pump is defined as the following expression:

$$P_{HP,ww} = \frac{G_{ww}}{COP_{ww}} f_{flp,ww}(PLR_{ww}) \tag{4.1}$$

and the G_{ww}, COP_{ww} and $f_{flp,ww}$ quantities needed to calculate P_{HP} are related on different ways with the operational variables (see the appendix A.2).

Fan Coil (FC). A central fan coil is used to heat or cool the office area. A fan coil unit is a simple device consisting of a heating or cooling coil and an air fan. The coil receives hot or cold water from a central plant, and removes or adds heat from the air through heat transfer in order to condition a space.

The simplified fan coil model considers that the final air temperature is the average temperature of the fluid in the coil. The only complication in the scheme is that in order to find the average water temperature in the coil, it is necessary to guess an outlet temperature and iterate until the energy transferred from the air stream matches the energy transferred into the water stream. The heat absorbed by the fluid is the same extracted from the air minus the losses due to condensation as can be read in the following equation:

$$\dot{Q}_{fluid} = \dot{m}_{air}(h_{air,in} - h_{air,out}) - \dot{m}_{cond} h_{cond} \tag{4.2}$$

Device	Parameter	Value
Heat Pump	Rated capacity in heating of the WWHP	10 KW
	Rated capacity in cooling of the WWHP	9 KW
	Rated coefficient performance of the WWHP	3
	Set point temperature in cooling	5-10°C
	Set point temperature in heating	35-45°C
Fan Coil	Rated air mass flow	2700 kg/h
	Rated power for the electric motor of the fan	366 W
Water Pump	Rated water mass flow for the IWP	1650 Kg/h
	Rated water mass flow for the EWP	1500 Kg/h
	Rated power for the IWP	400 W
	Rated power for EWP	360 W

Table 4.2: Value of the parameters for the heat pump, fan coil and water pumps.

The effect of the condensation only is to produce when is cooling the air stream and the amount of condensate is given by the equation:

$$\dot{m}_{cond} = (\omega_{air,out} - \omega_{air,in}) \tag{4.3}$$

In particular, the electrical consumption of this device comes from the fan electric motor and it is computed as follows:

$$P_{fan} = P_{rated,fan} \left(\frac{\dot{m}_{air}}{\dot{m}_{rated,air}} \right)^2 \tag{4.4}$$

where $P_{rated,fan}$ and $\dot{m}_{rated,air}$ are the rated fan power consumption and the rated air mass flow when the fan is operating at full-speed, see table 4.2. Finally, $\dot{m}_{air}$ is the air mass flow through the fan in each time step.

Water Pump (IWP, EWP). We use variable speed water pumps for the internal and external hydraulic circuit. The pump speed will be adjusted by a pressure regulator so that the pressure drop keeps constant in the hydraulic circuit. As a consequence the electric pumping consumption is linear with respect to the water mass flow through the pump. This linear relation is defined in the following expression:

$$P_{pump} = P_{rated,pump} \frac{\dot{m}_{water}}{\dot{m}_{rated,water}} \tag{4.5}$$

where $P_{rated,pump}$ and $\dot{m}_{rated,water}$ are the rated pump power consumption and the rated water mass flow when the pump is operating at full capacity, see

table 4.2. Finally, $\dot{m}_{water}$ is the water mass flow through the pump in each time step.

Total electrical consumption of the air conditioning system. The addition of the consumption from the different devices is the total electric power consumption of our air conditioning system. Equation (4.6) allows us to calculate this total power consumption at every time step. In this expression, the constant coefficients C_{FC}, C_{IWP}, C_{EWP} and C_{WWHP} can be obtained by looking in the previous electrical consumption expressions for each device, equations (4.1), (4.4) and (4.5).

$$\begin{aligned} P_{total} &= C_{FC}\dot{m}_{air}^2 + C_{IWP}\dot{m}_{IWP} + C_{EWP}\dot{m}_{EWP} + \\ &+ C_{WWHP}\frac{G_{ratio}(T_{set}, T_{ground,out})}{COP_{ratio}(T_{set}, T_{ground,out})} \cdot \\ &\cdot f_{flp}(T_{load,in}, T_{ground,out}, T_{set}, \dot{m}_{IWP}) \end{aligned} \tag{4.6}$$

This equation shows the relation between the electrical consumption of the air conditioning system and six system variables: air mass flow ($\dot{m}_{air}$), internal water mass flow ($\dot{m}_{IWP}$), external water mass flow ($\dot{m}_{EWP}$), heat pump set point temperature (T_{set}), heat pump inlet temperature from the ground heat exchanger ($T_{ground,out}$) and heat pump inlet temperature from the load ($T_{load,in}$). Out of these six variables the first four are management variables ($\dot{m}_{air}$, $\dot{m}_{IWP}$, $\dot{m}_{EWP}$, T_{set}). A proper understanding of the behaviour of this power consumption expression is the key to design a management strategy that will improve the energy efficiency of the system.

The consumptions of the fan coil electric motor and of the water pumps only depend on the air mass flow and the water mass flow respectively, and they are independent of the electric consumptions of the other devices. In contrast, the consumption of the heat pump depends on its set point temperature and the internal water mass flow and this last variable is included in the consumption equation of the internal water pump.

Let study this expression for given conditions for the variables $T_{ground,out}$ and $T_{load,in}$. The behaviour of equation (4.6), corresponding to the heat pump plus water pumping power consumption is shown in figure 4.3. The figure shows the overall electric consumption of these two devices as a function of the internal water mass flow and the set point for the outgoing temperature in the cold side when delivering 5 KW in cooling mode with a heat pump inlet temperature from the ground of 24^oC.

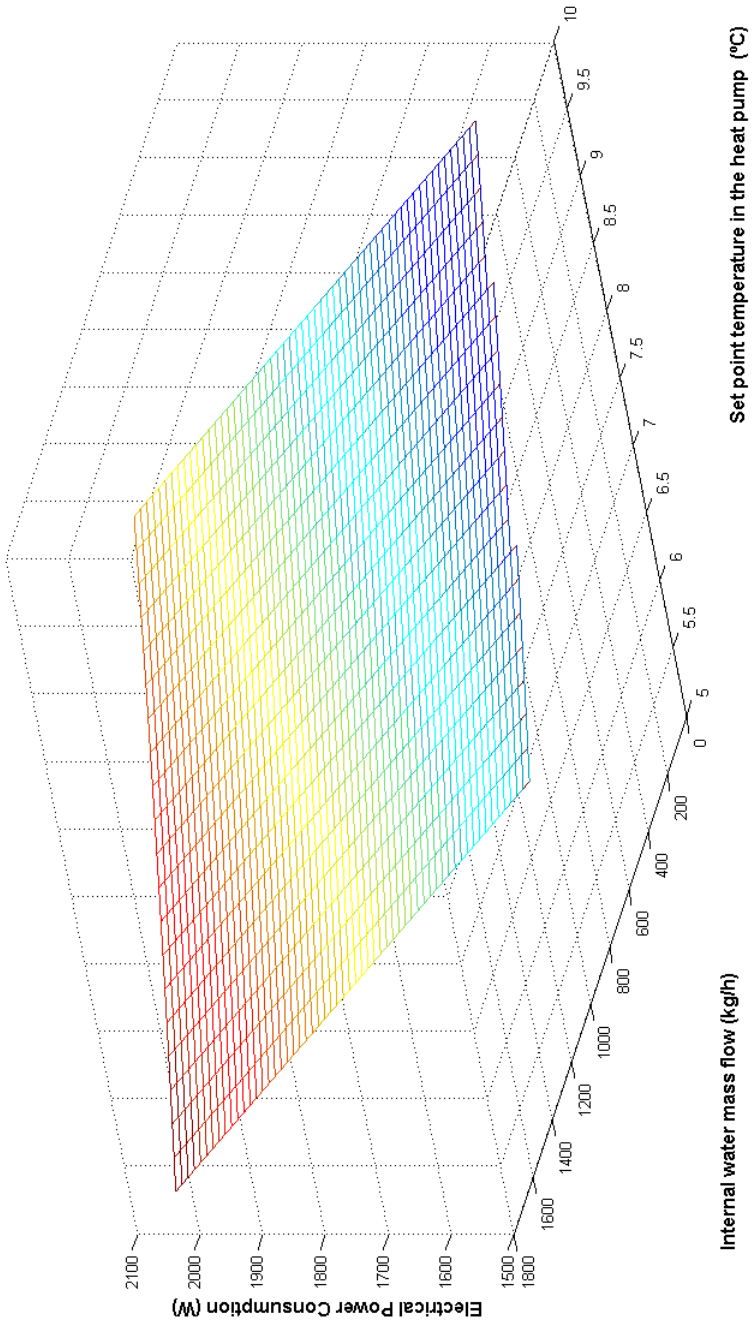

Figure 4.3: Electrical power consumption for the heat pump and the internal water pump when the heat pump supplies 5 KW in cooling mode with a heat pump inlet temperature from the source of $24°C$.

From figure 4.3, we see that to achieve energy savings it is desirable to work with low water flows and high set point temperatures. Notice that the change in electric power consumption is bigger in the direction of the internal water mass flow than in the set point temperature of the heat pump. Therefore, if it is necessary to supply more energy it is more convenient to modify first the set point temperature keeping low water mass flows. Once the set point temperature achieves its minimum allowed value the water pump starts to increase the water mass flow rate.

In addition to the conclusions derived from figure 4.3, it would be desirable to have similar flows in both sides of the heat pump. Therefore, the ratio between internal and external water mass flow must be the same with the time. Finally, notice that the electric motor of the fan is the unique device which can be switched on with independence of the other ones. The other devices, the internal and external water pumps along with the heat pump have to be switched on all together.

4.5 Management Strategies

In this section we present both management strategies: the new one based on the behaviour of equation (4.6) and the conventional one.

For both systems, we have fixed two aspects: the working period and the heating and cooling seasons. The working period in the office is fixed from 9:00 to 18:00, which is the period when is switched on the air conditioning system. The heating season is considered from November to December and from January to March and the cooling season from April to October. Finally, there are not holiday periods, as a consequence the air conditioning system works every day.

4.5.1 New management strategy

Description of the new management strategy.

The objective of the new management strategy is to improve the energy efficiency of the air conditioning system by adapting its thermal capacity to the actual thermal comfort demand in the office. This new management strategy is detailed in the following paragraphs.

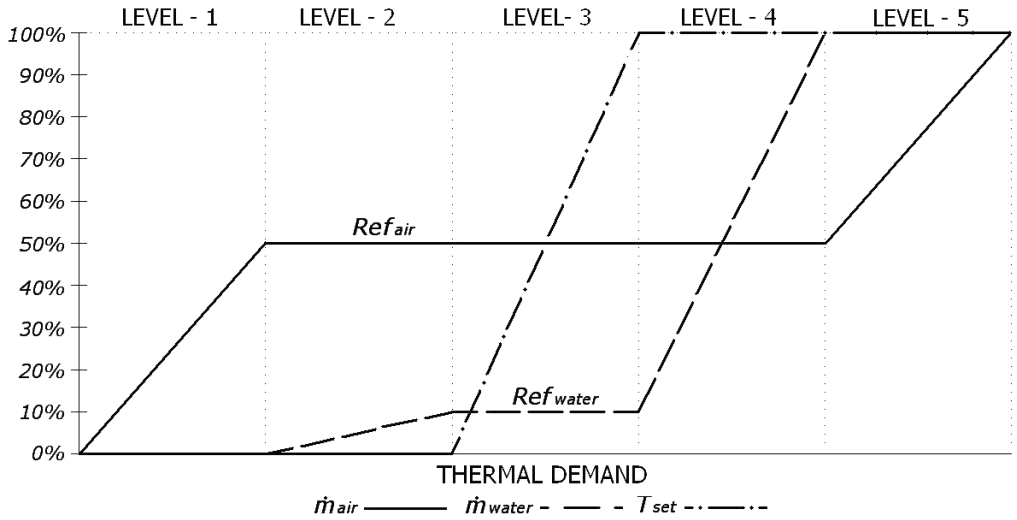

Figure 4.4: Diagram illustrating the classification in capacity levels of the system capacity given by the steady state values of the control variables. For a given thermal demand there is a unique choice for the operational point of the air conditioning system.

To maintain neutral comfort conditions in the office the PMV value should be zero in the Thermal Comfort Scale. The deviation of the PMV from zero indicates a variation of the thermal demand in the office area. Notice that, to satisfy this thermal demand, there are several configurations of the management variables which are suitable to compensate this PMV deviation. Our management strategy is based on the choice of a particular configuration of these variables. This choice classifies the air conditioning system capacity in five capacity levels given by the steady state value of the management variables. In figure 4.4, we show a diagram illustrating this classification. We now describe each capacity level.

- First capacity level; in steady state conditions the fan capacity is between the 0% and the 50% of its maximum capacity and the other devices are switched off. In this level the blown air by the fan modify the convective factor and homogenize the temperature in the office to achieve the thermal comfort.

- Second capacity level; the fan, the hydraulic pumps and the heat pump are switched on. In steady state conditions the air blown by the fan is fixed to the 50% of its maximum capacity, the water mass flows of

the internal and external hydraulic pumps are between the 0% and the 10% of its maximum allowed value, and the set point temperature is 0%, which indicates the lowest or highest set point temperature for heating or cooling mode respectively.

- Third capacity level; in steady state conditions the air blown by the fan is fixed to the 50% of its maximum capacity, the water mass flows of the internal and external hydraulic pumps are fixed to the 10% of its maximum allowed value and the set point temperature is between 0% and 100%, meaning that the set point temperature can be any value of its range in heating or cooling mode.

- Fourth capacity level; in steady state conditions the air blown by the fan is fixed to the 50% of its maximum capacity, the water mass flows of the internal and external hydraulic pumps are between the 10% and the 100% of its maximum allowed value and the set point temperature is 100% which indicates the highest or lowest set point temperature for heating or cooling mode respectively.

- Fifth capacity level; in steady state conditions the fan capacity is between the 50% and the 100% of its maximum capacity, the water mass flows of the internal and external hydraulic pumps are fixed to the 100% of its maximum allowed value and the set point temperature is 100%.

If the energy supplied by the air conditioning system when all the active devices are given the 100% of its capacities is not enough to maintain the thermal comfort conditions, the PMV diverts from zero and the thermal demand is not satisfied.

The choice of these five capacity levels is based on the behaviour of equation (4.6). This equation, explained in previous section, indicates that to achieve energy savings is desirable to work with low water mass flows in the air conditioning system. For this reason, the new management strategy tries to achieve a steady state in which the water mass flow is maintained as low as possible, using first all other possibilities to supply energy.

We also want to point out that in actual conditions a high air flow blown by the fan can produce an excessive noise due to the vibration in the fan coil, to avoid this effect, the new management strategy tries to maintain in steady state conditions the air mass flow blown by the fan around half of its maximum capacity.

Implementation of the new control strategy through a cascade control structure.

A cascade control structure with PID regulators is a suitable choice to implement our management strategy (see appendix B.3). We explain in the following paragraphs the cascade control structure used for this purpose, [75] and [76]; a diagram showing this control structure is included in figure 4.5.

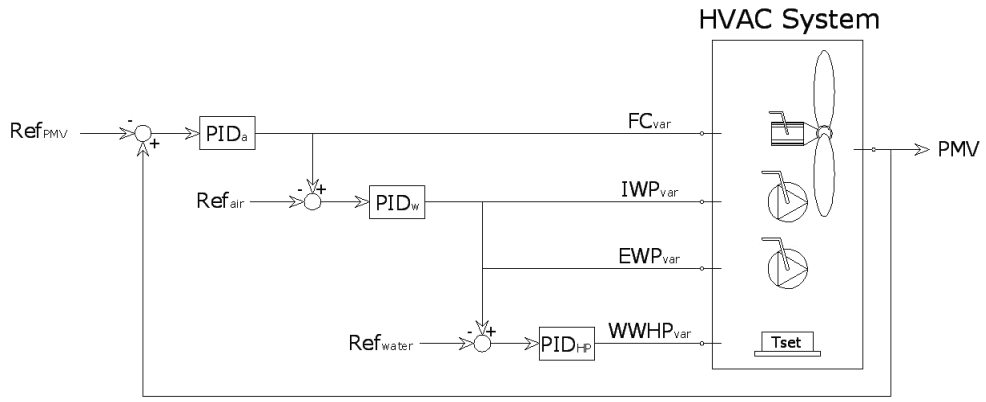

Figure 4.5: Control structure diagram for the new strategy.

A primary loop regulated by PID_a, acts as a master loop adjusting the air mass flow in order to achieve a correct PMV given by the value of its reference, Ref_{PMV}, equal to zero. A second loop regulated by PID_w, acts as slave loop of the primary one adjusting the water mass flow in the internal and external water pumps in order to achieve an air mass flow given by the value of its reference, Ref_{air}, equal to the 50% of its maximum allowed value. The internal and external water mass flows have the same signal; therefore, both devices change their flows with the same rate. A third loop regulated by PID_{HP}, acts as slave loop of the second one adjusting the set point temperature of the water to water heat pump in order to achieve water mass flows given by the value of its reference, Ref_{water}, equal to the 10% of its maximum allowed value.

This control structure is able to drive the air conditioning system to the steady state conditions explained previously. Notice that in the transient period in which the system is driven to the desired steady state the management variables are not limited to any value within its physically allowed ranges. As a consequence, when a change in the thermal demand occurs, the control

structure is able to quickly supply the needed energy to achieve the thermal comfort and, subsequently, a new steady state is reached to accommodate the change in thermal demand.

4.5.2 Conventional management strategy

In the following paragraphs, we are going to describe the employed conventional management strategy for the air conditioning system.

This strategy uses on/off regulators to manage the air conditioning system. This kind of regulators has only two possible operation points. They give its maximum capacity when switched on and nothing when switched off. The on/off regulators are installed in active elements: the heat pump, the electric motor of the fan coil and the internal and external water pumps.

In this strategy, three aspects are important. First, the difference between the set point temperature and the inlet temperature of fluid in the heat pump from the office area indicates the connection or disconnection of the generator energy system, composed by the heat pump, the external water pump and the ground heat exchanger. Therefore, the internal water pump is always switched on to have a measure of this difference during the working period. Second, to maintain the comfort conditions, the PMV is located in a comfort band between 0.5 and -0.5, in order to try to avoid an excessive number of connections and disconnections of the system which, in an actual situation, could damage the actuators of the fan coil. Finally, the set point temperature in the heat pump is constant, for the heating season is fixed to $45^{o}C$ and for the cooling season to $7^{o}C$.

In heating mode the conventional management strategy works as follows. When the value of the PMV variable is below the lower limit of the comfort band, PMV equal to -0.5, the electric motor of the fan is switched on. Then, the air goes through the coil, where a constant water mass flow is pumped from the internal circulation pump. This heat exchange produces a variation of the temperature of the water in the internal circuit which is detected by the heat pump; immediately this device and the external water pump are switched on to provide the necessary energy to fix the value of the PMV to the upper limit of the comfort band, PMV equal to 0.5. After achieving this value, the heat pump, the external water pump and the electric motor of the fan are switched off.

In cooling mode the conventional management strategy is the same as

the previous one except that the references of the comfort band are inverted. The electric motor of the fan is connected when the PMV is above the upper limit, PMV equal to 0.5, and the air conditioning system stops supplying energy when the PMV arrives to -0.5.

Finally, figure 4.6 shows the control structure diagram of this strategy.

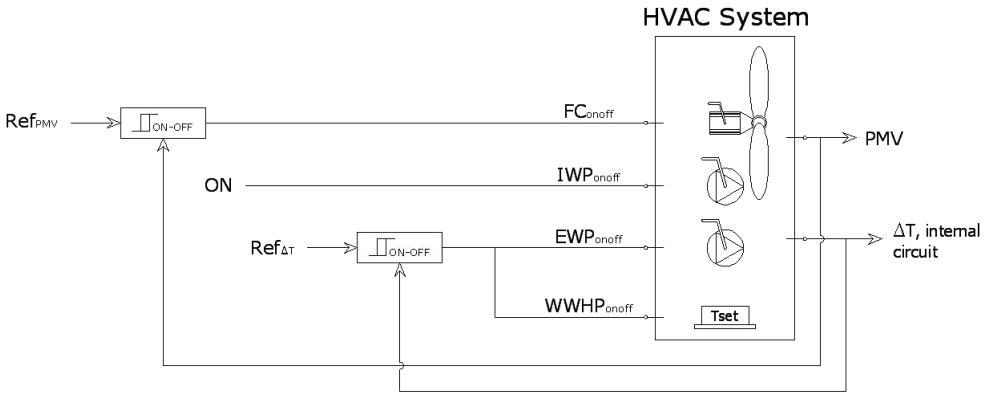

Figure 4.6: Control structure diagram for the conventional strategy.

4.6 Simulation results and discussion

In the following paragraphs, we present and discuss the results obtained from the simulations. First, we evaluate the accuracy of the obtained results. Second, we show the correct behaviour of the new management strategy. Finally, we present the energy consumption of the air conditioning system for both management strategies, and we evaluate the energy savings achieved by the new one.

4.6.1 Accuracy of the simulation results

We present in this subsection a study of the accuracy of the simulation results. These results have to show a tendency towards a value independent

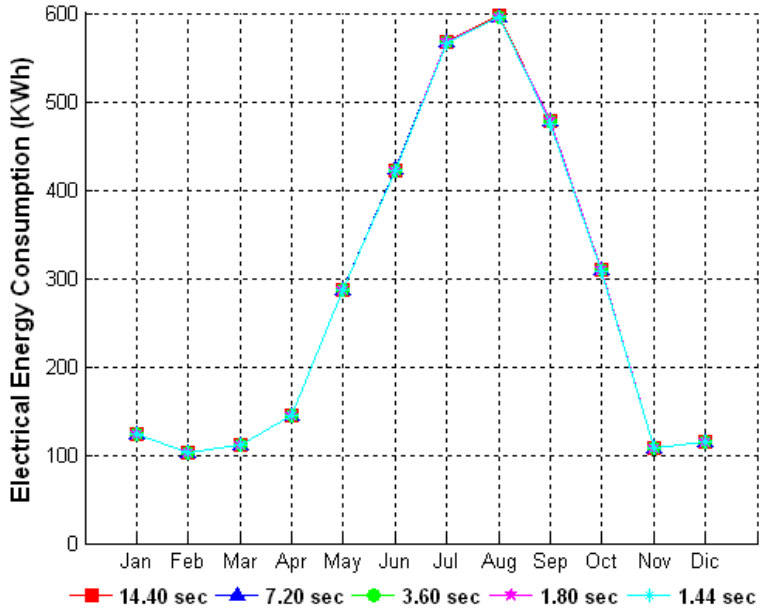

Figure 4.7: Monthly electrical energy consumptions of the air conditioning system for conventional strategy.

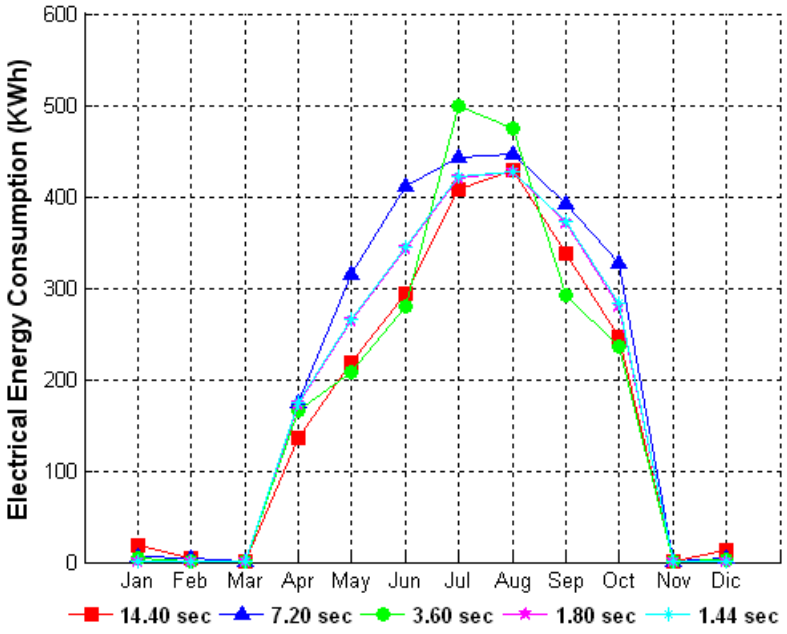

Figure 4.8: Monthly electrical energy consumptions of the air conditioning system for new strategy.

of the time step employed to solve the set of differential equations programmed in our software package. Therefore, a set of simulations are carried out for several time steps. The smaller time scale of the system is the one given by the action of the controllers. In all the simulations this scale is fixed to 28.8 seconds, which is fast enough in comparison with the building dynamic behaviour. Therefore, we choose the solver time step as a fraction of this smaller physical time scale, and we perform simulations at the following solver time steps: 14.40 seconds, 7.20 seconds, 3.6 seconds, 1.8 seconds and 1.44 seconds.

Figure 4.7 and figure 4.8 show the monthly electrical energy consumption of the air conditioning system when is managed by the conventional strategy and by the new one, respectively, and for the different solver time steps mentioned before. For the conventional strategy, the results obtained are almost independent of the solver time step chosen and it does not notice significant variations among them. Nevertheless, the results from the simulation of the new management strategy show a higher dispersion. This behaviour is due to the fast dynamic introduced by the controllers which are not possible to simulate correctly when the solver time step is not small enough. In spite of this, the tendency of the electrical energy consumptions in all the simulations is the same through the year. In the cases where is used the smallest time steps, 1.80 seconds and 1.44 second, the obtained results do not show significant variation among them and points to the same continuum values.

4.6.2 Behaviour of the cascade control structure in the simulation

The purpose of this subsection is to show the correct behaviour of the new management strategy. This one achieves quickly the thermal comfort state and, after this, drives the management variables to the steady state of one of the capacity levels of the new management strategy.

Figure 4.9 shows the evolution of the thermal comfort and the management variables for three days in heating and cooling mode. In this particular case the steady state achieved belongs to the third capacity level of the new management strategy. The steady state conditions achieved are shown in the figures, the PMV achieves quickly a value equal to zero which corresponds to thermal comfort (see figures 4.9-a1 and 4.9-a2), the air blown by the fan achieves the 50% of its maximum allowed value (see figures 4.9-b1 and 4.9-b2), the water mass flows of the internal and external hydraulic pumps

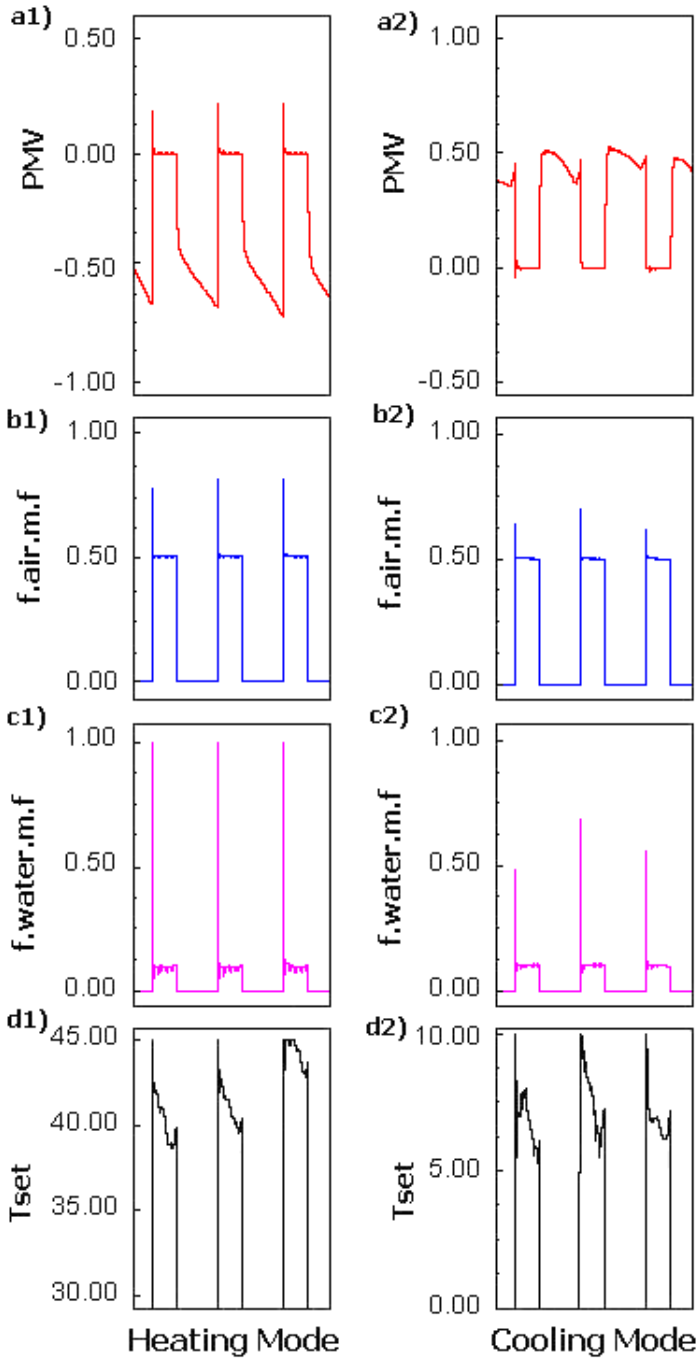

Figure 4.9: Evolution of the input and output control variables for three days in heating mode (left) and three days in cooling mode (right). From top to bottom, PMV index, fraction of air mass flow (f.air.m.f.), fraction of water mass flow (f.water.m.f.) and set point temperature (T_{set}).

achieve the 10% of its maximum allowed value (see figures 4.9-c1 and 4.9-c2) and the set point temperature is between 30°C and 45°C in heating mode and 7°C and 10°C in cooling mode (see figures 4.9-d1 and 4.9-d2).

4.6.3 Electrical consumption comparison between the two management strategies

In this subsection, we present the energy consumption of the air conditioning system for both management strategies, and we evaluate the energy savings achieved by the new one. In the simulation conditions, the weather database employed models of the Mediterranean coast weather, which is characterized to have hot summers and warm winters and the working period coincides when the external ambient temperature and the solar radiation is the highest throughout the day. The combination of these two factors produces that the energy demand in cooling mode is much higher than in heating mode.

In figure 4.10, we present the monthly electrical energy consumptions of the air conditioning system for the two management strategies. These data correspond to the simulations employing a solver time step equal to 1.8 seconds. From this figure we can see that in all months, except April, the system consumes less electrical energy when it is managed by the new management strategy.

In winter season, our simulation results show that the influence of the external temperature and the solar radiation in the office area during the working period is enough to maintain the thermal comfort in it, therefore the energy provided by the air conditioning system is very low. A remarkable difference between both management strategies exist because the conventional management strategy employs the temperature change of the water in the internal hydraulic circuit to communicate the energy demand in the office room to the generator system. As a consequence, the internal water pump is always switched on during the working time and, therefore, consuming electrical energy independently of the air conditioning necessities. Whereas, in the new strategy, the air conditioning system only consumes electrical energy according with the thermal demand in the office area. In this way, we avoided the unnecessary electrical consumptions, which can suppose a great energy lost throughout the year.

In summer season, the influence of the external temperature and the solar radiation which were an advantage during the winter season are now a

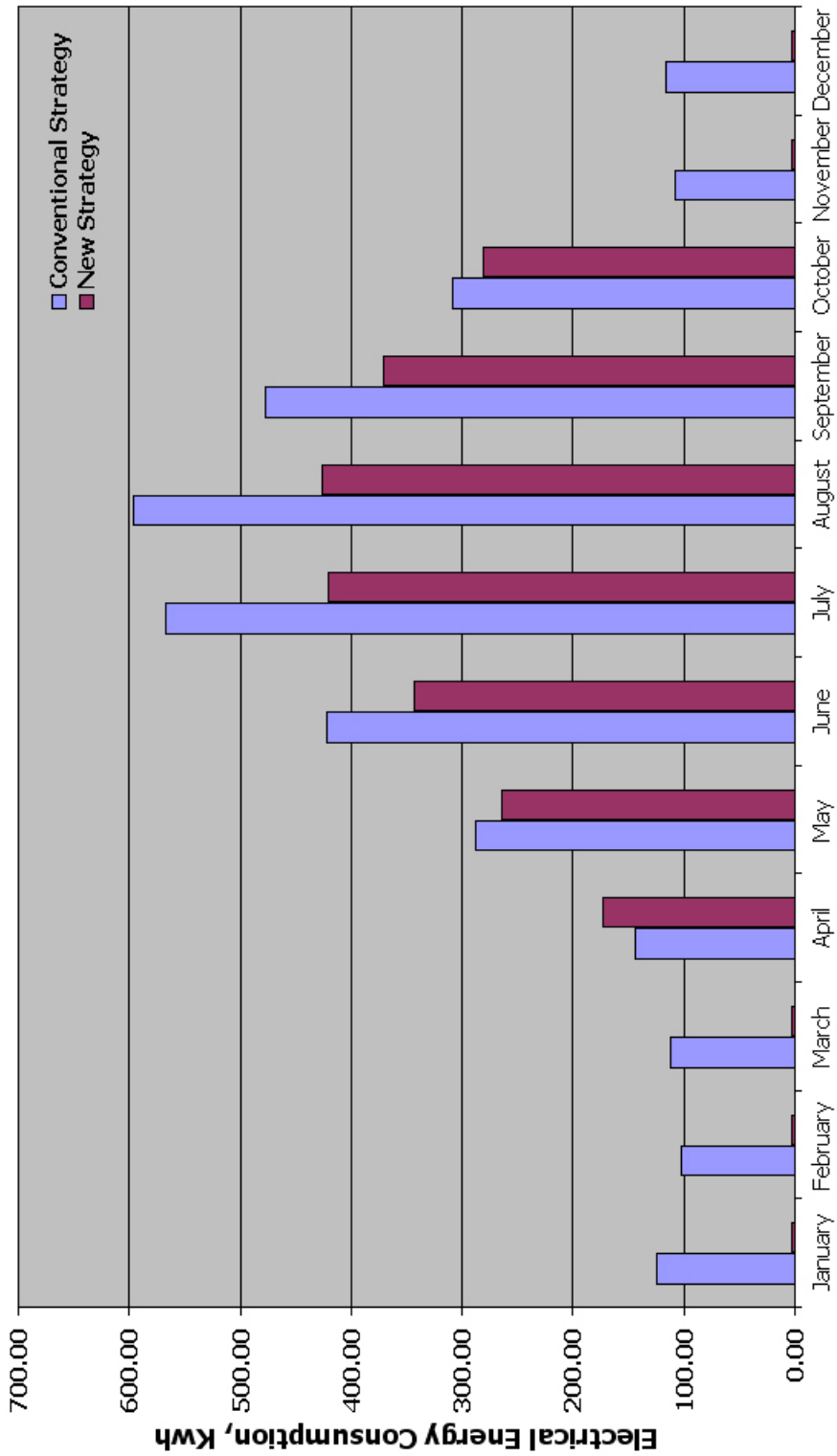

Figure 4.10: Electrical energy consumptions for the two control strategies.

disadvantage. Therefore, both management strategies are more active to provide the necessary high cooling power to achieve the thermal comfort. In these conditions is when the new one has more chances to manage the air conditioning system to reduce its electrical consumption. In figure 4.10, the electrical consumption for both strategies grows up in function of the cooling demand, being the maximum electrical consumptions during the warmest months, July and August. In all months during the cooling season, except April, the electrical consumptions of the air conditioning system when is employed the new management strategy are significantly lower than the ones achieved when using the conventional one. Furthermore, the new management strategy improves the efficiency of the air conditioning system as the cooling demand increases.

In April, the electrical consumption of the air conditioning system is lower when the conventional management strategy is used. This behaviour is because in the first day of this month the air conditioning system changes from heating mode to cooling mode. When the conventional management strategy manages the air conditioning system the value of the PMV index is between 0.0 and 0.5 most of the time belonging to the working periods. In these conditions, this management strategy keeps switched off the fan, the heat pump and the external water pump. Meanwhile, the new one activates these three devices to supply energy to the office to compensate the small deviation of the PMV variable from the thermal neutral state, PMV equal to zero. This shows us the difficulty to choose the suitable dates to change from heating mode to cooling mode and vice versa which are particulars for each environmental conditions. The previous situation can be avoided by delaying the date to activate the cooling mode of the heat pump.

We include in table 4.3 the annual electrical consumption of the air conditioning system when it is managed by the conventional management strategy and by the new management strategy. We also include in this table the percentage of energy savings achieved by the new one in comparison with the conventional one. These results are presented for all solver time steps used in the simulations.

In summary, looking at the results obtained for the different solver time steps used in the simulations, the annual energy savings obtained through the new management strategy are always above 24%. Furthermore, looking at the behaviour of these numerical results it is observed a tendency towards a value around the 30%.

Time step (*sec.*)	*AEC* (*CMS*) (*KWh*)	*AEC* (*NMS*) (*KWh*)	*Energy Savings* (%)
14.4	3365.86	2106.27	37.42
7.2	3365.96	2525.08	24.98
3.6	3365.67	2163.34	35.72
1.8	3365.24	2277.83	32.31
1.44	3359.16	2289.22	31.85

Table 4.3: Annual electrical consumptions (AEC) of the air conditioning system for the conventional management strategy (CMS) and the new management strategy (NMS) and energy savings achieved by the new one compared with the conventional one. These data are presented for all solver time steps used.

Chapter 5
Conclusions

Let us summarize the main results obtained in this Ph.D. thesis. The objective of this research was improving the energy efficiency of an air conditioning systems driven by a ground coupled heat pump at the same time that we kept the thermal comfort in cooling dominated offices. The proposed energy management strategies were oriented to improve the thermal energy generation and the thermal energy distribution in this air conditioning system through the following ideas: combining several thermal generation systems (ground coupled heat pump and air to water heat pump), decoupling thermal generation from thermal distribution (employing a thermal storage device) and, finally, the management of some parameters of the devices of the ground coupled heat pump system (the air mass flow in the fan coil, the water mass flow in the internal and external hydraulic systems and the set point temperature in the water to water heat pump).

In chapter 3, we studied the energy efficiency improvement of ground coupled heat pump systems when energy generation is decoupled from energy distribution and when it is supported by other generation systems. Following these ideas we evaluated the electrical energy consumption of several air conditioning layouts combining a ground coupled heat pump, an air to water heat pump and a thermal storage device. This air conditioning configuration has been linked to a office building. This building has been evaluated in the weather conditions of the cities of Athens, Rome and Valencia which are representatives of the different Mediterranean climatic areas (cooling dominated conditions).

The procedure to evaluate the energy efficiency improvement was as follows. We calculate the electrical energy consumption of the air conditioning system when was composed only by an air to water heat pump ('Air' configuration) or a ground coupled heat pump ('GCHP' configuration). These values where used as a reference to evaluate the energy savings achieved by

the proposed layouts. Then, we calculated the electrical energy consumption of a system composed by a ground coupled heat pump which was supported by an air to water heat pump ('GCHP + Air' configuration) and evaluated its energy savings. Next, we combined a thermal storage device with a ground coupled heat pump or an air to water heat pump to study their behaviour when was decoupled energy generation from energy distribution ('Air + S' and 'GCHP + S' configurations). And finally, we presented three hybrid configurations ('HA', 'HB' and 'HC' configurations) combining the three elements: a ground coupled heat pump, an air to water heat pump and a thermal storage device.

The result of our simulations showed that decoupling thermal energy generation from thermal energy distribution through a thermal storage device and a suitable combination of a ground coupled heat pump with an air to water heat pump allowed a reduction of the electrical energy consumption and, therefore, an improvement of the cooling mode performance factor (CMPF). The hybrid configuration type C was the most suitable combination. This configuration obtained the highest cooling mode performance factor and the electrical energy savings were estimated around the 40% and the 18% when were compared with the 'Air' and 'GCHP' configurations respectively.

We have also included the assessment of the cost effectiveness for the different air conditioning configurations in the three climatic areas. From this economic study we see that for the three climate areas the initial investment for the 'Air' configuration is the lowest. This is because the installation of a thermal storage device and a GCHP, due to the ground heat exchanger, produce a high increase in the initial cost in an air conditioning system. Nevertheless, this configuration has the highest annual electrical energy consumption which produces that it has the most expensive final economic cost for the thermal energy. Furthermore, the incorporation of a thermal storage device increase the cost effectiveness of the air conditioning system and the combination of both generation systems has around the same thermal energy cost than the 'GCHP' configuration. Finally, the hybrid configurations, which combine the three equipments, has the best cost effectiveness in the three climatic areas. This is specially good for the hybrid configuration type C which has the best CMPF and the best cost effectiveness.

In chapter 4, we presented a new management strategy based on the power equation of the air conditioning system driven only by a ground coupled heat pump. The air mass flow in the fan coil, the water mass flow in the internal and external hydraulic system and the set point temperature in

the heat pump are managed to obtain the desired thermal comfort in the office area while reducing the electrical consumption of the air conditioning system. We compare the total power consumption of the HVAC system when it is managed by the new strategy and by a conventional one.

This new management strategy has five capacity levels developed from the total electrical power equation of the HVAC system. This equation indicates that to achieve energy savings is desirable to work with low water flows in the air conditioning system. For this reason, the new management strategy tries to achieve a steady state in which the water mass flow is maintained as low as possible, using first all other possibilities to supply energy.

The annual electrical energy savings achieved by the air conditioning system managed by the new management strategy are above the 24% of the electrical consumption of the system managed by a conventional one for all solver time step used. This result was the lower bound obtained from the simulations, nevertheless, we have observed a continuum tendency of the savings towards a value around a 30%. In addition to these savings results it was relevant to point out that the new strategy improves the efficiency of the air conditioning system as the thermal demand increases.

Finally, we think that the present ideas can be adapted to other buildings with similar characteristics and conditions and the energy savings achieved should be of the order of the savings obtained in this research work.

Future research

- Experimental verification of the obtained results in the simulations in an actual system.
- Development of management strategies and hybrid layouts which allow a thermal equilibrium between heat extracted from the ground and heat rejected to the ground.
- Development of management strategies based on the power equation which manage the different devices of a hybrid ground coupled heat pump system.
- Combination of a ground coupled heat pump with other generation systems such an absorbtion machine.

Appendix A
Thermal energy model of the heat pump and the ground heat exchanger

A.1 Introduction

In this appendix we describe with more detail the thermal model of the water to water heat pump and the air to water heat pump used to heat or cool the different acclimatized areas in our simulations as well as the model of the ground heat exchanger employed in the different energy studies presented in this thesis.

A.2 Thermal energy model of the heat pump

As we said previously, a heat pump is a device that cool a fluid stream on the evaporator side while rejecting heat to a fluid on the condenser side. Because this device can be employed to cool or heat an area of a building depending on if in the building is located the evaporator or the condenser.

Now, we describe the way in which the model calculates the heat pump power consumption from the operational variables. By definition, heat pump power consumption is equal to the ratio between the heat pump capacity, G, and its nominal coefficient of performance, COP. Nevertheless, the model takes into account that the heat pump is working at partial load. In this case, the actual heat pump power consumption is calculated multiplying this theoretical consumption by the fraction of full load power, f_{flp} , which is a function of the heat pump partial load ratio, PLR (ratio between the load, Q_{load}, and the heat pump capacity, G, [77]. Then, the actual consumption for the heat pump is defined as the following expression:

$$P_{HP} = \frac{G}{COP} f_{flp}(PLR) \tag{A.1}$$

These three quantities needed to calculate P_{HP} are related on different ways with the operational variables. The heat pump capacity, G, and the coefficient of performance, COP, are calculated using the following expressions:

$$G = G_{rate} G_{ratio}(T_{set}, T_{exch,out}) \tag{A.2}$$

$$COP = COP_{rate} COP_{ratio}(T_{set}, T_{exch,out}) \tag{A.3}$$

First, G_{rate} and COP_{rate} are the heat pump capacity and the coefficient of performance both in nominal conditions. And second, G_{ratio} and COP_{ratio} are dimensionless coefficients calculated from the values of the operational variables T_{set}, set point heat pump temperature, and $T_{exch,in}$, fluid inlet temperature from the ground heat exchanger for the water to water heat pump and the outdoor air temperature from the air exchanger for the air to water heat pump. These quantities are read from two data files and characterize the behaviour of the heat pump for the different values of the operational conditions. Another data file is employed to relate the fraction of full load power, f_{flp}, and the partial load ratio, PLR.

A.3 Model of the ground heat exchanger

A ground heat exchanger is a system composed by a heat exchanger coupled directly in the ground. A heat carrier fluid is circulated through the ground heat exchanger and either rejects heat to, or absorbs heat from the ground depending on the temperatures of the heat carrier fluid and the ground. In typical U-tube ground heat exchanger applications, a vertical borehole is drilled into the ground. A U-tube heat exchanger is then pushed into the borehole. The top of the ground heat exchanger is typically several feet centimeters below the surface of the ground. Finally, the borehole is filled with a fill materia which can be virgin soil or a grout of some type, see figure A.1.

We use 'Duct Ground Heat Storage Model' to simulate our ground heat exchanger, [21]. In the model the temperature at a given point in the storage is a superposition of three parts: A global solution, a steady-flux solution around the nearest pipe, and a local radial solution.

The temperature of the heat carrier fluid at the inlet to the duct system is a function of time $T_{fin}(t)$. The variation of the fluid temperature along

the flow path through the ducts is accounted for by use of a heat balance equation. The rate of heat injection/extraction $Q(t)$, or the inlet fluid temperature $T_{fin}(t)$, or a $Q(t)$ that depends on $T_{fin}(t)$ may be specified.

The ground in the storage volume is assumed to have homogeneous thermal properties. The thermal properties of the ground and the arrangement of ducts are assumed to exhibit cylindrical symmetry with respect to a vertical axis through the middle of the storage region. The global problem, which does not include the local temperature fields, therefore becomes a function of the radial and the vertical coordinates. The heat flow process in the storage region and the surrounding ground is modeled using a rectangular two-dimensional mesh.

Figure A.1: Diagram of a ground heat exchanger in a building.

The storage volume is divided into a number of subregions. There is one local solution for each subregion. They also define the flow path of the heat carrier fluid. The injection/extraction of heat gives a distribution of sources and sinks for the global solution, which satisfies:

$$C\frac{\partial T}{\partial t} = \nabla(\lambda \nabla T) + q_{sf} + q_l \tag{A.4}$$

The source term q_{sf} uses the steady-flux solution to account for pulses that vary slowly in time. Here, it is used for the redistribution of heat in each subregion of the storage volume. The source term q_{sf} for a given cell in

the mesh is proportional to the difference between the mean temperature of the subregion in question and the temperature in that cell. There is no net energy contribution to the storage by this process.

The short-time effects of the injection/extraction through the ducts are simulated with the local solutions. This solution is assumed to be the same for all pipes within a given subregion. The solution depends only on a radial coordinate and covers the volume from the pipe to the radius r which is the radius of the cylindrical storage region. An energy pulse at a given moment from the pipes to the surrounding ground is retained in the local problem for a period of time corresponding to $at/r^2 = 0.2$ where a is the thermal diffusivity. The energy of the pulse is with this time lag added to the global solution as an increase of the temperature with the same amount in the whole subregion. The same temperature difference is subtracted from the local solution. The longtime effects are thus shifted over to the global solution.

The short-time variations are covered by the local problems. The slow redistribution of heat during injection/extraction and the interaction between the storage region and the surrounding ground are accounted for by the steady-flux and the global solution.

Appendix B
Control devices

B.1 Introduction

In this appendix is explained the behaviour of the On-Off controller as well as the PID controller employed to implement the conventional management strategy and the new management strategies presented in chapter four.

B.2 On-Off controller

The *two-position control mode* is the simplest mode of control. The controller output has only two possible values, depending on the sign of the error. If these two positions are fully open and fully closed, the controller is called an *On-Off controller*. Most of the two-position controllers have a neutral zone to prevent the chattering. The neutral zone is a range of values around zero before any control action takes place. Figure B.1 shows the input-output relationship of a two-position controller.

The two-position control mode supplies pulses of energy to the process, which cause a cycling controlled variable. The amplitude of the cycling depends on three factors: the capacitance of the process, the dead-time lag of the process, and the size of the load change that the process can handle. Two-position control is used whenever the cycling can be reduced to an acceptable level.

B.3 PID controller

A Proportional-Integral-Derivative controller (PID controller) is a generic control loop feedback mechanism widely used in industrial control systems. A PID controller attempts to correct the error between a measured process

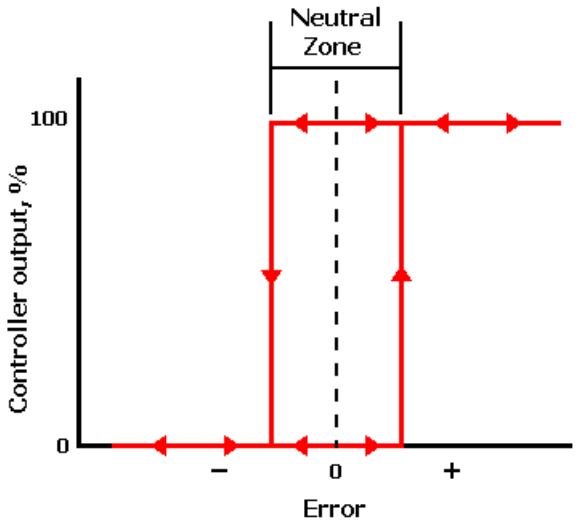

Figure B.1: Input-output relationship of a two-position controller.

variable and a desired setpoint by calculating and then outputting a corrective action that can adjust the process accordingly.

The PID controller calculation involves three separate parameters; the Proportional (P), the Integral (I) and Derivative (D) values. The *Proportional* value determines the reaction to the current error, the *Integral* value determines the reaction based on the sum of recent errors, and the *Derivative* value determines the reaction based on the rate at which the error has been changing. The weighted sum of these three actions is used to adjust the process via a control element such as the position of a control valve or the power supply of a heating element.

By "tuning" the three constants in the PID controller algorithm, the controller can provide control action designed for specific process requirements. The response of the controller can be described in terms of the responsiveness of the controller to an error, the degree to which the controller overshoots the setpoint and the degree of system oscillation. Note that the use of the PID algorithm for control does not guarantee optimal control of the system or system stability.

The *Proportional* , *Integral*, and *Derivative* terms are summed to calculate the output of the PID controller. Defining u(t) as the controller output, the

final form of the PID algorithm is:

$$\begin{aligned} u(t) &= P + I + D \\ &= K_p e(t) + K_i \int_0^t e(\tau)\, d\tau \; + K_d \frac{de}{dt} \end{aligned} \tag{B.1}$$

And the tuning parameters are: K_p is the Proportional gain, K_i is the Integral gain and K_d is the Derivative gain. Figure B.2 shows the behaviour of a PID controller respect its reference.

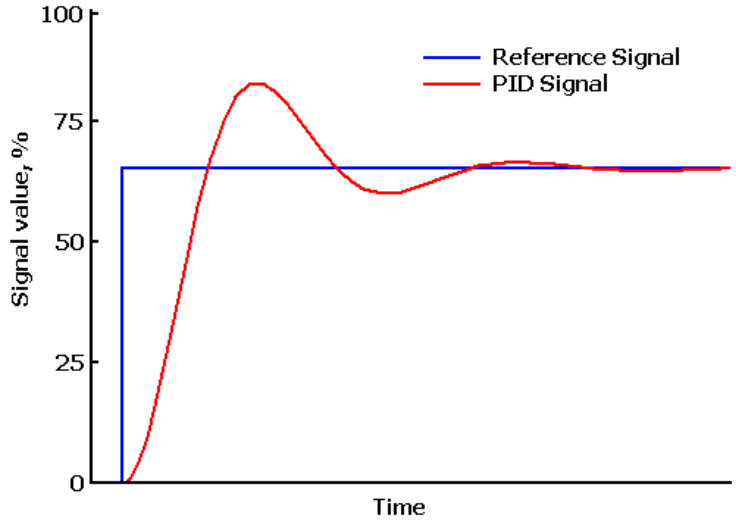

Figure B.2: Behaviour of a PID controller respect its reference.

Appendix C
Fanger's PMV Model

In this appendix is described with more detail the Predicted Mean Vote (PMV) index which was chosen to evaluate the thermal comfort in the presented thesis. This index represents the average thermal sensation felt by a large group of people in a space and it is one of the criteria to estimate the comfort state proposed by the ISO7730-1994 standard, [68] and [78]. It was developed by the Prof. P.O. Fanger of the International Centre for Indoor Environment and Energy at the Technical University of Denmark.

Fanger's PMV model was developed from laboratory and climate chamber studies. In these studies, the activities and the clothing of the participants where normalized and they where exposed to different thermal environments. In some studies the researchers choose the thermal conditions, and participants recorded how hot or cold they felt, using the Thermal Sensation Scale shown in figure C.1. In other studies, participants controlled the thermal environment themselves, adjusting the temperature until they felt thermally 'neutral'.

Thermal Sensation Scale						
-3	-2	-1	0	1	2	3
Cold	Cool	Slightly cool	Neutral	Slightly warm	Warm	Hot

Table C.1: Thermal Sensation Scale

PMV model is based on thermoregulation and heat balance theories. According to these theories, the human body employs physiological processes in order to maintain a balance between the heat produced by metabolism and the heat lost from the body. From this idea, Fanger proposed a model which describes the thermal comfort as the imbalance between the actual heat flow from the body in a given thermal environment and the heat flow required for

optimum comfort for a given activity. In this way, the PMV model combines four physical variables (air temperature, air velocity, mean radiant temperature, and relative humidity) and two personal variables (clothing insulation and activity level) into an index that can be used to predict thermal comfort.

Finally, the following equations show the Fanger's PMV model to predict the thermal comfort:

$$\begin{aligned} PMV &= [0.303 \cdot exp(-0.036 \cdot M) + 0.028] \cdot \{\ (M - W) - \\ &- 3.05 \cdot 10^{-3} \cdot [5733 - 6.99 \cdot (M - W) - p_a] - \\ &- 0.42 \cdot [(M - W) - 58.15] - 1.7 \cdot 10^{-5} \cdot M \cdot (5867 - p_a) - \\ &- 0.0014 \cdot M \cdot (34 - t_a) - 3.96 \cdot 10^{-8} \cdot f_{cl} \cdot \\ &\cdot \quad [(t_{cl} + 273)^4 - (\overline{t_r} - 273)^4] - f_{cl} \cdot h_c \cdot (t_{cl} - t_a)\} \end{aligned} \tag{C.1}$$

$$\begin{aligned} t_{cl} &= 35.7 - 0.028 \cdot (M - W) - I_{cl} \cdot \{\ 3.96 \cdot 10^{-8} \cdot f_{cl} \cdot \\ &\cdot \quad [(t_{cl} + 273)^4 - (\overline{t_r} - 273)^4] + f_{cl} \cdot h_c \cdot (t_{cl} - t_a)\} \end{aligned} \tag{C.2}$$

$$h_c = \begin{cases} 2.38 \cdot |t_{cl} - t_a|^{0.25} & \text{for } 2.38 \cdot |t_{cl} - t_a|^{0.25} > 12.1 \cdot \sqrt{v_{ar}} \\ 2.1 \cdot \sqrt{v_{ar}} & \text{for } 2.38 \cdot |t_{cl} - t_a|^{0.25} < 12.1 \cdot \sqrt{v_{ar}} \end{cases} \tag{C.3}$$

$$f_{cl} = \begin{cases} 1.00 + 1.290 \cdot I_{cl} & \text{for } I_{cl} \leq 0.078 \ \ m^2K/W \\ 1.05 + 0.645 \cdot I_{cl} & \text{for } I_{cl} > 0.078 \ \ m^2K/W \end{cases} \tag{C.4}$$

$$1\ metabolic\ unit = 1\ met = 58.2\ W/m^2,$$
$$1\ cloth\ unit = 1\ clo = 0.155\ m^2\ {}^{\circ}C/W.$$

Appendix D
Climatic Areas

There are several ways to classify climates into similar regimes. Originally, clime where defined to describe the weather depending upon a location's latitude. Modern climate classification methods can be broadly divided into genetic methods, which focus on the causes of climate, and empiric methods, which focus of the effects of climate.

In the European project GeoCool a subdivision of the South of Europe into climatic areas has been done considering the number of comfortable months and the prevalence of cold and warm months during the year, [67]. A identification label for each climatic area is obtained using a number indicating the comfortable months, followed by the letter F for an area with more than six cold months or a C in the other case.

Climatic Area	$T_{ma}(°C)$	$\Delta T_{ma}(°C)$	$T_{mmn}(°C)$	$T_{mmx}(°C)$
$0F$	$3 \div 6$	$15 \div 18$	$-6 \div -2$	$12 \div 14$
$1F$	$4 \div 7$	$17 \div 20$	$-6 \div -1$	$13 \div 16$
$2F$	$5 \div 8$	$17 \div 20$	$-5 \div 0$	$14 \div 17$
$3F$	$6 \div 9$	$17 \div 22$	$-4 \div 0$	$15 \div 18$
$4F$	$8 \div 13$	$13 \div 21$	$-2 \div 4$	$18 \div 23$
$5F$	$9 \div 13$	$17 \div 22$	$-1 \div 4$	$19 \div 23$
$2C$	$15 \div 17$	$16 \div 19$	$6 \div 10$	$24 \div 27$
$3C$	$12 \div 18$	$16 \div 23$	$3 \div 10$	$23 \div 27$
$4C$	$13 \div 18$	$14 \div 19$	$4 \div 11$	$22 \div 26$
$5C$	$14 \div 18$	$13 \div 17$	$6 \div 12$	$22 \div 26$

Table D.1: Climatic areas as defined by Petrarca

In table D.1 eleven climatic areas which are defined using the following temperature criteria: mean annual temperature (T_{ma}), annual variation of the

mean temperature (ΔT_{ma}), annual mean value od the minimum temperature (T_{mmn}) and annual mean value of the maximum temperature (T_{mmx}).

Appendix E
TRNSYS Software package

In this appendix we introduce the TRaNsient SYstem Simulation (TRNSYS) program which is the software package employed to model and to evaluate the different air conditioning layouts and the energy management strategies studied in this thesis, [64].

TRNSYS' beginnings can be found in a joint project between the Solar Energy Lab of the University of Wisconsin-Madison and the Solar Energy Applications Lab of the University of Colorado. In the 1970's a house was built in Colorado to study emerging solar energy technologies where the University of Wisconsin contributed by writing a Fortran program to predict the energy use in the building. In subsequent work, the same group developed a method of describing each component of the thermal system as a Fortran subroutine having inputs and outputs. As a consequence of this work took place the first commercial version available of this software package in 1975. This program was a flexible tool capable to simulate the transient performance of thermal energy systems.

Nowadays the modular structure of TRNSYS makes it one of the most flexible tools available according to the U.S. Department of Energy, [79]. This tool includes a graphical interface, a simulation engine, and a library of components that range from various building models to standard HVAC equipment to renewable energy and emerging technologies. TRNSYS also includes a method for creating new components that do not exist in the standard package. This characteristics has allowed that this simulation package has been used for more than 30 years for HVAC analysis and sizing, air conditioning systems, analysis of control schemes, building thermal performance, electric power simulation, multi-zone airflow analysis...

Due to its modular approach, TRNSYS is extremely flexible for modeling a variety of energy systems in differing levels of complexity. Supplied

source code and documentation provide an easy method for users to modify or add components not in the standard library; extensive documentation on component routines, including explanation, background, typical uses and governing equations; supplied time step, starting and stopping times allowing choice of modeling periods. The TRNSYS program includes a graphical interface to drag-and-drop components for creating input files (Simulation Studio), a utility for easily creating a building input file (TRNBuild), and a program for building TRNSYS-based applications for distribution to non-users (TRNEdit). Web-based library of additional components and frequent downloadable updates are also available to users. Extensive libraries of non standard components for TRNSYS are available commercially from TRNSYS distributors. TRNSYS also interfaces with various other simulation packages such as COMIS, CONTAM, EES, Excel, FLUENT, GenOpt and MATLAB.

Appendix F

Accuracy of the simulations results for the air conditioning layout configurations presented in Chapter 3

We include in this appendix a study of the accuracy of the simulation results for the air conditioning layouts in the different climate areas (Athens, Rome and Valencia) presented in Chapter 3. These results have to show a tendency towards a value independent of the time step employed to solve the set of differential equations programmed in our software package. Therefore, the simulation are carried out for several time steps. From this idea we perform simulations at the following solver time steps for each layout: 1.00 hour (60 minutes), 0.70 hour (42 minutes), 0.50 hour (30 minutes), 0.1 hour (6 minutes), 0.07 hour (4.2 minutes) and 0.05 hour (3 minutes).

For all configurations in Athens, Rome and Valencia, we presented a figure which includes the numerical error for the total electrical energy consumption in each time step. This error is calculated as the following equation:

$$Error(\%) = \frac{TEE_{\Delta t} - TEE_{\Delta t=0.05}}{TEE_{\Delta t=0.05}} \cdot 100 \tag{F.1}$$

where $TEE_{\Delta t}$ is the total electrical energy consumption for a particular time step. Notice that in the figure we show the results with respect to the $log(1/Time\_Step)$. This is done because this change allows compacting better the results.

Finally, the results from this study show a decreasing of the numerical error as we decrease the time step for all the configuration in Athens, Rome

and Valencia, obtaining a final numerical error lower than the 1‰. Furthermore, there is a clear tendency towards a value independent of the time step in each configuration.

F.1 Athens

'Air-A' configuration and 'GCHP-A' configuration

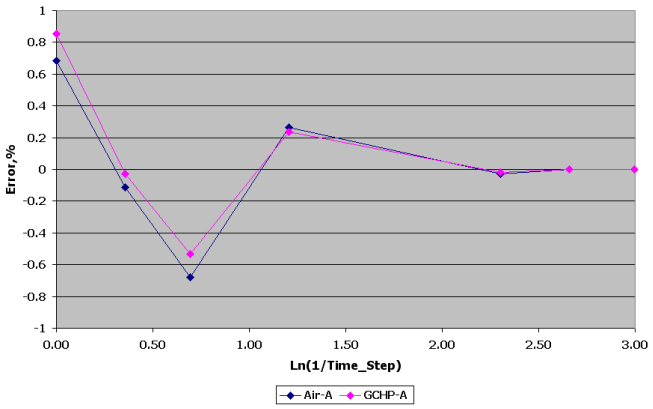

Figure F.1: Numerical error for the total electrical energy consumption for 'Air-A' configuration and 'GCHP-A' configuration.

'Air+S-A' configuration and 'GCHP+S-A' configuration

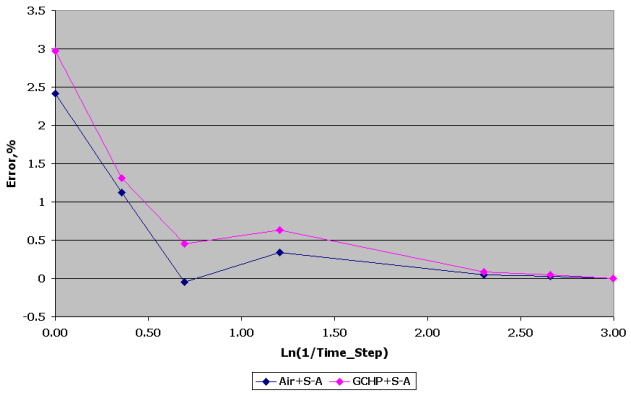

Figure F.2: Numerical error for the total electrical energy consumption for 'Air+S-A' configuration and 'GCHP+S-A' configuration.

'GCHP+Air-A' configurations

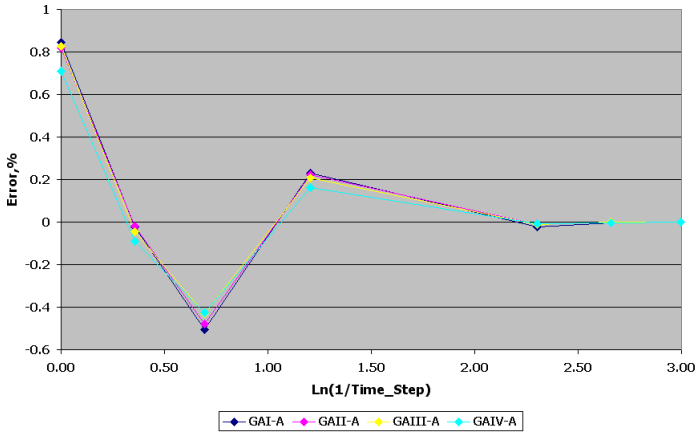

Figure F.3: Numerical error for the total electrical energy consumption for 'GCHP+Air-A' configurations.

'HA-A' configurations

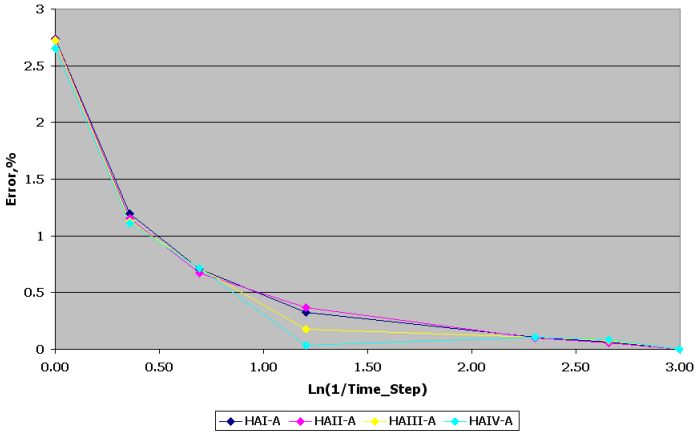

Figure F.4: Numerical error for the total electrical energy consumption for 'HA-A' configurations.

'HB-A' configurations

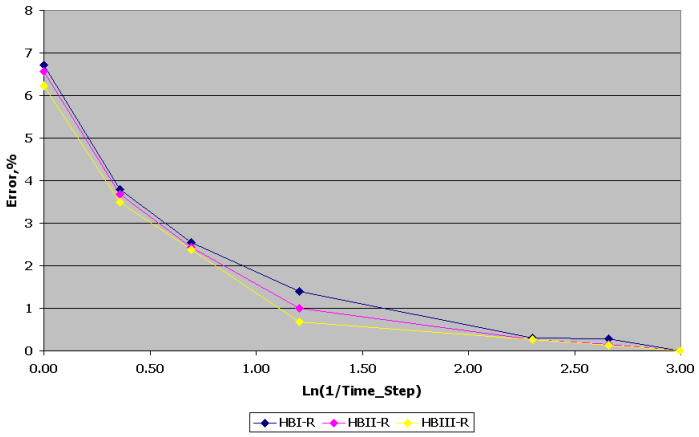

Figure F.5: Numerical error for the total electrical energy consumption for 'HB-A' configurations.

'HC-A' configurations

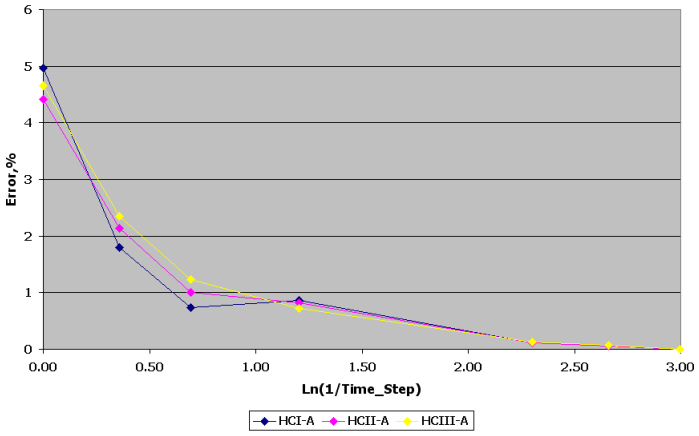

Figure F.6: Numerical error for the total electrical energy consumption for 'HC-A' configurations.

F.2 Rome

'Air-R' configuration and 'GCHP-R' configuration

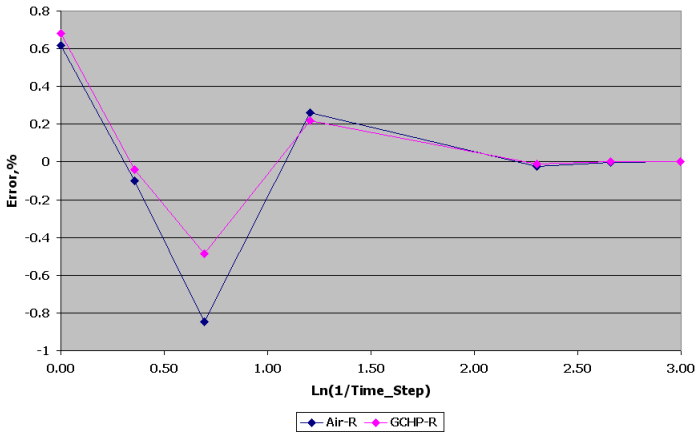

Figure F.7: Numerical error for the total electrical energy consumption for 'Air-R' configuration and 'GCHP-R' configuration.

'Air+S-R' configuration and 'GCHP+S-R' configuration

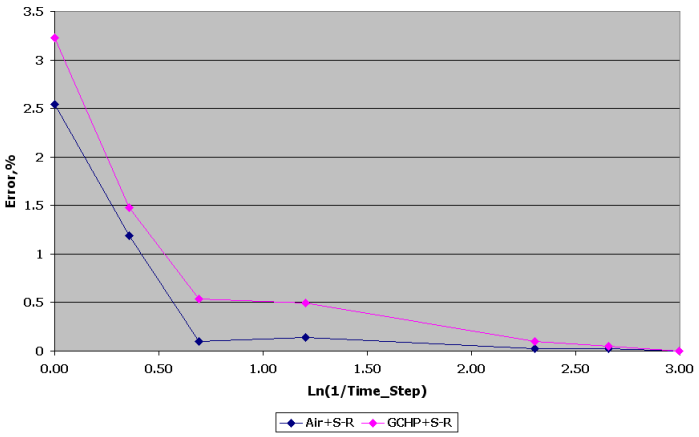

Figure F.8: Numerical error for the total electrical energy consumption for 'Air+S-R' configuration and 'GCHP+S-R' configuration.

'GCHP+Air-R' configurations

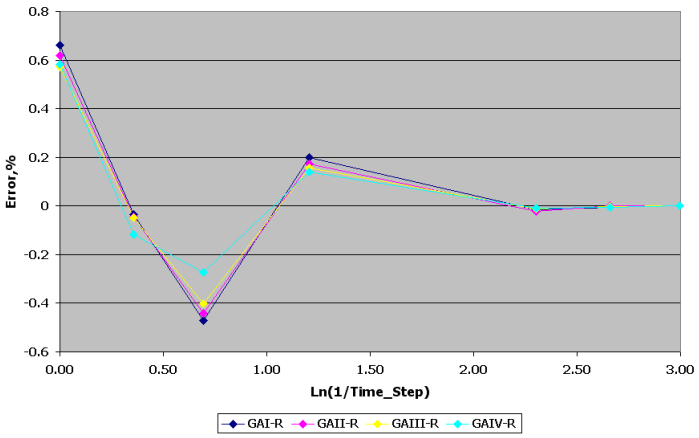

Figure F.9: Numerical error for the total electrical energy consumption for 'GCHP+Air-R' configurations.

'HA-R' configurations

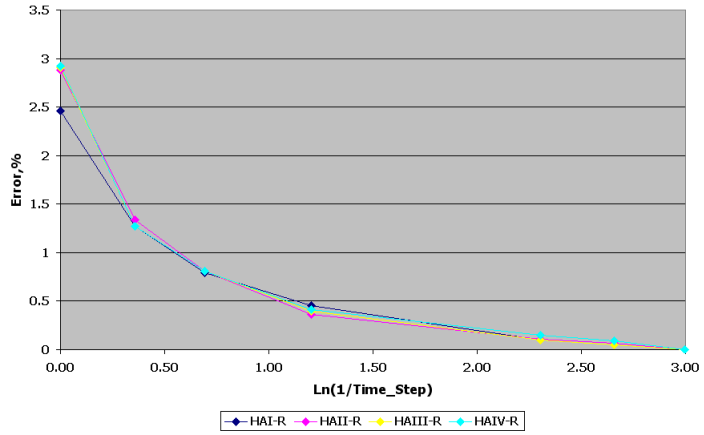

Figure F.10: Numerical error for the total electrical energy consumption for 'HA-R' configurations.

'HB-R' configurations

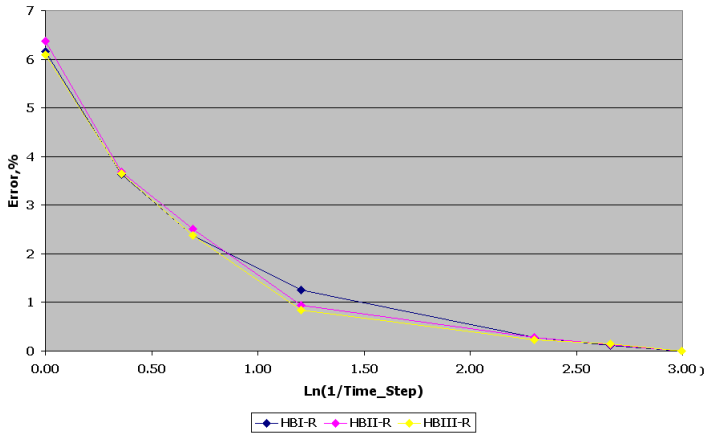

Figure F.11: Numerical error for the total electrical energy consumption for 'HB-R' configurations.

'HC-R' configurations

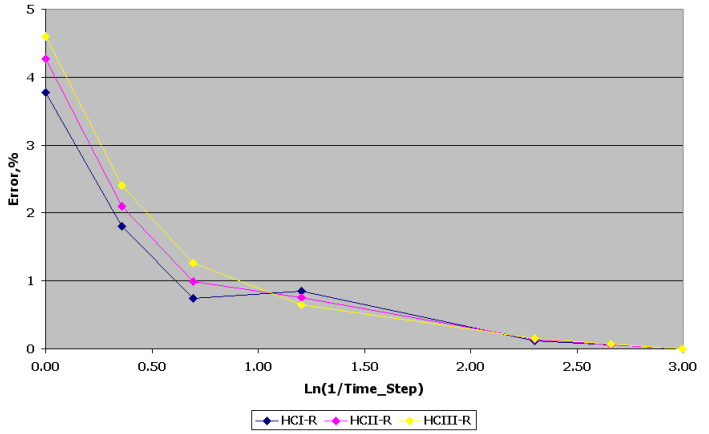

Figure F.12: Numerical error for the total electrical energy consumption for 'HC-R' configuration.

F.3 Valencia

'Air-V' configuration and 'GCHP-V' configuration

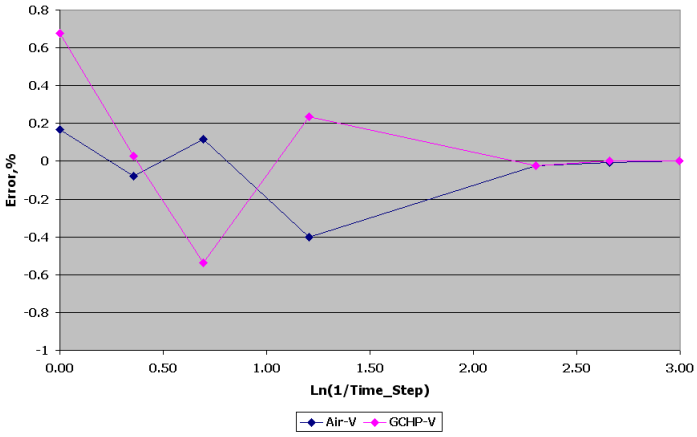

Figure F.13: Numerical error for the total electrical energy consumption for 'Air-V' configuration and 'GCHP-V' configuration.

'Air+S-V' configuration and 'GCHP+S-V' configuration

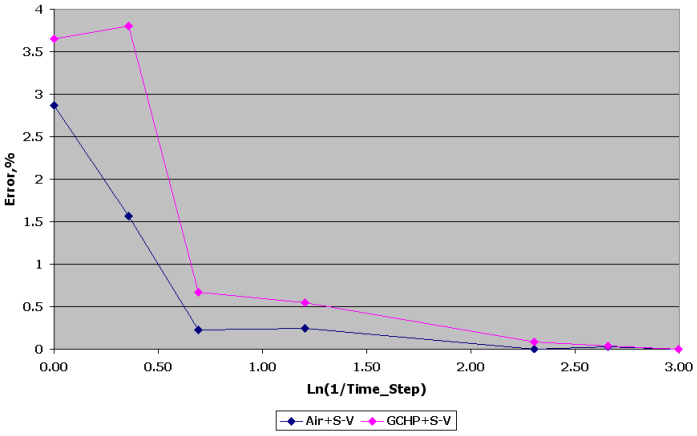

Figure F.14: Numerical error for the total electrical energy consumption for 'Air+S-V' configuration and 'GCHP+S-V' configuration.

'GCHP+Air-V' configurations

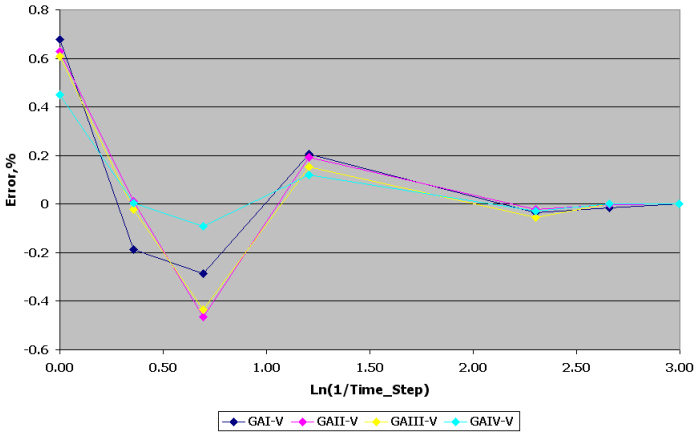

Figure F.15: Numerical error for the total electrical energy consumption for 'GCHP+Air-V' configurations.

'HA-V' configurations

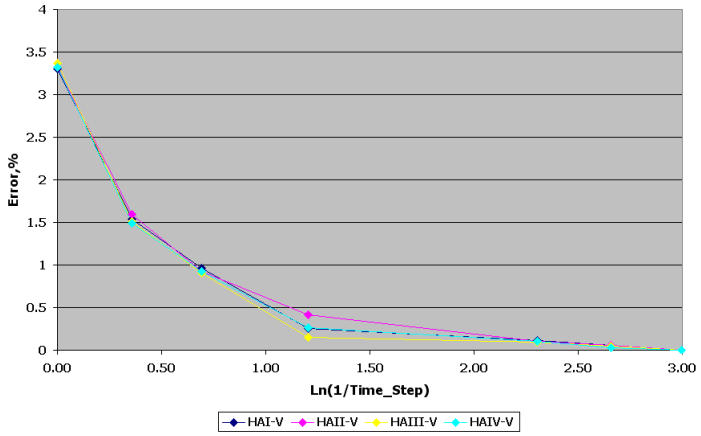

Figure F.16: Numerical error for the total electrical energy consumption for 'HA-V' configurations.

'HB-V' configurations

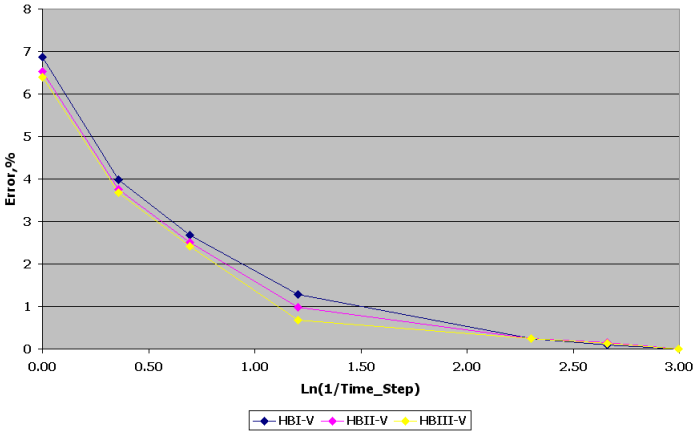

Figure F.17: Numerical error for the total electrical energy consumption for 'HB-V' configurations.

'HC-V' configurations

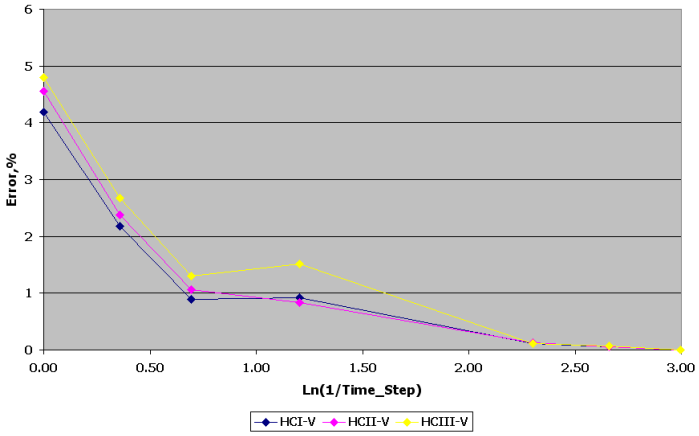

Figure F.18: Numerical error for the total electrical energy consumption for 'HC-V' configuration.

Nomenclature

$P_{HP,ww}$	Heat pump electrical power consumption at current conditions of the water to water heat pump
G_{ww}	Heat pump capacity at current conditions of the water to water heat pump
COP_{ww}	Heat pump coefficient of performance at current conditions of the water to water heat pump
$f_{flp,ww}$	Heat pump fraction of full load power of the water to water heat pump
PLR_{ww}	Heat pump partial load ratio of the water to water heat pump
$P_{HP,aw}$	Heat pump electrical power consumption at current conditions of the air to water heat pump
G_{aw}	Heat pump capacity at current conditions of the water to air heat pump
COP_{aw}	Heat pump coefficient of performance at current conditions of the air to water heat pump
$f_{flp,aw}$	Heat pump fraction of full load power of the air to water heat pump
PLR_{aw}	Heat pump partial load ratio of the air to water heat pump
m_i	Water mass of node i in the thermal storage device
Cp_{water}	Specific heat of the water
dTi/dt	Variation of the temperature in node i in the thermal storage device
$\dot{Q}_i^{dp}$	Energy change of the node i in the thermal storage device
$\dot{Q}_i^{cond}$	Thermal conduction to neighboring nodes of the node i in the thermal storage device
$\dot{Q}_i^{loss}$	Thermal losses to the ambient of the node i in the thermal storage device
P_{pump}	Water pump electrical power consumption

$P_{rated,pump}$	Rated water pump electrical power consumption
γ_{pump}	Water pump control signal
P_{fan}	Air fan electrical power consumption
$P_{rated,fan}$	Rated air fan electrical power consumption
γ_{fan}	Air fan control signal
$CMPF$	Cooling Mode Performance Factor
$Q_{load,cool}$	Total cooling thermal load
$W_{elec,cool}$	Total electrical energy consumption of the air conditioning configuration
$\dot{Q}_{fluid}$	Thermal energy absorbed by the water in the coil
$h_{air,in}$	Enthalpy of air entering the coil
$h_{air,out}$	Enthalpy of air exiting the coil
$\dot{m}_{air}$	Mass flow rate of air passing through the fan
h_{cond}	Enthalpy of condensate draining from the coil
$\dot{m}_{cond}$	Flow rate of condensate draining from the coil
$\dot{m}_{air}$	Mass flow rate of air passing through the fan
$\dot{m}_{rated,air}$	Maximum mass flow rate of air that can pass through the fan
$\omega_{air,in}$	Absolute humidity ratio of air entering the coil
$\omega_{air,out}$	Absolute humidity ratio of air exiting the coil
$\dot{m}_{water}$	Mass flow rate of fluid passing through the circulation pump
$\dot{m}_{rated,water}$	Maximum mass flow rate of fluid that can pass through the circulation pump
$\dot{m}_{IWP}$	Water mass flow from the load to the water to water heat pump (internal water mass flow)
$\dot{m}_{EWP}$	Water mass flow from the ground heat exchanger to the water to water heat pump (external water mass flow)
T_{set}	Heat pump set point temperature
$T_{exch,out}$	Heat pump inlet temperature from the external heat exchanger
$T_{load,in}$	Heat pump inlet temperature from the load
$COP_{heating}$	Coefficient of Performance index of a heat pump in heating mode
$Q_{heating}$	Heat provided by the heat pump in the heating mode
$COP_{cooling}$	Coefficient of Performance index of a heat pump in cooling mode
$Q_{cooling}$	Heat absorbed by the heat pump in the cooling mode
$W_{compressor}$	Work developed by the compressor of the heat pump
P_{HP}	Heat pump electrical power consumption at current conditions of the water to water heat pump
G	Heat pump capacity at current conditions of the heat pump

COP	Heat pump coefficient of performance at current conditions of the heat pump
f_{flp}	Heat pump fraction of full load power of the heat pump
PLR	Heat pump partial load ratio of the heat pump
G_{rate}	Heat pump rated capacity
G_{ratio}	Heat pump capacity at current conditions divided by the rated capacity
COP_{rate}	Heat pump rated coefficient of performance at current conditions
COP_{ratio}	Heat pump COP at current conditions divided by the rated COP
λ	Conductivity of the thermal ground storage
q_{sf}	Steady-flux solution in the thermal ground storage
q_l	Local solution in the thermal ground storage
r	Radius of the cylindrical thermal ground storage region
a	Diffusivity of the thermal ground storage
$u(t)$	Output of the PID controler
$e(t)$	Error between the reference and the measure of the PID controler
K_p	Proportional gain of the PID controler
K_i	Integral gain of the PID controler
K_d	Derivative gain of the PID controler
PMV	Predicted Mean Vote index
M	Metabolic rate (W/m^2)
W	External work (W/m^2)
I_{cl}	Insulation of the cloth (m^2K/W)
f_{cl}	ratio of the man‘s surface area while clothed to man‘s surface area while nude
t_a	Air temperature (^oC)
$\overline{t_r}$	Mean radiant temperature (^oC)
v_{ar}	Relative air velocity (relative to human body) (m/s)
p_a	Partial water vapour pressure (Pa)
h_c	Convective heat transfer coefficient between air and clothes (W/m^2K)
t_{cl}	Surface temperature of clothing (^oC)
$FCost_{cool}$	Final economic cost in cooling (€/KWh)
Q_{total_cool}	total cooling thermal energy (KWh)
$TCost$	Total economic cost (€)

List of Tables

List of Figures

Publications

2009. Efficiency improvement of ground coupled heat pumps when combined with air source heat pump and thermal storage, N. Pardo, Á. Montero, J. Martos, J.F. Urchueguía, submitted to Applied Thermal Engineering.

2009. Efficiency improvement of a ground coupled heat pump system from energy management, N. Pardo, Á. Montero, A. Sala, J. Martos, J.F. Urchueguía, submitted to Applied Thermal Engineering.

2009. Simulation study of a control strategy for improving the energy efficiency of a ground coupled heat pump HVAC system, N. Pardo, Á. Montero, A. Sala, J. Martos, J.F. Urchueguía, in: 11th International Building Performance Simulations Association and Exhibition in 2009,Glasgow (Scotland).

2009. Energy efficiency of study of a hybrid ground coupled heat pump system in several layouts combinations, N. Pardo, Á. Montero, J. Martos, J.F. Urchueguía, Thermal Energy Storage for Efficiency and Sustainability (EFFSTOCK 2009), Stockholm (Sweden).

2009. Efficiency study of a ground coupled heat pump combined with an air source heat pump and thermal storage, N. Pardo, Á. Montero, J. Martos, J.F. Urchueguía, Energy, Climate and Indoor Comfort in the Mediterranean Countries (CLIMAMED 2009), Lisbon (Portugal).

2008. Advanced Control Structure for Energy Management in Ground Coupled Heat Pump HVAC System, N. Pardo, A. Sala, A. Montero, J. F. Urchueguía, J. Martos, Energy, 17th World Congress. The International Federation of Automatic Control, Seoul (Corea).

2007. Advance control structures for HVAC with a geothermal heat pump applied to an office building in the Mediterranean area, N. Pardo, A. Sala, Á. Montero, J. Martos, J.F. Urchueguia Energy, Climate and Indoor Comfort

in the Mediterranean Countries (CLIMAMED 2007), Genoa (Italy).

2007. Monitoring systems to evaluate building energetic response and comparison with simulated data, N.Pardo, B.Paz, J. Martos, J.F. Urchueguía, Á. Montero, Renewables in a Changing Climate - Innovation in the Built Environment (CISBAT 2007), Lausanne (Swiss).

2007. Instrumento para la validación de modelos de edificación en simulaciones de respuesta térmicas con TRNSYS, N. Pardo, B. Paz, A. Montero, J. Martos, 2nd International Congress, Energy and Environment Engineering and Management (ICIIEM), Badajoz (Spain).

Bibliography

[1] International Energy Agency (IEA), in: http://www.iea.org.

[2] Energy Star Program from US Environment Protection Agency, in: http://www.energystar.gov.

[3] P.F. Healy, V.I. Ugursal. Performance and economic feasibility of ground coupled heat pumps in cold climate. International Journal of Energy Research 1997; 21(10) 857-70.

[4] P.J. Petit, J.P. Meyer. Economic potential of ground-coupled heat pumps compared to air-coupled air conditioners in South Africa. Energy 1998; 23(2) 137-43.

[5] Y. Hwang, J. Lee, Y. Jeong, K. Koo, D. Lee, I. Kim, S. Jin, S.H. Kim, Cooling performance of a vertical ground-coupled heat pump system installed in a school building, Renewable Energy 34 (2009) 578-582.

[6] J.F. Urchueguía, M. Zacarés, J.M. Corberán, Á. Montero, J. Martos, H. Witte, Comparison between the energy performance of a ground coupled water to water heat pump system and an air to water heat pump system for heating and cooling in typical conditions of the European Mediterranean coast, Energy Conversion and Management 49 (2008) 2917-2923.

[7] J.D. Spitler, Ground-Source Heat Pump System Research - Past, Present and Future, HVAC & Research 11 (2) (2005).

[8] Jr. Jones, Malcom, The history of the air conditioning, Air conditioning - Newsweek 130 (1997) 24-42.

[9] D.A. King, Architecture and Astronomy: The ventilation of medieval Cairo and their secrets, Journal of the American Oriental Society 104 (1) (1984) 97-133.

[10] D.A. Ball, R.D. Fischer, and D.L. Hodgett, Design methods for ground-source heat pumps, ASHRAE Transactions 89 (2) (1983) 416-440.

[11] C. Orio, Water Energy Distributors, (2005).

[12] L.R. Ingersoll, O.J. Zobel, Heat conduction: with engineering, geological and other applications. Madison: University of Wisconsin Press, 1954.

[13] H.S. Carslaw, J.C. Jaeger, Conduction of heat in solids. Oxford: Claremore Press, 1959.

[14] E.R. Ambrose, Heat Pumps and Electric Heating, Winley New York, USA, 1966.

[15] B. Sanner, Some history of shallow geothermal energy use. International Summer School on Direct Application of Geothermal Energy, Skopje, (2001).

[16] J.D. Kroeker, In a comment on the paper: Guernsey, E.W., P.L. Betz, and N.H. Skau. Earth as a heat source or storage medium for the heat pump. ASHVE Transactions (55) 321-324. Kroeker's comments may be found on 336-337 (1949).

[17] J.E. Bose, J.D. Parker, and F.C. McQuiston, Design/Data Manual for Closed-Loop Ground-Coupled Heat Pump Systems, ASHRAE (1985).

[18] Geothermal Heat Pump Consortium, http://www.geoexchange.org/

[19] D.P. Hart, R. Couvillion, Earth coupled heat transfer, National Water Well Association, 1986.

[20] IGSHPA. Design and installation standards, stillwater, Oklahoma: International Ground Source Heat Pump Association, 1991.

[21] G. Hellstrom. Ground heat storage. Thermal analysis of duct storage systems: part I. Theory. Doctoral Thesis, Department of Mathematical Physics, University of Lund, Sweden, 1991.

[22] F. Hikari, I. Ryuichi, I. Takashi, Improvements on analytical modeling for vertical U-tube ground heat exchangers. Geotherm Resources Council Trans (28) (2004) 73-7.

[23] P. Eskilson, Thermal analysis of heat extraction boreholes. Doctoral Thesis, Department of Mathematical Physics and Building Technology, University of Lund, Sweden, 1987.

[24] H. Zeng, N. Diao, Z. Fang, Heat transfer analysis of boreholes in vertical ground heat exchangers, Int Journal Heat Mass Transfer (46) (2003) 4467-81.

[25] L. Lamarche, B. Beauchamp, A new contribution to the finite linesource model for geothermal boreholes. Energy and Buildings (2) (2007) 188-98.

[26] T.V. Bandos, Á. Montero, E. Fernández, J.L.G. Santander, J.M. Isidro, J. Pérez, P.J. Fernández de Córdoba, J.F. Urchueguía, Finite line-source model for borehole heat exchanger: effect of vertial temperature variations. Geothermics, in: 10.1016/j.geothermics.2009.01.003

[27] C. Yavuzturk, Modeling of vertical ground loop heat exchangers for ground source heat pump systems. Doctoral Thesis, Oklahoma State University, 1999.

[28] M.A. Bernier, P. Pinel, R. Labib, R. Paillot, A multiple load aggregation algorithm for annual hourly simulations of GCHP systems. HVAC&R Res (4) (2004) 471-87.

[29] C.K. Lee, H.N. Lam, Computer simulation of borehole ground heat exchangers for geothermal heat pump systems, Renewable Energy 33 (2008) 1286-1296

[30] Z. Li, M. Zheng, Development of a numerical model for the simulation of vertical U-tube ground heat exchangers, Applied Thermal Engineering (2008) (Available online).

[31] H. Esena, M. Inallib, A. Sengurc, M. Esena, Predicting performance of a ground-source heat pump system using fuzzy weighted pre-processing-based ANFIS, Building and Environment 43 (2008) 2178-2187.

[32] W. Yang, M. Shi, G. Liu, Z. Chen, A two-region simulation model of vertical U-tube ground heat exchanger and its experimental verification, Applied Energy 86 (2009) 2005-2012.

[33] J. Gao, X. Zhang, J. Liu, K. S. Li, J. Yang, Thermal performance and ground temperature of vertical pile-foundation heat exchangers: A case study, Applied Thermal Engineering 28 (2008) 2295-2304.

[34] T. Katsura, K. Nagano, S. Narita, S. Takeda , Y. Nakamura, A. Okamoto, Calculation algorithm of the temperatures for pipe arrangement of multiple ground heat exchangers, Applied Thermal Engineering (2008) (Available online).

[35] H. Demir, A. Koyun, G. Temir, Heat transfer of horizontal parallel pipe ground heat exchanger and experimental verification, Applied Thermal Engineering 29 (2009) 224-233.

[36] O. Ozgener, A. Hepbasli, Modeling and performance evaluation of ground source (geothermal) heat pump systems, Energy and Buildings 39 (2007) 66-75.

[37] A. Hepbasli, Exergetic modeling and assessment of solar assisted domestic hot water tank integrated ground-source heat pump systems for residences, Energy and Buildings 39 (2007) 1211-1217.

[38] V. Trillat-Berdal, B. Souyri, G. Achard, Coupling of geothermal heat pumps with thermal solar collectors, Applied Thermal Engineering 27 (2007) 1750-1755.

[39] Z. Han, M. Zheng, F. Kong, F. Wang, Z. Li, T. Bai, Numerical simulation of solar assisted ground-source heat pump heating system with latent heat energy storage in severely cold area, Applied Thermal Engineering 28 (2008) 1427-1436.

[40] H. Wang, C. Qi, E. Wang, J. Zhao, A case study of underground thermal storage in a solar-ground coupled heat pump system for residential buildings, Renewable Energy 34 (2009) 307-314.

[41] Y. Bi, T. Guo, L. Zhang, L. Chen, Solar and ground source heat-pump system, Applied Energy 78 (2004) 231-245.

[42] ASHRAE, Commercial/Institutional Ground-Source Heat Pump Engineering Manual, American Society of Heating, Refrigerating and Air-Conditioning Engineers, Inc., Atlanta, 1995.

[43] C.S. Gilbreath, Hybrid ground-source heat pump systems for commercial applications, Master‘s Thesis, University of Alabama, Tuscaloosa, Alabama, 1996.

[44] S.P. Kavanaugh, K. Rafferty, Ground-source Heat Pumps: Design of Geothermal Systems for Commercial and Institutional Buildings, American Society of Heating, Refrigerating and Air-Conditioning Engineers, inc: Atlanta, 1997.

[45] G. Phetteplace, W. Sullivan, Performance of a hybrid ground-coupled heat pump system, ASHRAE Transactions 104 (1b) (1998) 763-770.

[46] C. Yavuzturk, J.D. Spitler, Comparative study of operating and control strategies for hybrid ground-source heat pump systems using a short time step simulation model, ASHRAE Transactions 106 (2) (2000) 192-209.

[47] M. Yi, Y. Hongxing, F. Zhaohong, Study on hybrid ground-coupled heat pump systems, Energy and Buildings 40 (2008) 2028-2036.

[48] S.M. Hasnain, N.M. Alabbadi, Need for a thermal-storage air-conditioning in Saudi Arabia, Applied Energy 65 (1-4) (2000) 153-164.

[49] T. Nagota, Y. Shimoda, M. Mizumo, Verification of the energy-savings effect of the district heating and cooling system - Simulation of an electrical-driven heat pump system, Energy and Buildings, 40 (2008) 732-741.

[50] P. Mogensen, Fluid to duct wall heat transfer in duct system heat storages, in: Proceedings from International Conference on Subsurface Heat Storage in Theory and Practice, Stockholm, (1983), pp. 652-657.

[51] C. Eklöf, S. Gehlin, TED - a mobile equipment for thermal response test, MSc Thesis, 198, Luleå University of Technology, 1996, p. 62

[52] S. Gehlin, B. Nordell, Thermal response testŮa mobile equipment for determining thermal resistance of boreholes, in: Proceedings of the Megastock'97, Sapporo, Japan, (1997), pp. 103-108.

[53] W. Austin, Development of an in situ system for measuring ground thermal properties, MSc Thesis, Oklahoma State University, 1998, p. 164

[54] W. Austin, C. Yavuzurk, J.D. Spitler, Development of and in situ system for measuring ground thermal properties, ASHRAE Transactions 106 (1) 2000 365-379.

[55] L. Laloui, G. Steinmann, Finalisation du module de lŠEPFL pour les tests de responses, ENET Swiss Energy, No. 220188, 2002 (in French).

[56] N. Mattsson, G. Steinmann, L. Laloui, Advanced compact device for the in situ determination of geothermal characteristics of soils, Energy and Buildings 40 (2008) 1344-1352.

[57] B. Sanner, E. Mands, M.K. Sauer, Larger geothermal heat pump plants in the central region of Germany, Geothermics, vol. 32, Elsevier, 2003, pp. 589-602.

[58] H.J.L. Witte, G.J. van Gelder, J.D. Spitler, In situ measurement of ground thermal conductivity: the Dutch perspective, ASHRAE Transactions 108 (1) (2002).

[59] M.L. Allan, S.P. Kavanaugh, Thermal conductivity of cementitious grouts and impact on heat exchanger length design for ground source heat pumps, International Journal of HVAC&R 5 (2) (1999) 85-96.

[60] M.L. Allan, A.J. Philippacopoulos, Thermally conductive cementious grouts for geothemal heat pumps, World Geothemal Congress 2000, in press.

[61] M.L. Allan, A.J. Philippacopoulos, Ground water protection issues with geothermal heat pumps, in: http://www.osti.gov.

[62] M.L. Allan, Materials characterization os superpasticized cement-sand grout, Cement and Concrete Research 30 (2000) 937-942.

[63] J.M. Corberán, Bombas de Calor Geotérmicas, Conferencia en la Universidad de Valladolid 28 de Noviembre 2008.

[64] TRNSYS 16.1: Transient System Simulation Program. University of Wisconsin, Madison (USA): Solar Energy Laboratory.

[65] Ground-source heat pump project analysis, in: Clean Energy Project Analisys, CANMET Energy Technology Centre - Varennes (CTEC), Minister of Natural Resource Canada 2001-2005.

[66] Ground Reach project, in: http://groundreach.fiz-kalsruhe.de/en

[67] Geothermal Heat Pump for Cooling and Heating along the European Coastal Areas, in: Report of the european project NEE-2001-00847

[68] ISO. International Standard 7730-1994, Moderate thermal environments-determination of the PMV and PPD indices and specification of the conditions for thermal comfort, in: International Standard Organization, Switzerland, 1994.

[69] Norma Básica de la Edificación - Comportamiento Térmico en los Edificios (CNE-CT-79) Ed: Ministerio de Fomento, Spain.

[70] Agencia Valenciana de la Energía, in: www.aven.es

[71] Grundfos Company, in: www.grundfos.com

[72] Ciatesa Company, in: www.ciatesa.es

[73] Asociacion Española de la Industria Electrica, in: www.unesa.es

[74] EUROSTAT in: http://epp.eurostat.ec.europa.eu

[75] P. Albertos, A. Sala Piqueras, Springer-Verlag New York, Inc. Secaucus, NJ, USA, 2002.

[76] C.P. Underwood, Robust control of HVAC plant. Part 1, Modelling, Building Services Engineering Research and Technology 21 (2000) 53-61.

[77] E. Bettanini, A. Gastaldello, L. Schibuola, Simplified models to simulate part load performance of air conditioning equipments, in Proceedings of the Eighth International IBPSA Conference, Eindhoven, Netherlands, 2003.

[78] P.O. Fanger, Calculation of thermal comfort: Introduction of a basic comfort equation, ASHRAE Transactions, 73(2) (1967) III4.1-III4.20.

[79] U.S Department of Energy - Energy Efficiency and Renewable Energy, in: http://www.eere.energy.gov/

[80] ASHRAE Research, 2004 ASHRAE Handbook, HVAC Systems and Equipments, 2004, pp.11.1-11.2

[81] C.E. Dorgan, J.S. Elleson, Design Guide for Cool Thermal Storage, USA, 1993.

[82] M. Ibáñez, L.F. Cabeza, C. Solé, J. Roca, M. Nogués, Modelization of a water tank including a PCM module, Applied Thermal Engineering 26 (2006) 1328-1333.

[83] J. Bony, S. Citherlet, Numerical model and experimental validation of heat storage with phase change material, Energy and Buildings 39 (2007) 1065-1072.

[84] W. Chen, K. Wong, H. Chou, A reliable one-dimensional method applied to heat-transfer problems associated with insulated rectangular tanks in refrigeration systems, International Journal of Refrigeration 29 (2006) 485-494.

[85] F.M. McQuiston, J.D. Parker, J.D. Spitler, Heating, ventilation, and air conditioning, John Wiley & Sons, Inc (Ed.), USA, 2000.

[86] Fundamentals of HVAC systems - SI version, American Society of Heating, Refrigeration and Air-Conditioning Engineers (ASHRAE) (Ed.), USA, 1999

[87] R.N. Bateson, Introduction to control system technology, Prentice Hall intenational, London, UK, 1993.

[88] S. Gupta, Elements of control systems, Prentice Hall intenational, London, UK, 2002.

[89] T.Q. Qureshi, S.A. Tassou, Variable-speed capacity control in refrigeration systems, Applied Thermal Engineering 16 (1996) 103-113.

[90] C. Aprea, R. Mastrullo, C. Renno, G. Vanoli, An evaluation of R22 substitutes performances regulating continuously the compressor refrigeration capacity, Applied Thermal Engineering 24 (1) (2004) 127-139.

[91] H.M. Henning, T. Pagano, S. Mola, E. Wiemkem, Micro tri-generation system for indoor air conditioning, Applied Thermal Engineering 27 (2007) 2188-2194.